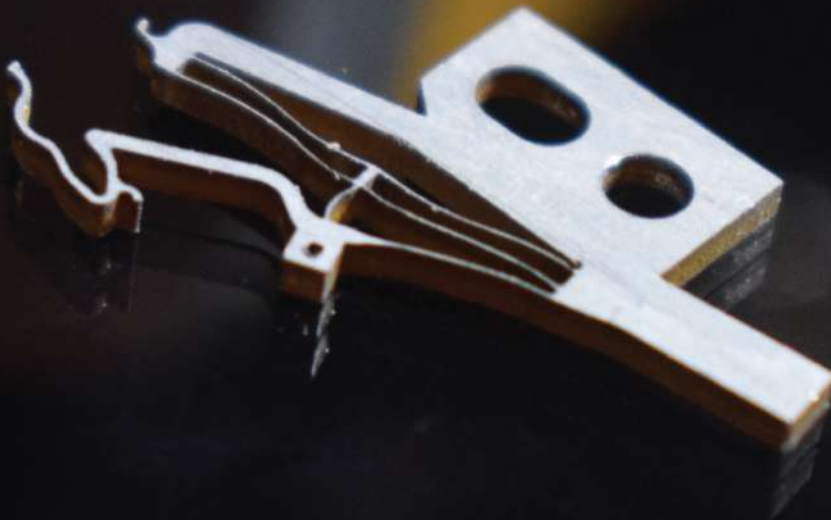


Department of Precision and Microsystems Engineering

DESIGN OF A BISTABLE STAPES PROSTHESIS

E.J. GIUFFRÉ

Report no. : MSD 2018.024
Coach : Dr. N. Tolou
Professor : Prof. dr. ir. J.L. Herder
Specialisation : Mechatronic System Design
Type of report : MSc Thesis
Date : August 17, 2018



Design of a bistable stapes prosthesis

by

E.J. Giuffré

to obtain the degree of Master of Science
at the Delft University of Technology,
to be defended publicly on Friday August 31, 2018 at 1:00 PM.

Student number:	4624599
Project duration:	September 1, 2017 – August 31, 2018
Thesis committee:	Prof. J. Herder, TU Delft, Chair
	Dr. N. Tolou, TU Delft, supervisor
	Ir. R. Kuppens, TU Delft, supervisor
	Dr.ir. G. Smit, TU Delft
	Dr. H. Blom, Hagaziekenhuis

An electronic version of this thesis is available at <http://repository.tudelft.nl/>.

Acknowledgements

Presented in this document is the research I have performed in the design and development of a bistable stapes prosthesis. During the process I received valuable help from many people.

Firstly, I would like to thank my supervisor Nima Tolou, for his insights and words of encouragement, and for his impromptu coffee catch-ups at IO. Thank you to my daily supervisor Reinier Kuppens, for the time he spent giving me feedback and for his constant support and optimism. I would also like to thank the surgeon, Dr. Henk Blom, for initiating the project and providing valuable insights on the clinical perspective.

A big thank you to David Jaager from DEMO for his patience and perfectionism in manufacturing the titanium prototypes, and to Paul Breedveld for his input and for connecting me with David. I would like to acknowledge Davood, for letting me use his force-displacement measurement setup, the technicians Spiridon and Wim for assisting with the machining of parts, and Jos for helping with setting up the force sensor.

Finally to my family, friends and Rayco, for their support through what was a rewarding but challenging year. Thank you.

E.J. Giuffré
Delft, August 2018

Abstract

Otosclerosis is a bone disease of the middle ear that often causes conductive hearing loss. This type of hearing loss can be treated by implanting a prosthesis, which replaces the stapes bone and attaches to the adjacent bone: the incus. Current stapes prostheses produce excellent hearing results, however the procedure is difficult to perform and success is not assured. With current prostheses, safe clamping forces cannot be accurately controlled, despite being crucial to the surgery's long-term success. Inappropriate clamping force may cause slipping of the prosthesis or necrosis of the incus.

The objective of this study was to first create an overview of current prostheses and subsequently examine their pitfalls, and to design a new stapes prosthesis that addresses these pitfalls. Throughout the literature review a classification and evaluation system was developed to catalogue existing and future prostheses based on, for example, air bone gap difference, force controllability and ease of implantation. From this study we found the category of prostheses that utilise elastic material behaviour to securely clasp around the incus to have the most potential in a new prosthesis design.

Presented in this thesis is a novel prosthesis which features a bistable, fully compliant, two-dimensional mechanism, designed to be simpler to insert and with a more predictable clamping force compared with existing prostheses. For any incus diameter within the recorded range, the force around the incus is sure to be safe by design. The new prosthesis can be placed around the bone without causing unwanted stresses in the ossicles and joints, and is easily clicked shut.

Contents

Abstract	v
1 Introduction	1
2 Literature review paper: Towards the next-generation of stapes prostheses	3
3 Paper: Design of a bistable stapes prosthesis	21
4 Reflection	33
4.1 Line of thought	33
4.2 Timeline review	34
4.3 Contributions	34
4.4 Future steps	34
5 Conclusion	35
A Conceptual process	37
A.1 Morphological chart process	38
A.2 Concept generation and evaluation	39
A.3 Shortlisted concepts	39
A.4 Final concept	41
A.5 Morphological chart 1: general solutions	44
A.6 Concept brainstorm	47
A.7 Morphological chart 2: mechanical solutions	48
A.8 Evaluation: bistable concepts	51
A.9 Evaluation: multistable concepts	52
A.10 4-bar tristable mechanism synthesis	53
B Dimensional design	55
B.1 PRBM: initial concept	55
B.2 PRBM: final concept	57
B.3 FEM modelling process	58
B.3.1 Setting up COMSOL model	58
B.3.2 Convergence	60
B.3.3 Varying parameters	60
B.4 Concept revision	62
B.5 Determining minimum prototype scale	64
B.6 CAD drawings	65
C Manufacturing and measurements	67
C.1 Manufacturing techniques	67
C.1.1 2D Laser cutting	67
C.1.2 2D Wire Electron Discharge Machining (EDM)	68
C.1.3 2D Deep Reactive Ion Etching (DRIE)	68
C.1.4 3D Selective laser melting	68
C.1.5 3D Micro milling	69
C.2 Materials	69
C.3 Prototypes	69
C.3.1 Design process demonstrators	69
C.3.2 Wire EDM: copy of existing prosthesis	70
C.3.3 Wire EDM: bistable prosthesis	71

C.4	Test setup and measurements.	74
C.4.1	First test series	75
C.4.2	Second test series	78
D	Final design	81
E	Code	83
E.1	PRBM python code	83
E.2	ANSYS code.	85
F	Extra material	89
F.1	Photographs from stapedotomy surgery	89
F.2	KNO Conference	90

Introduction

Otosclerosis is a bone disease of the middle ear which often causes severe conductive hearing loss. It is particularly prevalent in the Caucasian population, affecting 7.3% of Caucasian males and 10.3% of Caucasian females. The disease affects 0.3% of the population in general. Otosclerosis induced conductive hearing loss can be treated by the insertion of a passive prosthesis. The procedure typically has excellent results, with the potential to completely restore hearing to the patient. However, it is difficult to perform and success is not assured. There is very little space in the middle ear and the view of the surgeon is highly restricted. The middle ear is accessed via the narrow ear canal, and the entire operation is done under a microscope. Failure modes are, for example, an inappropriate clamping pressure which may cause slipping of the prosthesis or necrosis of the incus. According to Fisch [3], the most common cause of failure for a stapedotomy is the displacement of the prosthesis from the incus, likely caused by under-crimping. Another common complication of the stapedotomy which can be recognised in revision surgeries is necrosis of the long process of the incus, which may be caused by over-crimping. Thus in current crimping prostheses safe clamping forces cannot be accurately controlled, despite being crucial to the surgery's long term success.

The objective of this study was to first create an overview of current prostheses and subsequently examine their pitfalls, and to design a new stapes prosthesis that addresses these pitfalls. There does not exist in literature a comprehensive review of all the variations of stapes prostheses. Therefore, the review paper presents a classification and evaluation system to categorise all existing and future prostheses. Two strategies of classifying the prostheses are combined to form a 2-dimensional array of solutions. These classification systems are (1) the working principle employed in the attachment of the prosthesis to the long process of the incus, and (2) the geometry of the coupling between the prosthesis and incus.

The physics of attachment includes the five possible categories: multibody prostheses, prostheses which use plastic deformation to attach to the incus, prostheses which use elastic deformation, thermally actuated prostheses, and finally any combination of these four attachment principles. For the first category, attachment is achieved by forcing the prosthesis to plastically deform around the adjacent ossicle, the incus, via manual crimping. However, crimping to the correct pressure without damaging the delicate bones, ligaments and nerves of the middle ear is a complex task, and either over-crimping or under-crimping will result in detrimental long-term effects to the patient's hearing. These effects are discussed in more detail in Section 2 of the literature review paper. Prostheses which attach via elastic deformation are typically in the form of clips which are pushed onto the long process of the incus, however this involves putting a high lateral force on the delicate ossicles. Thermally actuated prostheses require a laser to be used directly in the middle ear, risking damage to middle ear tissue.

Presented in this thesis is a prosthesis design that is simpler and safer to insert compared with conventional prostheses. The new design features a bistable, fully compliant mechanism which reliably applies an appropriate clamping force, independent of the experience of the operating surgeon. For any incus diameter within the recorded range, the force around the incus is sure to be safe by design. The new prosthesis can be placed around the bone without causing unwanted stresses in the ossicles and joints, and is easily clicked shut.

The body of this thesis is comprised of two papers. The first paper, in Chapter 2, is a review of the current stapes prosthesis technology. Chapter 3 contains the second paper, in which we detail a novel prosthesis design. The two papers are followed in Chapter 4 by a reflection on the project, a conclusion in Chapter 5, and finally the appendix. The appendix contains all the background information pertaining to the project,

and is organised into six chapters. Appendix A steps through the conceptual design process; from generating solutions with morphological charts, to refining the final solution. In Appendix B the PRBM analysis and FEM dimensioning of the design is shown. Appendix C reviews the manufacturing options, and details the prototype manufacturing and measurement processes. Drawings and photographs of the final device are collected in Appendix D, and the code written for the project is found in Appendix E. Finally, Appendix F contains extra material, such as photographs taken from the presentation of the literature review paper at the national KNO conference in April 2018.

2

Literature review paper: Towards the next-generation of stapes prostheses

Towards the next-generation of stapes prostheses

Lola Giuffré, Nima Tolou, Reinier Kuppens, Henk Blom

Dept. of Precision and Microsystems Engineering Delft University of Technology

Delft, 2628 CD, The Netherlands

lolagiuffre@gmail.com, n.tolou@tudelft.nl, p.r.kuppens@tudelft.nl, h.blom@hagaziekenhuis.nl

ABSTRACT

Current stapes prostheses produce excellent clinical hearing results, however the surgical procedure is complex and requires the hand of a highly experienced surgeon. The procedure is technically difficult, and the surgeon may not be confident that the prosthesis is clamped at a correct pressure around the incus. The objective of this study is to characterise and evaluate current state-of-the-art in stapes prostheses, with the incentive to lay the groundwork for the next generation of prostheses. We have developed a classification and evaluation system to catalogue existing and future prostheses, and we have evaluated 17 existing prostheses according to this framework. From these results we could identify the categories most promising for further development. We found the category of prostheses that utilise elastic material behaviour to securely clasp around the incus to have the most potential in future designs.

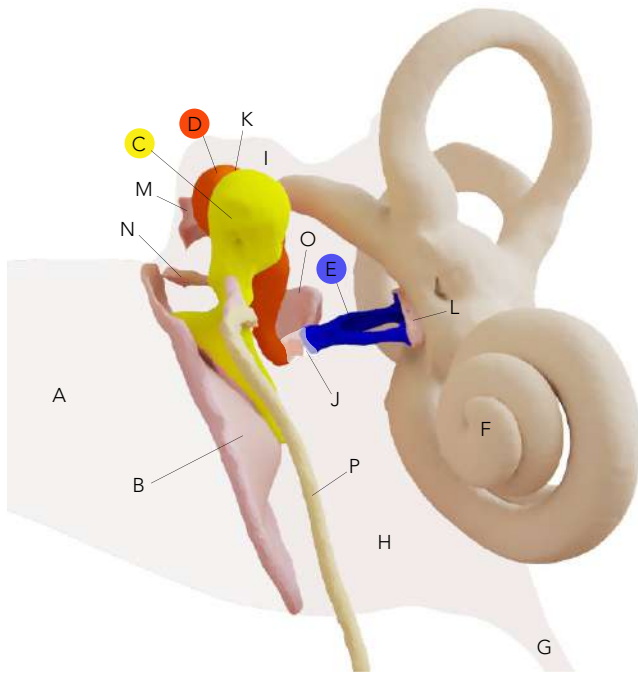
1 Introduction

Otosclerosis is a bone disease of the middle ear causing conductive hearing loss of the patient, and can be effectively treated through surgical implantation of a passive prosthesis. Although current solutions produce excellent hearing results for the patient, they are difficult to perform. The long-term success of the operation is highly sensitive to the skill of the operating surgeon [26]. In an affected patient, abnormal bone mineralisation leads to fixation of the ossicles, which impedes proper sound transfer from the eardrum through to the inner ear. The form of otosclerosis that concerns this paper is the fixation of the innermost ossicle, the stapes. The preferred surgical procedure for this instance of otosclerosis is called a stapedotomy, and involves the insertion of a prosthesis to replace the function of the stapes. What current prosthesis designs have in common is an ability to effectively transfer sound, however there is not yet an 'ideal' prosthesis [19] which can be inserted with confidence and ease.

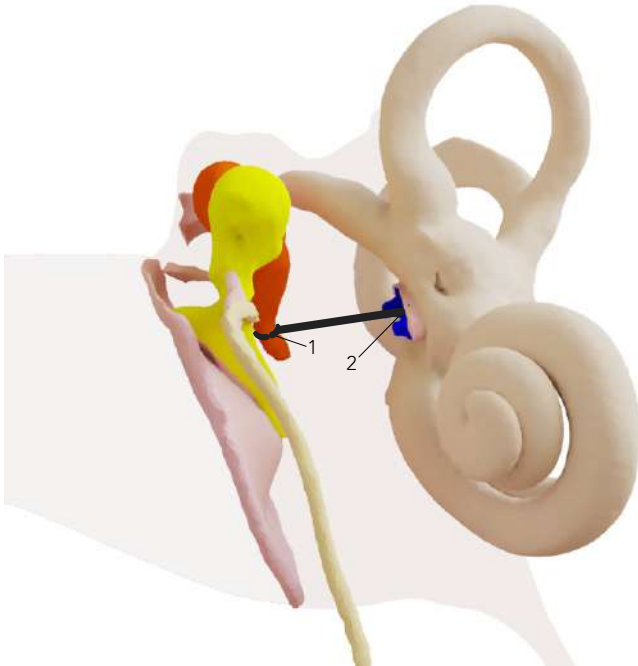
Since all prostheses examined are for a stapedotomy procedure, and are hence all piston-type prostheses, the focus of this study is on the varying attachment

methods to the incus. Most commonly, prosthesis attachment is achieved by forcing the prosthesis to plastically deform around the adjacent ossicle, the incus, via manual crimping. Crimping to the correct pressure without damaging the delicate bones, ligaments and nerves of the middle ear is a complex task, and either over-crimping or under-crimping will result in detrimental long-term effects to the patient's hearing. These effects are discussed in detail in Section 2. A second class of prostheses is those that attach to the incus via elastic deformation. These prostheses are typically in the form of clips which are pushed onto the long process of the incus, however this involves putting a high lateral force on the delicate ossicles. Several other approaches to the attachment of the prosthesis to the incus are described and evaluated later in this paper. Another issue with current prostheses is their failure to accommodate the tapered cylindrical geometry of the long process of the incus, resulting in a nonuniform pressure distribution around the incus. More research is therefore required to improve current prosthesis technology. In particular a simpler and safer method for attachment and better shape fitting to the varied geometries of the incus. The incus diameter varies considerably patient to patient, posing a challenge when designing a universal prosthesis [28].

The present investigation, through examination of state of the art prosthesis technology and relevant literature, sets up a classification system and list of requirements for current and future prosthesis designs. A set of existing prostheses and patent designs are organised into the proposed classification system and evaluated using the framework described in this paper. A foundation is made to provide a structured approach in generating and evaluating concepts for the next phase - design of an improved prosthesis. In Section 2 background information is given. In Section 3 the method is outlined. Results are presented in Section 4, and a discussion and conclusion are provided in Section 5 and 6.



(a) Anatomy of the normal middle ear. A: external auditory meatus, B: tympanic membrane, C: malleus, D: incus, E: stapes, F: bony canals which comprise the inner ear, G: eustachian tube, H: tympanic cavity proper, I: epitympanic recess, J: incudostapedial joint, K: incudomalleolar joint, L: annular ligament, M: posterior incudal ligament, N: lateral malleolar ligament, O: stapedius muscle and tendon, P: Chorda Tympani



(b) Diagram of an ear reconstructed via a stapedotomy. The stapes superstructure has been removed and replaced with a piston prosthesis. 1: attachment of prosthesis to incus process, 2: the piston end protrudes into the inner ear through a hole drilled into the stapes footplate

Figure 1: Diagrams of the healthy and reconstructed middle ear. Images adapted from the geometric data from De Greef *et al.* 2015

2 Background

This section provides fundamental background information. It is divided into three parts: firstly the mechanics of a healthy middle ear, including an outline of the basic anatomy and the dynamics of the system. The second part is the mechanics of the diseased middle

ear, which includes a description of conductive hearing loss, approaches of modelling otosclerosis and several methods to clinically test the degree of hearing loss. The final part discusses the mechanics of the reconstructed middle ear, where the steps of the stapedotomy procedure are given, and results and causes of failure are discussed.

2.1 Mechanics of the normal middle ear

2.1.1 Basic anatomy

The middle ear is an air-filled, mucosa-lined cavity, which houses three small bones; the malleus, incus and stapes, together referred to as the ossicular chain. These bones are attached to each other by synovial joints, and suspended from the walls of the middle ear cavity by a series of ligaments. The tympanic membrane (TM), commonly known as the eardrum, resides at the boundary between the outer and the middle ear. Two membrane windows, the round window and the oval window, form the boundary between the middle ear and the fluid-filled inner ear. The middle ear cavity is directly connected to the nasal cavity via the eustachian tube for two purposes: to control air pressure and to release fluid that is constantly produced in the middle ear. The eustachian tube is closed at rest, but can be opened briefly by swallowing or yawning. [12]

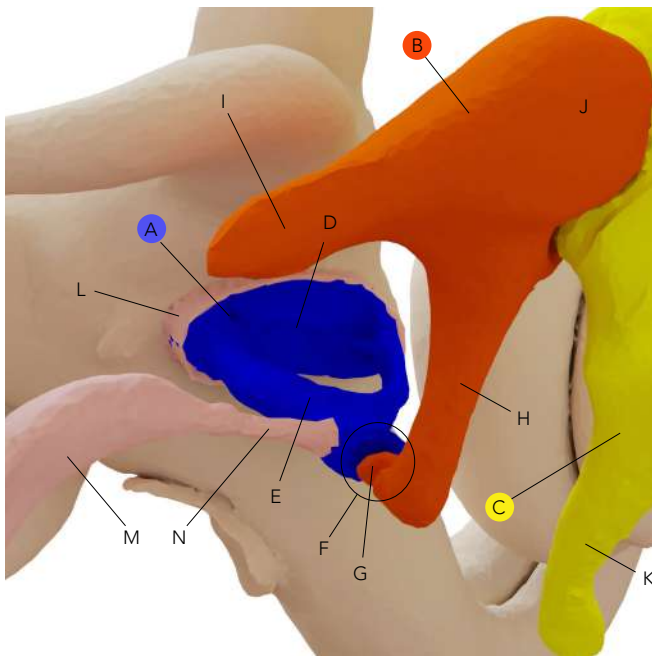
A branch of the facial nerve responsible for taste, the Chorda Tympani, travels through the middle ear. Though it performs no functional role in the ear, it is an important piece of anatomy to consider when designing for a stapedotomy. Special care must be taken not to damage it since doing so may lead to taste disruption or facial nerve paralysis [29]. Figure 1(a) and Figure 2(a) show anatomical diagrams of the healthy middle ear.

2.1.2 Dynamics

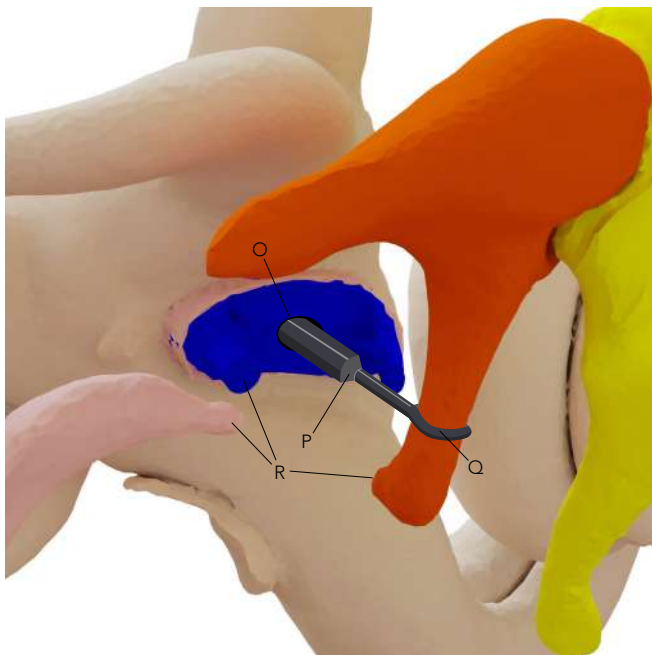
The ossicular chain essentially acts as an impedance matching mechanism. It transfers the vibrations of the tympanic membrane, caused by sound waves travelling through the external auditory meatus, to the fluid in the inner ear. Since the air in the external auditory canal has a far lower impedance compared to the fluids in the inner ear [13], a mechanism is required to minimise energy loss in the transfer of sound vibrations. Multiple attempts have been made to model the three dimensional vibrations of the ossicular chain, either through experimental analyses [24], finite element modelling [9] [45], or multibody models [21] [46] [13] [14] [16]. It is generally agreed that these motions are extremely complex, due especially to frequency dependent axes of rotation.

Helmholtz's lever model

In 1868 Helmholtz [21] proposed a model of the ossicular dynamics, which consisted of 3 independent levers. The first lever is the mechanical advantage provided by the TM (about 2:1), referred to as the catenary lever. The second lever, the ossicular lever, has the least significant mechanical advantage (around 1.3:1), and is produced by the rotation of the incus and malleus about a similar axis. Finally, Helmholtz refers to the force amplification resulting from the area ratio between the large TM and the small stapes footplate as the



(a) A: stapes, B: incus, C: malleus, D: stapes footplate, E: stapes superstructure, F: incudostapedial joint, G: lenticular process, H: long process of the incus, I: short process of the incus, J: incus body, K: manubrium, L: annular ligament, M: stapedius muscle, N: stapedius tendon



(b) Reconstructed middle ear details. O: hole drilled into the stapes footplate, P: piston shaft of prosthesis, Q: attachment of incus to prosthesis

Figure 2: Details of healthy and reconstructed middle ear. Images adapted from the geometric data from De Greef *et al.* 2015

'hydraulic lever'. This lever produces the most significant mechanical advantage, around 20.8:1. Each of these three amplification factors increase the sound pressure at the oval window, compared with the pressure at the tympanic membrane. The final pressure gain over the middle ear is found by multiplying the three mechanical advantages, and approximates to 35 dB:

$$\frac{P_{\text{oval}}}{P_{\text{TM}}} = 2.6 \times 20.8 = 54 \approx 35\text{dB}$$

Finite element modelling

Williams *et al.* investigated the mechanics of the middle ear through the development of finite element models [45]. They modelled the tympanic membrane and the ossicular chain separately, simplifying their respective geometries to a series of nodes in 3 dimensional space. The incudostapedial joint was simulated by adding joint elements at the tip of the incus. The stiffness of these elements were kept at a constant at 100N/mm in all 3 principal directions, since this configuration is known to result in realistic mode shapes. An analysis was carried out to characterise the effects of incudostapedial joint stiffness. The known configuration of 100N/mm in all 3 directions was in fact found to be optimal, with the nodes vibrating in phase and with maximum amplitude. Williams *et al.* determined the frequency response of the ear to be sensitive to the damping in the incudostapedial joint.

Experimental analysis

Huber *et al.* (1996) [24] attempted to gain further understanding of the 3-dimensional vibrations through *ex vivo* experimental analysis. In their experiments they used four human temporal bones, removed from the cadaver within 24 hours after death. The TM in each cadaver specimen was excited with a loudspeaker that was producing pure tones. They set up an optical system which consisted of 6 reflective balls attached via capillary force to each ossicle, forming the targets of a laser Doppler vibrometer. Only one-dimensional movement was recorded for each point, but they were arranged in such a way as to reveal the 3-dimensional movement of the ossicle. Huber *et al.* found results which indicate a complex spatial motion, consisting of both translational and rotational components that change with frequency. The malleus exhibited almost pure rotation around a fixed axis up to 1kHz and above 2 kHz. At low frequencies the incus rotated about the same axis of rotation as the malleus, though at higher frequencies a translational element was also present. Finally, their results indicate that the stapes vibrates in a piston-motion at low frequencies, however at higher frequencies this is combined with a rocking motion.

2.2 Mechanics of the diseased middle ear and conductive hearing loss

The function of the middle ear is to transfer the vibrations from the external ear to the fluid in the inner ear. In a patient with otosclerosis, conductive hearing loss arises due to abnormal mineralisation which, in one form of the disease, fixates the stapes ossicle. Due to this fixation the stapes-cochlear impedance, which comprises the impedance from the annular ligament and the impedance from the cochlea fluid, increases. As a result the amplification of the sound waves passing through to the inner ear is decreased [30]. Conductive hearing loss first occurs at low frequencies, and as the disease gets more severe higher frequencies will also become affected [41].

Huber *et al.* [23] used an existing, extensively tested, finite element model [44] to study the effects of stapedial fixation. They were able to simulate otosclerosis in the model by increasing the Young's Modulus of the stapes

annular ligament until a reduction of sound conduction by approximately 30dB at low frequencies occurred. They found that otosclerosis is expressed by taking the Young's modulus of the stapedial annular ligament to be 100 times larger than that of a normal subject.

Several methods exist to clinically test conductive hearing loss in a patient. These include the Weber test, the Rinne test and pure tone audiometry. The Weber and Rinne tests are tests which can be performed quickly and easily by a GP, with a tuning fork. Pure tone audiometry provides a more complete understanding of the conductive hearing loss of the patient, over a range of frequencies. Pure tone sounds at various frequencies are generated, and the patient determines at which sound intensities they can no longer detect this frequency. This type of test can detect whether the patient has conductive, sensorineural or mixed hearing loss.

2.3 Mechanics of the reconstructed middle ear

Rendered diagrams of a diseased middle ear post stapedotomy reconstruction are shown in Figure 1(b) and Figure 2(b).

Surgical procedure: Stapedotomy

Surgical treatment for otosclerosis was first introduced by Shea in 1956, when he successfully removed the fixated stapes of an otosclerosis patient and sealed the opening with a tissue graft, replacing the stapes superstructure with a Teflon prosthesis. This technique is called a stapedectomy. Nowadays the preferred method is instead a stapedotomy, where, rather than fully removing the footplate, a small hole is drilled into it for placement of the prosthesis.

To perform a stapedotomy the surgeon must first gain access to the middle ear without damaging the tympanic membrane. This is achieved by making an incision around the wall of the external auditory canal and pushing aside the TM. If the view of the ossicles is impaired then removal of temporal bone may be necessary. At this point there are two options in the surgical procedure: the stapes superstructure can either be removed before or after the prosthesis is placed. Removing afterwards is a safer but technically more challenging approach, since the prosthesis is in the way when removing the stapes superstructure. The approach of first removing the superstructure is described below.

The surgeon severs the synovial joint connection between the stapes and the incus, and removes the superstructure from the stapes footplate. The distance

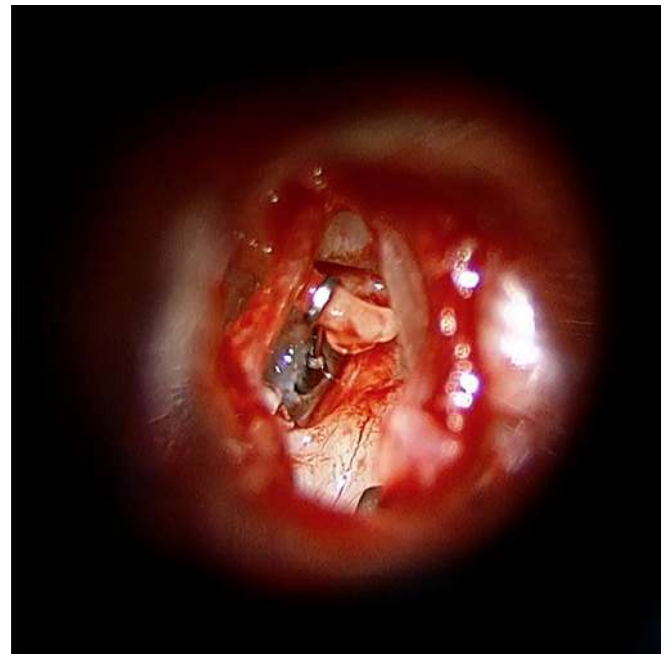


Figure 3: Micrograph of inserted prosthesis, taken during surgery

between the incus and the footplate is then measured, and the prosthesis is trimmed to the correct length if necessary. A small hole is drilled into the stapes footplate, and the rod-like end of the prosthesis is inserted into this hole, protruding slightly (no more than 0.75mm) into the inner ear fluid. The other end of the prosthesis must be secured to the next bone along in the ossicle chain, the incus. Depending on the design of the prosthesis this could involve placing a hook over the long process of the incus and manually crimping it in place, pushing an elastic clip over the incus or a variety of other methods. The surgeon probes the prosthesis-stapes connection to ensure that it is secure. Once the prosthesis is in place, the stapes superstructure is completely removed by cutting the stapedius muscle. The prosthesis can now perform the same piston movement as the original stapes structure, with its protrusion into the inner ear responsible for vibration transmission.

It is important to consider the environment that the surgeon is working in. The ear canal is approximately 25mm in length, with a diameter as small as 7mm [48]. The available space and field of view is hence extremely limited, and the entire surgery must be done under a microscope.

Cause of failure	Percentage of cases (n = 78)
Prosthesis displacement	45.5%
Incus erosion	32%
Fibrous tissue covering oval window	11.5%
Bony regrowth	10%
Fixation of incus and malleus	1%

Table 1: Results from Babighian et al.'s study of 78 revision stapedotomies [6]

Results of surgical intervention

Since first introduced by Shea in 1956, the treatment of stapes fixation by surgical intervention has proven to have excellent audiological results. Performed on patients with an air bone gap of at least 30dB, post-operative results show, in most cases, a closure of this air-bone gap to less than 10 dB. In large studies this success rate is about 95%, such as in Shea's 1998 study of 5444 cases [38] and the study of 3050 cases by Vincent *et al.* [43].

Causes of failure

According to Fisch [17], the most common cause of failure for a stapedotomy is the displacement of the prosthesis from the incus, likely caused by under-crimping. Under-crimping can also result in erosion of the incus, since micro gaps between the incus and prosthesis allow vibrations to wear at the bone, creating a localised erosion of bone tissue.

Another common complication of the stapedotomy which can be recognised in revision surgeries is necrosis of the long process of the incus, however the exact cause for this is disputed. Where some authors attribute it to over-crimping of the incus [45], [1], others [2], [3] argue the case that necrosis results from damage of the blood supply to the distal portion of the incus. During the operation, the incudostapedial joint is severed, disrupting the blood supply of the lenticular process through this joint. Also, it is hypothesised that over-crimping the prosthesis leads to strangulation of the mucosa lining of the lenticular process, and combined with the severing of the joint this results in an inadequate supply of nutrients to the distal portion of the incus.

I. Gerlinger *et al.* [18] studied the blood supply to the ossicles by reviewing literature and comparing with the authors' photodocumentation of 100 cadaver specimens. Through their observations they came to the conclusion that the supply of blood - through the incudal artery, the mucosa network on the surface, and the anastomoses between them - should be sufficient to supply the end of the incus. The exact cause for incus necrosis is an ongoing discussion and a satisfactory explanation that is widely agreed upon is yet to be found.

Other less common potential causes of failure include growth of fibrous adhesions, regrowth of otosclerotic bone over the footplate, or fixation of the malleus and incus. Table 1 shows the distribution of the causes of failure in Babighian *et al.*'s study of 78 revision stapedotomies between 1995 and 2005 [6].

3 Method

3.1 Classification system

In order to thoroughly evaluate all existing prosthesis designs and provide a framework to assess future concepts, a classification system is constructed along with a clear framework for concept evaluation. Two strategies of classifying the prostheses are combined to form a 2-dimensional array of solutions. These classification systems are (1) the working principle employed in the attachment of the prosthesis to the long process of the incus, and (2) the geometry of the coupling between the prosthesis and incus. The physics of attachment includes the five possible categories

listed below:

1. **Rigid multibody:** Multiple bodies move in respect to one another to form an attachment to the incus. The rigid bodies are connected via rigid body joints, such as pin, ball, slider, etc.
2. **Plastic deformation:** The prosthesis is coupled to the incus through a change of shape of the prosthesis which is *unrecoverable* upon removal of stress.
3. **Elastic deformation:** The prosthesis is coupled to the incus through a *recoverable* change of shape of the prosthesis.
4. **Thermally actuated shape memory:** The prosthesis is made partially or fully from a shape memory alloy (such as Nitinol) which, when heated with a laser, returns to a predetermined shape. The coupling of the prosthesis to the incus is a result of this heat-activated transformation.
5. **Combination:** Two or more of the first four options are used in combination to achieve the coupling between the prosthesis and the incus.

The second classification, a spatial property which can be viewed in a number of ways, refers to the size and geometry of the connection between the prosthesis and the incus. One approach would be to classify according to the degree of circulation ψ ($0 < \psi \leq p \cdot 2\pi$) around the long process of the incus, where $p > 1$ when the prosthesis makes more than one complete circulation of the incus. A second approach would be to consider the number, n , of contact points between the incus and the prosthesis. Finally, the width of the circulation: a wire around the incus would form a line of contact, whereas a band could in theory form a solid rectangle with a certain width. However in practice, due to the tapered cylindrical geometry of the incus, a prosthesis that is designed as a band may perform the same as a wire if it cannot conform to the geometry of the incus.

Since the dimensions of the prostheses were often not published in literature, it was decided that the number of contact points, n , would be the focus of the second method of classification. This choice also most clearly distinguishes between current prosthesis designs. The width of the circulation is also included in the classification system as a binary class: either 'line' or 'band'. Thus a table can be constructed with columns corresponding to the first system of classification, the working principle describing prosthesis-incus connection, and rows corresponding to the second classification system.

3.2 Desired properties and requirements

This section contains definitions of the prosthesis properties used to form evaluations. The following section, Section 3.3, provides a quantitative framework to assess each of these properties in a particular prosthesis.

Pressure controllability

An important factor in the success of stapedotomy surgery is how tightly the prosthesis is secured to the

incus. If it is too loose, displacement of the prosthesis along the long process of the incus could occur. Erosion of the incus is also a risk of under-tightening, due to repeated collisions between prosthesis and incus with ossicular vibrations, causing wear in an isolated location on the incus. On the other hand, over-tightening is speculated to cause necrosis of the incus, though the precise reasons for this are under debate.

Pressure controllability refers to the confidence the surgeon can have that the pressure around the incus bone by the secured prosthesis is within an appropriate range. Poor pressure controllability is found in prosthesis designs where the level of pressure around the incus is determined solely by the surgeon, and testing whether the pressure is in the correct range is done by probing the incus and applying intuition. Pressure controllability is adequate when, assuming the incus diameter is known, the pressure exerted on the incus can be accurately determined. The actions of the surgeon do not play a part. Excellent pressure controllability is a property of a constant force mechanism. Regardless of the diameter of the incus (within a realistic range), the pressure exerted on the incus bone is always known.

Ease of implantation

Ease of implantation refers to the ease at which the surgeon can place the device in the patient's middle ear. Factors to consider include how often the surgeon is required to change tools, how dangerous the required steps are in terms of damaging middle ear anatomy, and finally how reliant the success of the surgery is on the skill of the surgeon. Implantation of current prostheses is currently very difficult to master [27].

Shape adaptability to the incus

The long process of the incus approximates a tapered cylinder: wider near the connection to the incus body, and narrowing towards the end. As well as this diameter variation along a single incus, incus diameters also vary greatly patient to patient, ranging from about 0.52-1.15mm [42]. The property *shape adaptability* refers to two criteria. Firstly, the prosthesis design should be able to accommodate the tapered cylinder geometry. Many prostheses have a flat band design, with the intention of increasing the area of contact between the prosthesis and the incus. In most cases the band will not lie flat on the incus for its entire circumference, but will make a line of contact with the incus at the side of greatest incus diameter. It is possible that torsion will occur, causing the band to lie flat on the incus in some parts, however this still results in less contact than is intended by the band design. The second criteria refers to the ability of one size of prosthesis to fit a large range of incus diameters.

ABG difference

Air-bone gap (ABG) is an audiometric property that is commonly measured pre and post-operatively to determine the success of the operation. Surgical intervention should of course improve the hearing of the patient, hence this property is considered a requirement.

Prosthesis size

The middle ear is a cavity in the human temporal bone with limited available space, which is made even more restricted by the small field of view accessed by the surgeon. A prosthesis must conform to these restrictions in both the operative and post-operative phase. A prosthesis that is too big to fit at all is unacceptable, hence the size property is classified as a requirement. The preference is a small prosthesis that can be inserted with ease, with minimum risk of interfering with the Chorda Tympani. Figure 4 is a diagram of the proposed method of sizing each prosthesis, where D is taken as the maximum diameter of the prosthesis, centered around the midpoint of the lenticular process.

Mass

Bance *et al.* conducted a study in 2007 [7] to determine the effect of varying prosthesis mass on audiological results. They came to the conclusion that a lighter mass prosthesis may be preferred, since there is no drop in lower frequencies from lower masses, whereas they did observe a drop in higher frequencies with higher masses.

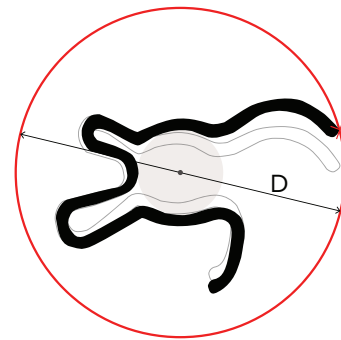


Figure 4: Guideline for size comparison

In their study, statistically significant effects were only observed above 4 kHz. The mass of the prosthesis is therefore a property of comparatively little importance, and thus should be weighted accordingly.

To give some indication of the mass ranges, the masses used in the experiments of M. Bance *et al.* are included in the evaluation shown in Table 2.

Biocompatibility

Biocompatibility is the capacity of a material to exist harmoniously within a living system, without triggering immune reactions or causing toxic harm to the body [31]. The minimising of reactions with the body results from the growth of a protective layer on the surface of the material, which stops ion flow to some degree. Some biocompatible materials include:

- **Metal:** stainless steel, Nitinol, gold alloys, platinum
- **Ceramics:** Alumina, Zirconia, calcium phosphates, porcelain, carbons

Property	Units	Requirement/ Wish	+	0	-
Pressure controllability	Pa	Wish	Post-operative distributed force around incus is known, and is constant for differing incus diameters (constant force mechanism)	Post-operative distributed force around incus is known, given particular incus diameter.	Post-operative pressure on incus is unknown. Falling within acceptable range depends entirely on the surgeon's intuition.
Ease of implantation by surgeon	*	Wish	Simple implantation. Success does not rely completely on the experience of the surgeon.	Moderately difficult operation, as judged by experienced surgeons.	Technically difficult operation, as judged by experienced surgeons. There exists a steep learning curve to master the operation.
Adaptability to the incus	*	Wish	Prosthesis adapts to the tapered geometry of the incus AND Prosthesis can accommodate 95% of incus diameters	Prosthesis adapts to the tapered geometry of the incus OR Prosthesis can accommodate 95% of incus diameters	NEITHER Prosthesis adapts to the tapered geometry of the incus NOR Prosthesis can accommodate 95% of incus diameters
Mass	mg	Wish	$M \leq 20$	$20 < M \leq 30$	$M > 30$
ABG difference	dB	Requirement	$0 < ABG \leq 10$	$10 < ABG \leq 20$	$ABG > 20$
Size	mm	Requirement	Compact design. $D \leq 1.5$	Bulky design, but still fits in middle ear. $D > 1.5$	Dimensions exceed that of the middle ear.
Biocompatibility	*	Requirement	Biocompatible AND CT scannable	Biocompatible BUT Can't be in CT scan	Not biocompatible

Table 2: Guide for evaluating solutions in respect to the desired properties

• **Polymers:** polyethylene, PTFE, polyurethanes, PVC, PMMA, silicones

(not essential, but should be strived towards when designing the ideal prosthesis).

A more comprehensive overview of biocompatible materials can be found in the ASM Handbook of Materials for Medical Devices [4]. Using biocompatible materials in the design of an ossicular prosthesis is crucial in ensuring the prosthesis will not be rejected by the body. This property is classified as a requirement.

3.3 Evaluation of concepts

In Table 2, guidelines are given to evaluate the six properties described in the previous section. For any given prosthesis, each property can be evaluated as one of three grades: '+' (good), '0' (has potential - the prosthesis possesses this property to an extent, but can be improved) and '-' (not achievable with this concept). Each property is classified as either a *requirement* (it is imperative that the device has this property) or a *wish*

4 Results

17 existing solutions are sorted and assessed according to the framework outlined in Section 3. On top of this, 6 prosthesis patents are placed in the classification system and evaluated qualitatively where possible. This section also includes an overview of the material properties for the different materials used in existing prostheses.

4.1 Prostheses descriptions

The seventeen different prostheses which were gathered from company catalogues are shown in Figure 5, labelled from (a)-(q), and the descriptions for each prosthesis are given below. Figure 6 shows drawings of six patented designs, labelled (1)-(6).



Figure 5: 17 state of the art stapes prostheses

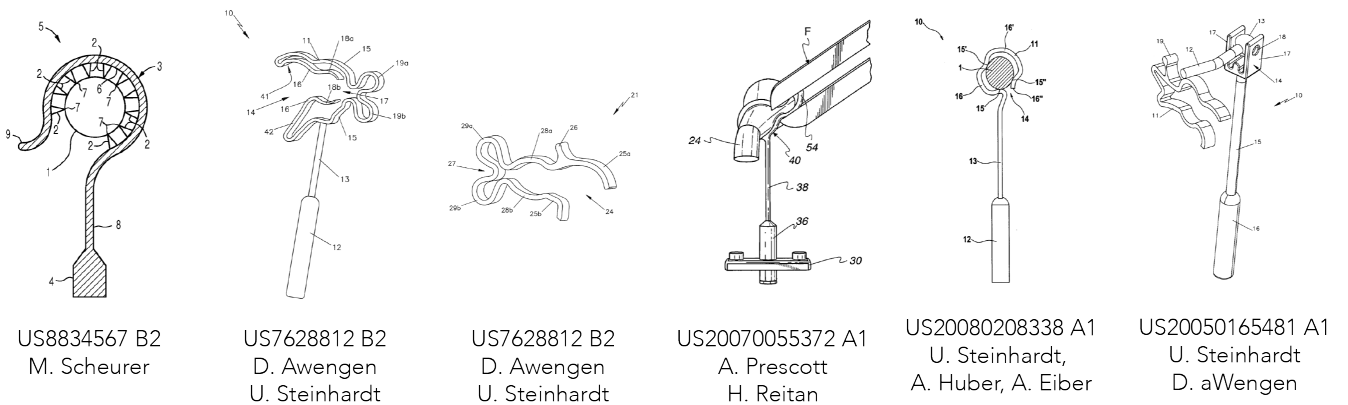


Figure 6: 6 patent designs for stapes prostheses

(a) Causse Teflon piston

Material: *Teflon*

Teflon pistons were an early but popular choice for surgeons performing stapedotomy or stapedectomy procedures. The entire piston is made from a single polymer material, Teflon (brand name for the chemical compound polytetrafluoroethylene). Teflon is completely inert, so does not react with surrounding tissue. The loop end of the prosthesis is opened up and placed over the long process of the incus. Due to the material memory, the loop deforms back to its original shape, forming a secure connection with the incus. Gentle crimping may be done to assist the deformation.

(b) Causse Gold piston

Material: *Gold*

Gold was introduced as a possible prosthesis material in the 1990s. As with Teflon, the gold does not react with tissue. The main difference between Teflon and gold prostheses is the higher mass and higher ductility of the latter, as well as the differing techniques in attaching to the incus. The gold K-piston is placed over the LPI, and secured by using alligator forceps to manually crimp the loop. The straight extension of the loop is designed to ease the crimping process. Due to its higher ductility, less force is required to crimp the gold prosthesis closed around the incus. This prosthesis has a circular cross section (wire type), therefore the circumferential force is concentrated in a line around the incus.

(c) Richards Platinum Fluoroplastic

Material: *Teflon, Platinum*

Richards Platinum Fluoroplastic piston is a nonmonolithic prosthesis made from a composite of Teflon piston and platinum hook. The hook is attached to the incus via manual crimping - the same method as described above for the Causse Gold piston.

(d) Olympus Mangham Piston

Material: *Teflon, Platinum*

The Mangham piston is a nonmonolithic prosthesis comprised of a platinum double-fold hook which requires manual crimping, and a Teflon piston. A depth gauge on the piston functions to verify that the correct length of piston is protruding into the inner ear.

(e) Grace Medical Eclipse

Material: *Teflon, Nitinol*

The eclipse piston is a nonmonolithic design, made partially from Teflon (the piston) and a shape memory alloy, Nitinol (the hook attachment to the incus). The shape memory behaviour does not occur along the entire hook, but in one local area. This prosthesis is a wire-type piston, and fully encloses the incus over the entire circumference.

(f) Olympus SMart 360° Piston

Material: *Teflon, Nitinol*

The SMart 360° Piston is made from Nitinol, a shape memory alloy that returns to its original position when heated. In the stapedotomy surgery the hook is placed loosely, and is made to enclose around the incus by

directing a laser beam at the prosthesis, heating the hook and activating shape memory. The danger in this technique is the potential for excessive heating of the ossicles themselves, risking necrosis or damage to the blood supply.

(g) Grace Medical Megerian Nitinol

Material: *Teflon, Nitinol*

The Megerian piston is another thermally actuated shape memory prosthesis, comprising six tapered arms which enclose the incus. The additional arms aim to increase the stability of the connection, and can accommodate the tapered cylinder geometry of the lenticular process. The attachment section is made from one flat piece of Nitinol, which is cut and bent to shape. This Nitinol structure is secured to a Teflon piston which protrudes into the inner ear.

(h) KURZ Bucket

Material: *Titanium*

The KURZ bucket prosthesis is a standard bucket-type prosthesis. It is classified as 'multibody' since it comprises rigid bodies which interact via pin joints. Bucket type stapes prostheses use an alternative method to attach to the incus. To insert, the surgeon positions the prosthesis so that the lenticular process is sitting in the bucket. The wire is then rotated up and over the bone, and, if necessary, is crimped around the incus to increase stability.

(i) Bartels Bucket

Material: *Titanium*

The Bartels Bucket design uses the same working principle as the KURZ Bucket described above, however it features an adjustable diameter. Three tabs surrounding the distal lenticular process can be plastically deformed to provide a tighter fit. Since this design uses plastic deformation as well multiple bodies connected with kinematic joints, it is classified as a 'combination' type using the system proposed in this paper.

(j) KURZ K-Piston

Material: *Titanium*

The KURZ K-piston functions in exactly the same way as the Causse Gold piston (b) and the Richards Platinum Fluoroplastic piston (c), however it is made from one material: titanium. Titanium is more lightweight compared to the materials used in (b) and (c) (gold and platinum respectively). Furthermore, titanium is highly MRI compatible, and exhibits improved biocompatibility.

(k) KURZ Skarzynski Piston

Material: *Titanium*

The Skarzynski piston is a slim, lightweight prosthesis, which requires manual crimping to secure to the incus. The entire structure is made of pure titanium, which has low mass and high rigidity. The minimal design of the prosthesis is intended to enable a clear intraoperative view.

(l) KURZ Matrix

Material: *Titanium*

The KURZ Matrix piston uses the same working principle at the K-piston. In the Matrix design, perforations have been introduced over the wide band loop with the intention to increase malleability and ease the crimping process.

(m) KURZ Angular Piston

Material: *Titanium*

The KURZ angular piston is designed for use in revision surgery, when the incus has eroded to an extent that coupling with conventional prostheses is not practical. The surgeon must manually crimp the two titanium bands onto the eroded lenticular process.

(n) KURZ CliP Piston aWengen

Material: *Titanium*

The KURZ aWengen prosthesis, designed by Daniel à Wengen and first implanted in 2000, was the first in a series of 'clip' type prostheses that utilise elastic deformation to secure to the incus, as opposed to plastic deformation in traditional crimping designs. To form the attachment the surgeon must push the clip over the lenticular process. The stiffness in the clip, and the diameter of the incus, determines the circumferential pressure. Once pushed onto the incus, the pressure is completely independent of the surgeon's intuition, and can be accurately determined if the incus diameter is known.

Unlike traditional crimping style prostheses [(b), (c), (d), (j), (k), (l)], the aWengen CliP does not completely encircle the lenticular process, but rather clamps onto the process via contact at two separated sections. This design choice is to minimise the possibility of mucosa strangulation - a hypothesised cause of incus necrosis. This prosthesis is monolithic and made entirely from titanium, which is a light, biocompatible and low MRI risk material.

(o) KURZ Soft CliP

Material: *Titanium*

The KURZ Soft CliP is a further development of the aWengen prosthesis, and is based on the same working principle. This new prosthesis is designed to apply a force on the incus that is 40% less than its predecessor [8]. The design is also more compact, virtually eliminating the spatial problems found with the slightly bulkier aWengen CliP [20]. As with the aWengen CliP, the Soft CliP does not fully encircle the lenticular process, but contacts only about 60% of the circumference to protect the vascular supply.

(p) KURZ Nitiflex

Material: *Titanium, Nitinol*

Nitiflex is the next generation in clip type prostheses, following from the KURZ Soft CliP described above. In this design, the clip is no longer made from titanium but from Nitinol, an alloy of titanium and nickel with superelastic properties. The combination of using Nitinol instead of titanium, the reduction in thickness by 50%, and a slightly different geometry, results in a

greatly reduced application force on the long process of the incus. Where the Soft CliP applied 200 mN, Nitiflex applies only 50 mN [32].

(q) KURZ Nitibond

Material: *Titanium, Nitinol*

The Nitibond prosthesis is comprised of a titanium piston which protrudes into the inner ear, and a Nitinol loop which closes around the incus as the surgeon heats it with a laser. The unique shape of the Nitinol loop is designed so that the locations where the surgeon directs the laser are not in direct contact with the incus, hence minimising risk of tissue damage from over-heating. Another purpose of the unique loop shape is so that the incus and the prosthesis are coupled via four contact points, which can conform to the irregular geometry of the incus. The loop is designed to fit most lenticular processes, regardless of the diameter or presence of irregularities.

The prosthesis comes with a thermo dummy, with the purpose of calibrating the laser intensity so that risk of tissue damage is minimised.

Patents

As well as the 17 existing prosthesis designs which have been described above, six design patents are also included in this study. They are briefly described below:

- 1. Middle ear prosthesis having discrete projections for purposes of ossicular attachment** [36]: This prosthesis is designed under the hypothesis that necrosis results from impaired blood supply to the distal portion of the incus. Instead of complete circulation of the incus, the prosthesis attaches via a series of discrete projections. The idea is to minimise the contact area between the prosthesis and the incus, while maintaining a secure connection.
- 2, 3. Ossicle prosthesis** [5]: Two alternative designs for a clip-type prosthesis.
- 4. Crimp assist middle ear prosthesis** [33]: This patent details a proposed improvement for crimping-type prostheses. Instead of applying the crimping force directly to the lenticular process, the surgeon instead crimps a 'crimp-assist' portion which extends outside the circle.
- 5. Auditory ossicle prosthesis** [40]: A modification of the typical crimp-type prosthesis, where at least three sections of the loop do not come in contact with the incus.
- 6. Ossicular replacement prosthesis** [39]: This design consists of an elastic clip to secure to the incus, and a hinged connection between the piston and the clip. According to the inventors, the lever ratios in this prosthesis are greatly improved since the transmission mimics anatomical conditions, leading to better audiological results.

4.2 Materials

The material properties for the materials used in the set of prostheses examined in this study are shown in

Material		Young's Modulus (GPa)	Yield strength (MPa)	Poisson's ratio	Density (g/cm ³)
Titanium		116	880	0.32	4.506
Nitinol	Austenite	83	195-690	0.33	6.45
	Martensite	28-41	70-140		
Gold		79		0.4	19.30
Teflon		0.55	0.862 - 41.4	0.46	2.16
Platinum		168	35-180	0.38	21.45

Table 3: Material properties for materials used in current prostheses

Table 3. Aside from Teflon, all other materials are metals. The metals used in older prostheses (gold, platinum) are about four times heavier than the more recently adopted titanium and Nitinol. From the Young's Modulus data it is evident that platinum is the stiffest choice of material, and thus would require more force to be crimped onto the incus if it were used in a *plastic deformation* category of prostheses.

Nitinol is the newest material to be used in stapes prostheses, and its special properties make it an appealing choice in the design of improved prostheses. Nitinol has two unique properties, namely it is a shape memory alloy, and it exhibits superelasticity. The first effect is utilised in the thermally actuated prostheses, where a laser is used to heat the prosthesis so that it returns to its original position. The second unique property, superelasticity, is used in the KURZ Nitiflex. The choice of Nitinol for the clip greatly reduces the force required to push the prosthesis onto the stapes, and increases the maximum incus diameter that it can attach to.

4.3 Classification and evaluation of state of the art

The set of 17 existing prostheses and 6 patented designs are organised into the classification system described in Section 3.1, and categories of the system that contain an existing prosthesis are evaluated according to the criteria outlined in Section 3.3.

A graphic summary of the resulting classifications and evaluations is given in Table 4. In this table the columns indicate the first category of classifications: working principle of attachment, and the rows indicate the geometry of the connection. Each box is a unique class, which contains all of the prostheses (existing or patented) of that class. Empty boxes indicate classes where no prosthesis designs could be found. For each occupied class, an evaluation has been conducted in general, taking into consideration the performance of prostheses occupying that category. Only categories that contain an existing prosthesis are textually evaluated, since it is only in these cases where data exists and can be assessed. Categories containing only patents are assessed where qualitatively possible, with property evaluations left blank when real data is required (see Table 4).

The axes of Table 4 are labeled so that each classification subsystem can be indexed. For example,

the Causse Teflon Piston prosthesis (a) is located in *E1* - the class of prostheses which use elastic deformation as a working principle, and fully encircle the lenticular process. Below are the textual evaluations of each occupied class. Properties described in Section 3.2 are ranked as either Grade 1 (+), Grade 2 (0) or Grade 3 (-), according to the guidelines given in Section 3.3. The permutation of the properties can be seen in the bottom right of Table 4, and results of evaluating these properties are shown for each category.

P0 & P1

Under the classification *plastic deformation*, two classes are filled with existing prosthesis designs: P0 and P1. P1 in particular is a class with a large amount of variations, likely due to the popularity of these crimping style prostheses. Prostheses in these two categories perform poorly in terms of pressure controllability. In each of these designs, the surgeon manually crimps the loop over the incus using a tool such as alligator forceps. There is no precise way of knowing what force the prosthesis is applying to the incus after crimping, thus the success of the operation depends heavily on the surgeon's skill and intuition. Following the evaluation guidelines in Table 2, P0 and P1 clearly fall under class 3 for the property *pressure controllability*.

Crimping is considered to be the most problematic step in stapedotomy surgery, and it is very difficult to master the technique [27]. Both P0 and P1 rely on crimping, and therefore are evaluated as Grade 3 for the property *ease of implantation*.

An advantage of the prostheses classed as P0 and P1 is their ability to adapt to a range of incus diameters. Depending on the diameter of the lenticular process, the surgeon is able to apply more or less deformation.

A. J. G. De Buijn *et al.* [10] conducted a retrospective study of the Causse gold piston (P1), analysing audiometric results of 65 patients before and after implantation. Frequencies of 0.5kHz, 1kHz, 2kHz and 4kHz were tested in each audiometric analysis. In about 80% of all patients, the patient's air-bone gap was closed to less than 10dB. An equivalent study [47] was conducted for the KURZ K-Piston, by the same A. J. G. De Buijn, C. Zuur, and another group of colleagues. This study also showed excellent air-bone gap closure (less than 10dB for 79% of cases). S. Rösch *et al.* studied the audiometric results of the KURZ Matrix prosthesis

[35], and K. Huttenbrink *et al.* [25] studied the results of implanting the KURZ Angular Piston. Each of these studies conclude excellent air-bone gap closure, thus the classification categories P1 and P0 have their ABG property evaluated as Grade 1.

Another advantage of the P0 and P1 classes of prostheses is their relatively small size and low mass. According to the size definition in Section 3.2, these prostheses easily fall into Grade 1 for the size property. Although the prosthesis in P0 is larger, this prosthesis is used in the case of excessive incus erosion, hence is replacing more bone mass than other designs.

The masses of the P1 prostheses do differ due to varying materials, however even the heaviest - the Causse Gold Piston - weighs only 10 mg [10].

T0 & T1

Although the problematic manual crimping seen in categories P0 and P1 is not needed in classes T0 and T1, the surgeon must direct a laser at the thin band of the prosthesis, which adds complexity to the operation. Hence these categories also have poor (Grade 3) *ease of implantation*. Furthermore, the point of heating is in direct contact with the lenticular process, risking excessive heating of the tissue through conduction.

In terms of shape adaptability to the incus, category T0 scores higher than T1. The prostheses in T0 were able, to some extent, to adapt to the tapered geometry of the lenticular process. Both categories are able to accommodate a range of diameters.

T4

Evaluations for T4 are similar to T0 and T1. The problem of overheating the incus has been considered, and an attempt to minimise heat conduction to the bone tissue is done by including 'non-contact zones' where the prosthesis is elevated from the incus. At these zones, the prosthesis can be thermally actuated with less risk of overheating the tissue. T4 is adaptable to varying diameters of the lenticular process, however does not accommodate the tapered geometry as seen in category T0.

C. Roosli and A. M. Huber determined the closure of the air-bone gap to be successful, with tests done up to 12 months post-operatively [34]. Since this prosthesis design is relatively new, more long-term studies are still required.

E2 & E3

Classes E2 and E3 contain the new 'clip' style prostheses, which utilise elastic deformation to attach to the incus. An advantage of this type of prosthesis is their pressure controllability, since for a known diameter the contact force can always be determined. The method of application by the surgeon has no effect on the final pressure around the incus. It is also conceivable that a prosthesis could be designed within this category that applies a constant force on the incus, regardless of incus diameter. The Soft CliP prosthesis (o) in class E3 is a step towards this idea of constant force, since its particular shape was designed to minimise the variation in contact force for different cross sections [22]. Though

none of these prostheses adapt to the tapered geometry of the lenticular process, they are able to accommodate a large range of diameters. The Soft CliP prosthesis can fit on incuses ranging between 0.52 and 1.15mm in diameter [14]. G. Schimanski and A. Eiber [37] measured the incus diameter in 100 cases, and found that they ranged between 0.5 and 1mm.

The major downside of this style of prostheses, considering the existing prostheses, is the difficulty of implantation. During insertion, a high lateral force is applied to the incus, risking the integrity of the delicate ossicular chain. Another disadvantage is the relative bulkiness of the current designs. The diameter, D , of each device (from the definition of D in Figure 4) is approximately 2-3 times larger than the incus diameter in each device within classes E2 and E3. Though it fits within the middle ear cavity once inserted, the bulkiness increases the difficulty of insertion.

Studies of the acoustic properties of these classes of prostheses show satisfactory results. A. Hornung *et al.* [22] measured pre and post-operative air bone gaps for the insertion of aWengen (n) and Soft CliP (o) prostheses, for frequencies 0.5kHz, 1kHz, 2kHz, and 3kHz. They found that each prosthesis resulted in air bone gaps less than 10 dB, with no statistically significant difference between the two.

All prostheses within classes E2 and E3 are made from titanium or Nitinol - both biocompatible, lightweight materials.

M1 & C1

M1 and C1 both currently only contain bucket style prostheses. Bucket prostheses are a popular choice due to the fact that crimping is not usually required, however in some cases crimping may be necessary to provide extra security. The difference between the prosthesis in category M1 and the prosthesis in C1 is the adaptability of the bucket diameter for the C1 prosthesis. This addition of plastically deformable tabs allows it to accommodate a greater range of incus diameters. In both cases, however, the pressure is not controllable. There is a risk that the prosthesis will be too loosely secured to the incus, resulting in erosion or displacement.

Farrior and Temple compared the post-operative air-bone gaps for 82 surgeries where either a classic Teflon-wire prosthesis or the KURZ bucket prosthesis was inserted [15]. They found no statistical difference between the two.

E1

The only prosthesis contained in the E1 class is the Teflon prosthesis, introduced in the early 60s [41]. After the prosthesis is deformed and placed around the incus, it tries to deform back to its original shape due to the biocompatible memory of the material. The difference in behaviour between this Teflon prosthesis and the titanium/Nitinol prostheses found in categories E2 and E3 is the rate that the material returns to its original position. The pressure controllability for category E1 is also rated as grade 2 (0) since the prosthesis is always trying to return to the same shape, however differing incus diameters will change the final circumferential

Index	Connection type	M Multibody	P Plastic	E Elastic	T Thermal	C Combination
0			 7		 11	
1	n = 1 	 4	 5	 11	 9	 6
2	n = 2 			 7		
3	n = 3 		 7	 7		 8
4	n > 3 		 7		 9	

Pressure controllability	
Ease of implantation	
Shape adaptability to LPI	
Mass	
ABG difference	
Size	
Biocompatibility	

Table 4: Results of classification system for range of current prostheses

pressure.

There are three significant differences between this prosthesis and the prostheses in categories E2 and E3: shape adaptability, size and mass. It should be noted, however, that these differences are more likely due to the difference in material rather than the differences between the categories, so these observations should be considered with some caution. Due to its elasticity, the Teflon prosthesis is able to more effectively cater

to the tapered geometry of the incus. In terms of size, where the E2 and E3 prostheses were relatively bulky, the Teflon prosthesis fits within the first grade (+) according to the framework in Table 2. The mass of the Teflon prosthesis is about 3mg, which is approximately the same mass as an average stapes.

Durko *et al.* [11] studied the pre and post-operative air-bone gaps of 160 surgeries for frequencies 0.5 kHz, 1 kHz and 2 kHz, and found that in 81.3% of the cases the

Requirement	Factor	M1	P0	P1	E1	E2	E3	T0	T1	T4	C1
Pressure controllability	4	-1	-1	-1	0	0	0	0	0	0	-1
Ease of implantation	4	-1	-1	-1	-1	-1	-1	-1	-1	-1	-1
Shape adaptability	2	0	1	0	1	0	0	1	0	0	1
Mass	1	0	1	1	1	1	1	1	1	1	0
ABG difference	5	1	1	1	1	1	1	1	1	1	1
Size	2	1	1	1	1	0	0	1	1	1	1
Biocompatibility	5	1	1	1	1	1	1	1	1	1	1
Total		4	7	5	11	7	7	11	9	9	6

Table 5: Total scores for each prosthesis category, with weighted requirements

Category	M1	P0	P1	E1	E2	E3	T0	T1	T4	C1
Raw total scores	4	7	5	△ 11	7	7	△ 11	9	9	6
Improved requirement	Improved total scores									
Pressure controllability	10	7	5	▲ 15	△ 11	△ 11	△ 11	9	9	▲ 12
Ease of implementation	6	7	5	▲ 15	△ 11	△ 11	△ 11	9	9	8
Shape adaptability	6	7	7	△ 11	9	9	△ 11	△ 11	△ 11	6
Pressure + ease of implementation	▲ 14	7	5	▲ 19	▲ 15	▲ 15	△ 11	9	9	▲ 16
Pressure + shape adaptability	▲ 14	7	7	▲ 15	▲ 13	▲ 13	△ 11	△ 11	△ 11	▲ 14
Ease of implementation + shape adaptability	10	7	7	▲ 15	▲ 13	▲ 13	△ 11	△ 11	△ 11	10
Pressure controllability + ease of implementation + shape adaptability	▲ 18	7	7	▲ 19	▲ 17	▲ 17	△ 11	△ 11	△ 11	▲ 18

Table 6: Possible improved total scores for each prosthesis category. Yellow (unfilled triangle) indicate scores equal to the current high score of 11, green (solid triangle) indicate the scores higher than 11.

post-operative air-bone gap was less than 15 dB. They found no statistical difference between this prosthesis and platinum wire prostheses.

5 Discussion

In Section 4, evaluations for each requirement were made of all prosthesis categories that currently contain an existing prosthesis. In this section these evaluations are discussed, specifically in terms of their implications for the design of a new prosthesis.

5.1 Weighting factors and total scores

Table 5 details the method of obtaining total scores for each of the prosthesis categories. Each requirement/wish is given a weighting factor to control their relative influence on the scores. These factors are in the range 1-5; 1 assigned to the requirement(s) of least importance, and

5 assigned to the requirement(s) of greatest importance. These factor assignments are not completely repeatable, since somebody else making the evaluation may not necessarily assign the same importance to each requirement. The weighting factors given in Table 5 are in one possible permutation, evaluated by the author. The total score for each prosthesis category is the sum of the weighted requirement evaluations, which are evaluated as -1, 0 or 1 in Section 4.

As can be seen in Table 8, the highest scoring prosthesis categories are the thermally actuated mechanisms. The categories with the highest total score of 11 are E1 and T0. Another observation which can be made on the total scores is that in each working principle classification with a zeroth row, the zeroth row (i.e. P0, T0) always scores higher than any subsequent rows. In each case this is due to better shape adaptability.

5.2 Improvability

The total scores are based on the evaluations of prostheses that already exist, and are not the absolute limit for prostheses in that category. In some cases it is conceivable that the category score can be improved, through the design of a new prosthesis that addresses current limitations. *Pressure controllability*, for example, is a requirement that every category scores either 0 or -1. For a prosthesis to be given a score of 1 for *pressure controllability*, according to the evaluation framework in Section 3.3, the post-operative distributed force around the incus should be a known constant for differing incus diameters. Constant force mechanisms are a class of mechanisms which give a constant output force over a required range of motion, and can either be a rigid body mechanism with springs, or a compliant mechanism. The only categories that appear to have the potential to score a 1 for *pressure controllability* are *multibody*, *elastic* and *combination*.

Since rigid body mechanisms would require either torsional or linear springs to function as a constant force mechanism, it would be advantageous to instead design a constant force compliant mechanism (*elastic*) which could be a monolithic design. If the pressure controllability score for the elastic categories E2 and E3 was increased to 1, then their total score would be equivalent to the highest score of 11. Similarly, if just the ease of implantation could be increased to 0, then the total score could equal 11. Combining these two improvements would result in a total score of 15, which is higher than any current scores. Shape adaptability is another requirement evaluation which has the potential to be improved in the elastic categories, further increasing the total score.

Although the *thermal* categories appear to have the highest total scores, they are limited in how much they can be improved. Since they cannot be made into constant force mechanisms, *pressure controllability* cannot exceed 0. Also, their low score for *ease of implementation* is due to the fact that a laser is used to heat the implant and return it to a predefined shape. The need to heat the prosthesis is intrinsic to the thermal category, so improving this score is also not possible.

Table 6 shows the scores that can possibly be achieved when focusing on improving certain requirements. The top row is the current ranking, as detailed in Table 5. The next row of numbers indicates the potential scores of each of the categories, if a constant force mechanism was made where possible. The thermal and plastic scores stay the same because they cannot be made into a constant force mechanism, however the rest of the categories can theoretically be improved. Each subsequent row shows the potential ranking if certain requirements were improved where possible. The green components (solid triangle) indicate the scores that are higher than the current highest score, and the yellow components (unfilled triangle) indicate scores equal to the current high score of 11. From this table it is evident that the elastic and combination categories are the most promising in terms of designing a new, improved prosthesis.

Ease of implementation is a low-scoring requirement for every one of the prosthesis categories, however it

is a crucial one to consider since currently the success of the stapedotomy depends most critically on the skill of the surgeon [26]. The question is how prosthesis implantation can be made easier. In the plastic category of prostheses, the most difficult step is the crimping around the incus [27]. Thermally actuated prostheses require the use of a laser to heat the shape memory alloy, which must be calibrated to the correct intensity. Current elastic devices are designed as clips which are pushed onto the incus, however this pushing action puts excessive strain on the delicate ossicles. This difficulty with elastic prostheses could be addressed by designing a device that does not need to be pushed over the incus, but is instead a bistable compliant mechanism which is either open or closed, and is closed around the incus via a simple manoeuvre by the surgeon.

5.3 Manufacturability and materials

To design a device that is feasible to manufacture at this scale, it would be useful to either minimise or completely avoid assembly. For this reason the *multibody* class of prostheses should be avoided, especially if the designer's objective is to create a constant force device, since the required complexity would be unfeasible. Such a device could be manufactured more simply if it were monolithic, with the springs/joints replaced with distributed or continuous flexibility in the design (i.e. a compliant mechanism).

From the materials investigated in this review, the material that is most commonly used in recent prosthesis designs is titanium and, more recently, Nitinol. Both of these materials are extremely light, non-magnetic and biocompatible. If flexibility is desired in the design then Nitinol is more suited, due to its property of superelasticity (Young's Modulus between 28 and 41 GPa). Whereas, if the design requires more rigidity, then titanium is a better choice (Young's Modulus of 116 GPa).

5.4 Final comments

The finite element model investigation by Williams *et al.* [45] of the middle ear revealed the frequency response to be sensitive to incudostapedial joint damping, as discussed in Section 2.1.2. Since current stapes prostheses are rigid compared to a healthy ossicular chain, it could be beneficial to design a prosthesis that more closely mimics the damping in a healthy incudostapedial joint.

6 Conclusion

This paper gives an extensive overview of the various kinds of stapes prostheses and presents a new method to fairly compare them. There exists a need for a new stapes prosthesis design which is easier to implant, and can further minimise the need for revision surgery. Current prostheses reportedly give excellent hearing results, however they are difficult to implement and the success of the surgery relies heavily on the skill of the surgeon. By systematically reviewing current prosthesis designs, a classification and evaluation system was set up and applied to a set of existing and patented prostheses. From the results of this examination, the elastic deformation class of prostheses was deemed

to be the most promising for the next generation prosthesis, since they came out as the most likely to be able to fill all requirements. The biggest cause for revision surgeries, incorrect clamping force around the incus, can be addressed by using the predictable force-displacement curve of mechanisms which remain in the elastic regime. However, for current elastic prostheses, the insertion causes high lateral forces on the delicate ossicles when they are pushed over the incus.

References

- [1] M. E. Adams and H. K. El-Kashlan. "Tympanoplasty and Ossiculoplasty". In: *Cummings Otolaryngology - Head and Neck Surgery*. 2010, pp. 1999–2008.
- [2] P. W. Alberti. "The blood supply of the incudostapedial joint and the lenticular process." In: *The Laryngoscope* 73.5 (May 1963), pp. 605–628.
- [3] P. W. R. M. Alberti. "The Blood Supply of the Long Process of the Incus and the Head and Neck of Stapes". In: *The Journal of Laryngology & Otology* 79.11 (Nov. 1965), pp. 964–970.
- [4] ASM International. "Overview of Biomaterials and Their Use in Medical Devices". In: *ASM International* (2003), pp. 1–11.
- [5] D. F. Awengen and U. Steinhardt. *Ossicle prosthesis*. 2006.
- [6] G. G. Babighian and S. Albu. "Failures in stapedotomy for otosclerosis". In: *Otolaryngology - Head and Neck Surgery* 141.3 (2009), pp. 395–400.
- [7] M. Bance, D. P. Morris, and R. Van Wijhe. *Effects of ossicular prosthesis mass and section of the stapes tendon on middle ear transmission*. Apr. 2007.
- [8] C. Brase et al. "Stapes surgery : first experiences with the new Soft-Clip piston." In: *Hno* 57.5 (May 2009), pp. 509–13.
- [9] S. I. Daniel. "Finite-Element Model of the Human Eardrum and Middle Ear". (2002).
- [10] A. J. De Bruijn, R. A. Tange, and W. A. Dreschler. "Comparison of Stapes Prostheses: A Retrospective Analysis of Individual Audiometric Results Obtained after Stapedotomy by Implantation of a Gold and Teflon Prosthesis". In: *The American Journal of Otology* 20 (1999), pp. 573–580.
- [11] M. Durko et al. "Does the material of stapes prosthesis influence hearing improvement in stapes surgery - retrospective analysis of 350 cases". In: *Otolaryngologia polska = The Polish otolaryngology* 62.4 (Jan. 2008), pp. 480–482.
- [12] T. Ear. "The Tympanic Membrane and Middle Ear". In: *Encyclopedia Britannica*, pp. 72–81.
- [13] A. Eiber. "Mechanical Modelling and Dynamical Investigation of the Middle Ear". In: *Middle Ear Mechanics in Research and Otosurgery* (1996), pp. 61–66.
- [14] A. Eiber. "On the Simulation of Human Hearing". In: *International Journal for Computational Vision and Biomechanics* 2.2.
- [15] J. B. Farior and A. E. Temple. "Teflon-wire piston or stainless-steel bucket stapes prosthesis: Does it make a difference". In: *Ear, Nose and Throat Journal* 78.4 (Apr. 1999), pp. 252–260.18
- [16] B. Feng and R. Gan. "A lumped-parameter mechanical model of human ear for sound transmission". In: *Proceedings of the Second Joint 24th Annual Conference and the Annual Fall Meeting of the Biomedical Engineering Society Engineering in Medicine and Biology* 1 (2002), pp. 2–3.
- [17] U. Fisch. *Tympanoplasty, Mastoidectomy, and Stapes Surgery*. 2008, p. 396.
- [18] I. Gerlinger et al. "Necrosis of the long process of the incus following stapes surgery: New anatomical observations". In: *Laryngoscope* 119.4 (Apr. 2009), pp. 721–726.
- [19] R. Goode. "The Ideal Middle Ear Prosthesis". In: *Middle Ear Mechanics in Research and Otosurgery* (1996), pp. 169–174.
- [20] W. Grolman and R. A. Tange. "First Experience with a New Stapes Clip Piston in Stapedotomy". In: *Otology & Neurotology* 26.4 (2005), pp. 595–598.
- [21] H. Helmholtz. "The Mechanism of the Ossicles of the Ear and the Tympanic Membrane". In: *Pflügers Arch Physiol* (Bonn) 1 (1868), pp. 1–60.
- [22] J. A. Hornung et al. "First experience with a new titanium clip stapes prosthesis and a comparison with the earlier model used in stapes surgery". In: *Laryngoscope* 119.12 (Dec. 2009), pp. 2421–2427.
- [23] A. Huber et al. "Fixation of the anterior malleolar ligament: Diagnosis and consequences for hearing results in stapes surgery". In: *Annals of Otology, Rhinology and Laryngology* 112.4 (Apr. 2003), pp. 348–355.
- [24] A. Huber et al. "Analysis of Ossicular Vibration in Three Dimensions". In: *Mechanics of the Middle Ear* (1996).
- [25] K. B. Huttenbrink, J. C. Luers, and D. Beutner. "Titanium angular clip: A new prosthesis for reconstruction of the long process of the incus". In: *Otology and Neurotology* 30.8 (Dec. 2009), pp. 1186–1190.
- [26] J. Kujala. *Modern surgical treatment of otosclerosis*. July. 2009.
- [27] P. Kwok et al. "How to Avoid a Learning Curve in Stapedotomy". In: *Otology & Neurotology* 38.7 (Aug. 2017), pp. 931–937.
- [28] D. H. Lee et al. "Reconstruction and exploration of virtual middle-ear models derived from micro-CT datasets". In: *Hearing Research* 263.1-2 (2010), pp. 198–203.
- [29] S. Mahendran, R. Hogg, and J. M. Robinson. "To divide or manipulate the chorda tympani in stapedotomy". In: *European Archives of Oto-Rhino-Laryngology* 262.6 (June 2005), pp. 482–487.
- [30] S. N. Merchant et al. "Middle Ear Mechanics in Normal, Diseased and Reconstructed Ears". In: *Middle Ear Mechanics in Research and Otosurgery* (1996), pp. 175–182.
- [31] G. Merriam and C. Webster. *Biocompatibility*.
- [32] R. P. K. Plinkert et al. "Stapeschirurgie bei Otosklerose mit einer neuen Titanprothese mit superelastischem Nitinol-Clip". In: *HNO* 64 (2016), pp. 111–116.
- [33] A. Prescott and H. Reitan. *Crimp assist middle ear prosthesis*. 2005.
- [34] C. Roosli and A. M. Huber. "Mid-term results after a newly designed nitinol stapes prosthesis use in 46 patients". In: *Otology and Neurotology* 34.7 (Sept. 2013), e61–e64.

- [35] S. Rösch *et al.* "Initial experiences with the Matrix Type Stapes Prosthesis Introduction and question Results".
- [36] M. M. Scheurer. *Middle ear prosthesis having discrete projections for purposes of ossicular attachment*. 2012.
- [37] G. Schimanski and A. Eiber. "Measuring the long incudal process: Precondition for developing a new Clip Piston for stapes surgery".
- [38] J. J. J. Shea. "Forty Years of Stapes Surgery". In: *American Journal of Otology* 19.1 (Jan. 1998), pp. 52–55.
- [39] U. Steinhardt and D. AWengen. *Ossicular replacement prosthesis*. 2004.
- [40] U. Steinhardt, A. Huber, and A. Eiber. *Auditory ossicle prosthesis*. 2008.
- [41] R. A. Teasley and D. D. Backous. "43 Clinical Assessment and Surgical Treatment of Conductive Hearing Loss".
- [42] N. W. Todd. "Diameter of Long Process of Incus for Stapes Prosthesis". In: *Otology & Neurotology* 36.5 (June 2015), p. 941.
- [43] R. Vincent *et al.* "Surgical findings and long-term hearing results in 3,050 stapedotomies for primary otosclerosis: A prospective study with the otology-neurotology database". In: *Otology and Neurotology* 27.8 SUPPL. 2 (Dec. 2006), S25–S47.
- [44] H. Wada, T. Metoki, and T. Kobayashi. "Analysis of dynamic behavior of human middle ear using a finite-element method." In: *The Journal of the Acoustical Society of America* 92.6 (Dec. 1992), pp. 3157–3168.
- [45] K. R. Williams, A. W. Blayney, and H. J. Rice. "Middle Ear Mechanics as Examined by the Finite Element Method". In: *Middle Ear Mechanics in Research and Otosurgery* (1996), pp. 67–75.
- [46] Y.-L. M. Ying, T. A. Hillman, and D. A. Chen. *Patterns of failure in heat-activated crimping prosthesis in stapedotomy*. Jan. 2011.19
- [47] C. L. Zuur *et al.* "Retrospective Analysis of Early Postoperative Hearing Results Obtained After Stapedotomy With Implantation of a New Titanium Stapes Prosthesis". In: *Otology and Neurotology* 24.6(Nov. 2003), pp. 863–867.

3

Paper: Design of a bistable stapes
prosthesis

Design of a bistable stapes prosthesis

Lola Giuffré, Nima Tolou, Reinier Kuppens, Henk Blom

Dept. of Precision and Microsystems Engineering Delft University of Technology
Delft, 2628 CD, The Netherlands

lolagiuffre@gmail.com, n.tolou@tudelft.nl, p.r.kuppens@tudelft.nl, h.blom@hagaziekenhuis.nl

ABSTRACT

Current stapes prostheses can treat otosclerosis induced conductive hearing loss. The procedure typically has excellent results, however it is difficult to perform and success is not assured. The surgeon may not be confident that the prosthesis is clamped at a correct clamping force around the incus. This paper presents the design of a novel stapes prosthesis. The new prosthesis is a bistable, monolithic mechanism, which is designed to be simpler to insert and with a more reliable clamping force compared with existing devices. We have used a pseudo rigid body modelling approach to analyse the system. We then simulated the mechanism with FEM and from this determined exact dimensions. A 3:1 titanium prototype has been manufactured using wire EDM. The prototype verifies the intended bistability of the design. It has two stable positions, and requires a force of 60mN to switch from the second positions back to the first, zero-energy state position. This force was designed in the modelling stages to be 65mN. More research is required to verify the surgeon's improved user experience when inserting into the middle ear.

1 Introduction

Otosclerosis induced conductive hearing loss can be effectively treated by the insertion of a passive prosthesis. The procedure typically has excellent results, with the potential to completely restore hearing to the patient. However, it is difficult to perform and success is not assured. Otosclerosis causes fixation of the stapes, hindering the sound vibration transmission from the middle to the inner ear. The prosthesis attaches to the incus and bypasses the fixated stapes, restoring sound transmission. Implanting the prosthesis is difficult due to limited space in the middle ear cavity and the delicacy of the ossicles. Safe clamping forces cannot be accurately controlled, despite being crucial to the surgery's long term success [1].

A typical prosthesis consists of a wire that is plastically deformed around the incus by crimping, the degree

of crimping determined intuitively. Over recent years new prostheses have been developed to improve the method of clamping the prosthesis. For example, clip-type prostheses which secure to the incus via elastic deformation [2] [3], and prostheses made from shape memory allows (SMAs) [4] [5], which are secured by heating them with a laser. Even though elastic clips exert a predictable amount of force when in place, insertion causes high lateral forces on the delicate ossicles when they are pushed over the incus. The long term success of the operation is strongly influenced by the skill of the surgeon [5]. This is due to the delicacy of elastic clip insertion or the difficulty of crimping to an appropriate pressure.

High lateral forces on the ossicles can be removed by keeping the prosthesis open during insertion, then closing once in place. Behaviour of this kind can mechanically be achieved with bistable mechanisms [6] [7]. These mechanisms exhibit two stable equilibrium positions, where no work is required to keep the device in each configuration. A typical force displacement curve of a bistable mechanism is shown in Figure 1. Upon

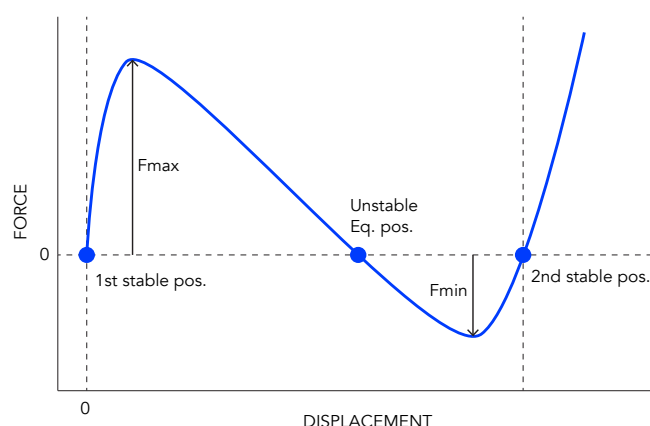


Figure 1: Typical force displacement graph of a bistable mechanism.

increasing displacement, a point is reached where the force changes sign and the mechanism, if released, will

jump to the second stable position.

To create such behaviour at the micro scale using traditional rigid body mechanical joints and springs is not practical, since this would require assembly and manufacturing would be excessively complex. Alternatively, the device can be designed as a compliant mechanism. These mechanisms transfer motion or force by utilising the flexibility in the structure [8]. The advantage of this is that they require less or no assembly and are thus easier to fabricate and, crucial to this application, easily minaturisable [6]. Furthermore, they are highly precise and require no maintenance and no lubricant due to the absence of frictional wear prevalent in rigid body joints.

Therefore, more research is needed to develop a stapes prosthesis with bistable behaviour. The idea is to shift some of the responsibility from the surgeon to the behaviour of the device, without applying dangerous forces to the ossicles and without the use of lasers. The device should not close prematurely due to unintentional collisions with the ear canal wall, thus the stability of the second position should be sufficiently strong. Also to be considered is the limited space in the middle ear and manufacturability. The device should be monolithic, biocompatible and easy to manufacture.

In this paper a new bistable prosthesis design is presented. The attachment of this prosthesis to the incus is simple: it can be placed around the bone without causing unwanted stresses in the ossicles and joints, and is easily clicked shut. For any incus diameter within the recorded range [9], the force around the incus is sure to be safe by design [10] (between 50mN and 200mN). Dependence on surgical intuition is thus eliminated. The prosthesis was designed as a monolithic, 2D structure. It is modeled and simulated using FEM. A prototype is manufactured out of titanium using wire EDM, and force displacement measurements have been done to verify the intended bistability and force-deflection behaviour.

In Section 2 background is given on the relevant anthropometric data, the procedural steps in a stapedotomy procedure, and the primary causes of failure for stapedotomies. In Section 3 the design problem is first given a framework by setting up the design specifications and functional requirements. The conversion from conceptual design to a dimensioned design and finite element model is detailed in Sections 3.3. In Section 3.4 the method of prototyping the device is discussed, and the experimental method to test the physical prototype is outlined in Section 3.5. Results are given in Section 4, where FEM analysis is compared with experimental data. A discussion and conclusion are provided in Section 5 and 6.

2 Background

2.1 Anatomy

The middle ear is an air-filled, mucosa-lined cavity, which houses three small bones; the malleus, incus and stapes, together referred to as the ossicular chain. The purpose of this chain is to efficiently transmit vibrations of the eardrum to the inner ear. These bones are attached to each other by synovial joints, and suspended from the walls of the middle ear cavity by a series of ligaments.

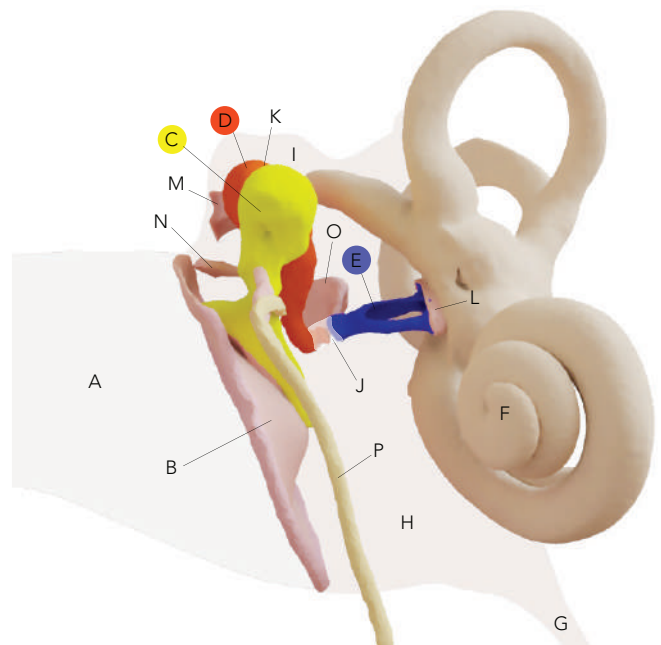


Figure 2: Anatomy of the normal middle ear. A: external auditory meatus, B: tympanic membrane, C: malleus, D: incus, E: stapes, F: bony canals which comprise the inner ear, G: eustachian tube, H: tympanic cavity proper, I: epitympanic recess, J: incudostapedial joint, K: incudomalleolar joint, L: annular ligament, M: posterior incudal ligament, N: lateral malleolar ligament, O: stapedius muscle and tendon, P: Chorda Tympani. Image adapted from the geometric data from De Greef *et al.* 2015 [21]

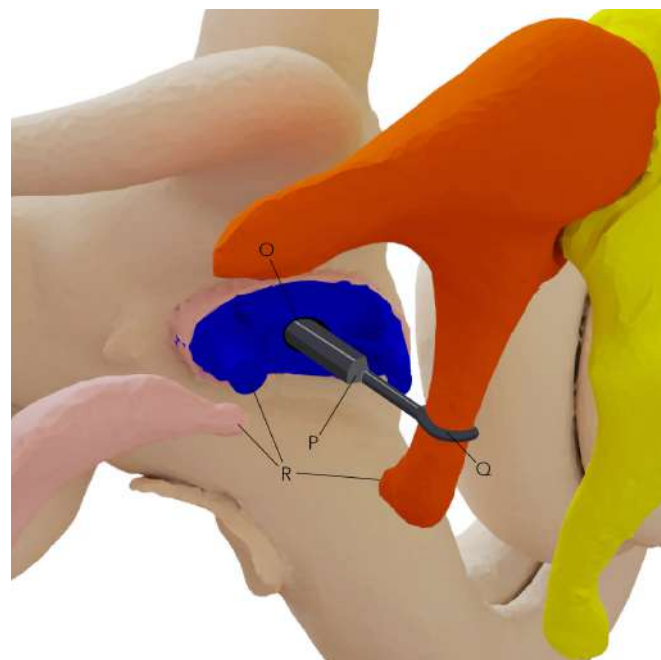


Figure 3: Reconstructed middle ear details. O: hole drilled into the stapes footplate, P: piston shaft of prosthesis, Q: attachment of incus to prosthesis. Image adapted from the geometric data from De Greef *et al.* 2015 [21]

The tympanic membrane (TM), commonly known as the eardrum, resides at the boundary between the outer and the middle ear. Two membrane windows, the round window and the oval window, form the boundary between the middle ear and the fluid-filled inner ear. A branch of the facial nerve responsible for taste, the Chorda Tympani, travels through the middle ear. Though it performs no functional role in the ear, it is an important piece of

anatomy to consider when designing for a stapedotomy. Special care must be taken not to damage it since doing so may lead to taste disruption or facial nerve paralysis [11]. A labelled diagram of the components of the middle ear is shown in Figure 2.

In otosclerosis, the footplate of the stapes bone becomes fixated, hindering the vibration transmission into the inner ear. During a stapedotomy procedure, the stapes superstructure is removed, a small hole is drilled into the footplate, and a prosthesis is inserted into this hole and secured to the adjacent bone, the incus. A diagram of the reconstructed ear is shown in Figure 3.

The ear canal is approximately 25mm in length, with a diameter as small as 7mm. The available space and field of view is hence extremely limited, and the entire surgery must be done under a microscope. The incus diameter at the location of prosthesis attachment is reported to vary between 0.52mm and 1.15mm [9], and the tapering angle of the conically shaped incus varies between 89.87 and 71.72 degrees [9].

2.2 Stapedotomy procedure

To perform a stapedotomy the surgeon must first gain access to the middle ear without damaging the TM. This is achieved by making an incision around the wall of the external auditory canal and pushing aside the TM. If the view of the ossicles is impaired then removal of temporal bone may be necessary. At this point there are two options in the surgical procedure: the stapes superstructure can either be removed before or after the prosthesis is placed.

The surgeon severs the synovial joint connection between the stapes and the incus, and, if following the first approach, removes the superstructure from the stapes footplate. The distance between the incus and the footplate is then measured, and the prosthesis is trimmed to the correct length if necessary. A small hole is drilled into the stapes footplate, and the rod-like end of the prosthesis is inserted into this hole, protruding slightly (no more than 0.75mm) into the inner ear fluid. The other end of the prosthesis must be secured to the next bone along in the ossicle chain - the incus. Depending on the design of the prosthesis this could involve placing a hook over the long process of the incus and manually crimping it in place, pushing an elastic clip over the incus or a variety of other methods [12]. The surgeon probes the prosthesis-stapes connection to ensure that it is secure.

Once the prosthesis is in place, the stapes

superstructure is completely removed by cutting the stapedius muscle, and severing its connection to the footplate if not done already. The prosthesis can now perform the same piston movement as the original stapes structure, with its protrusion into the inner ear responsible for vibration transmission.

2.3 Causes of failure

The most common cause of failure for a stapedotomy is the displacement of the prosthesis from the incus, according to Fisch [13]. This is likely caused by under-crimping. Under-crimping can also result in erosion of the incus, since micro gaps between the incus and prosthesis allow vibrations to wear at the bone, creating a localised erosion of bone tissue.

Another common complication of the stapedotomy which can be recognised in revision surgeries is necrosis of the long process of the incus, however the exact cause for this is disputed. Where some authors attribute it to overcrimping of the incus [14], [15], others [16], [17] argue the case that necrosis results from damage of the blood supply to the distal portion of the incus.

Other less common potential causes of failure include growth of fibrous adhesions, regrowth of otosclerotic bone over the footplate, or fixation of the malleus and incus. Table 1 shows the distribution of the causes of failure in 78 revision stapedotomies between 1995 and 2005 [18].

3 Method

3.1 Design specifications

The total length of the clasping mechanism is limited by the distance between the incus and the stapes footplate, and the amplitude of vibration. The incus-footplate distance is at minimum 4mm [19]. While transmitting sound vibrations the amplitude of the incus motion in the direction perpendicular to the footplate is 0.5mm [20]. Hence the length of the mechanism is less than 3.5mm.

The dimensions of the mechanism around the incus are also bounded due to the limited surrounding space. From anthropometric data [21] and existing prosthesis designs, the maximum distance from the centre of the incus cross section to the furthestmost point of the mechanism around the incus is restricted to 1mm. Before closing around the incus, the prosthesis must not be allowed to slip into the inner ear. Thus it is designed to hook over the incus before it is clicked shut.

The final clamping force of the prosthesis around the incus is crucial for the long term success of the operation. This force should be between 50 and 200mN for all incus diameters [10]. The force required to open the prosthesis should be larger than the force required to click shut. If revision surgery is required, it must be possible to open the prosthesis without damaging the delicate ossicles. In this case, the opening force is transferred to the incus in the posterior-anterior direction. Failures in the incudo-malleular joint begin to occur in this direction at 894mN [22], thus this is the absolute upper bound for the opening force. For safety, 800mN is taken as the limit. Within this bound, the force should be maximised to reduce the risk of the mechanism opening while performing its function.

Cause of failure	Percentage of cases (n=78)
Prosthesis displacement	45.5%
Incus erosion	32%
Fibrous tissue covering oval window	11.5%
Bony regrowth	10%
Fixation of incus and malleus	1%

Table 1: Results from Babighian et al.'s study of 78 revision stapedotomies [6]

Parameter	Symbol	Units	Requirement
Allowable incus diameter	D_{inc}	mm	$0.52 \leq D_{inc} \leq 1.1$
Length of mechanism	l_{base}	mm	$l_{base} \leq 3.5$
Distance from incus centre	r_{clamp}	mm	$r_{clamp} \leq 1$
Force of prosthesis on incus	F_{clamp}	mN	$50 \leq F_{clamp} \leq 200$
Force to open	F_{open}	mN	$F_{open} < 800$ Maximise
Force to close	F_{close}	mN	$F_{close} < F_{open}$

Table 2: Design specifications

An overview of these design specifications can be seen in Table 2.

3.2 Functional requirements

The required behaviour of an improved stapes prosthesis can be divided into four primary functional requirements:

1. Take action to open the prosthesis
2. Hold in open position
3. Take action to close prosthesis
4. Hold securely in closed position around the incus

The first function is performed outside of the body, possibly with the use of surgical tools or specially fabricated equipment. The second function is critical since the device should not close prematurely during the long passage into the middle ear cavity. The method of closing the device must be achievable in a simple motion, taking into consideration the lack of manoeuvrability allowed in the middle ear. The force required to close the device should be small enough such that it can be comfortably applied with existing stapedioplasty tools. Finally, once closed around the incus the device must not open unless by intention during revision surgery.

As well as these primary functions, the following sub-functions are also necessary for the device to be able to operate at a clinical level. The device must:

- adapt to the full range of incus diameters
- adapt to the full range of incus tapering angles
- transmit amplitude of incus vibration to the end of the piston at 1:1 for all audible frequencies

3.3 Dimensional Design

3.3.1 Final design

Illustrations of the final design are shown in Figure 4. The required function steps are shown. In the following sections, the analysis and dimensioning of the device is split into two parts: firstly of the bistable mechanism unit, and secondly a focus on the design of the clamping mechanism. The domain for each section is defined in Figure 4a.

3.3.2 Bistable mechanism design

A schematic of the fully compliant bistable mechanism is shown in Figure 4. The bistable mechanism cannot be thought of completely in isolation, as it is coupled with the clamping mechanism. F_{arm} refers to the force applied by the rotating arm (Figure 4a-C). The bottom length is given a fixed boundary condition, since it will be attached to the piston. When opening the prosthesis, the surgeon will hold somewhere along the backbone, and pull at point A (Figure 4). Hence the centre of the backbone is also fixed.

Pseudo rigid body model

A schematic of the pseudo rigid body equivalent used to approximate the fully compliant bistable mechanism is shown in Figure 5. Torsional springs represent the bending stiffness of the flexure beams. Their stiffness is given by:

$$K_t = 2\gamma K_\theta \frac{EI_B}{l}$$

where $K_\theta = 2.65$ and $\gamma = 0.85$, from standard pseudo rigid body mechanism equations [8].

The distance between the torsional springs, r , is also



Figure 4: Illustrations of final design

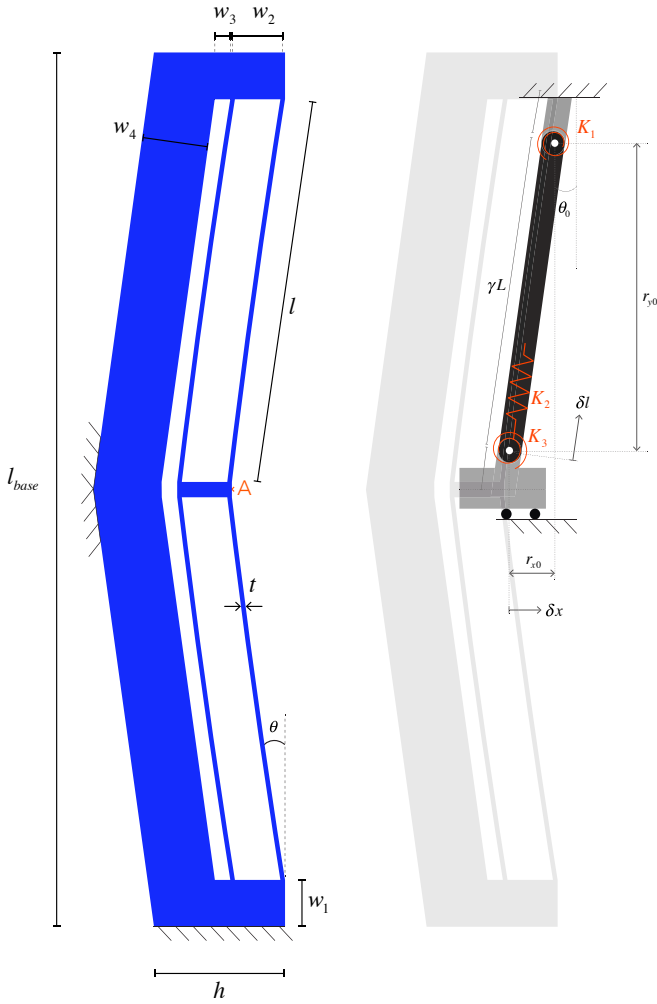


Figure 5: Bistable mechanism schematic and PRBM approximation

determined by PRBM standards: $r = \gamma L$.

The axial spring stiffness is calculated from the bending stiffness of the backbone:

$$\frac{1}{K_a} = \frac{(w_2 + w_3)^3}{3EI_1} + \frac{(l_{base}/2)^2}{3EI_2} \quad I_1 = \frac{dw_1^3}{12} \quad I_2 = \frac{dw_4^3}{12}$$

Linear and torsional springs deflections are found for varying deflections of the centre shuttle in the x direction δx_i , where $i = 1, 2, \dots, n$ is the number of load steps.

Upon deflection:

$$r_{xi} = r_{x0} - \delta x_i = r \sin(\theta_0) - \delta x_i$$

$$\theta_i = \tan^{-1} \left(\frac{r_{xi}}{r_{y0}} \right)$$

Hence the deflection of the first linear spring becomes:

$$\delta r_i = \sqrt{r_{xi}^2 + r_{y0}^2}$$

Torsional spring deflections:

$$\varphi_{1i} = \theta_0 - \theta_i$$

$$\varphi_{2i} = \theta_i - \theta_0$$

The total force on the shuttle at load step i is then:

$$F_i = 4g_{1i}K_t(|\varphi_{1i}| + |\varphi_{3i}|) + g_{2i}K_a\delta x_i - F_{arm}$$

where $g_{1i} = \frac{1}{r_{xi}}$ and $g_{2i} = \frac{r_{yi}}{r_{xi}}$ are the kinematic coefficients.

F_{arm} is due to the deflection in the rotating arm. It is determined through the standard beam deflection formula for a concentrated load at the free end of a cantilever:

$$F_{arm,i} = \frac{3EI_{arm}}{l_{arm}^3} \delta x_i \quad I_{arm} = \frac{dt^3}{12}$$

where δx_i is the deflection of point A at step i , and I_{arm} is the moment of inertia of the rotating arm.

Finite Element Analysis

The commercial finite element package COMSOL is used to dimension the design so that the desired performance is obtained in simulation. Through these simulations an understanding can be gained on the stress distributions and concentrations, and the sensitivities of each parameter on the mechanism's behaviour. In the interest of increased computational speed, the design was first simulated in 2D, and later checked by modelling in 3D. The relevant properties of titanium used in the simulation are the Young's Modulus ($E = 113.8$ GPa), and Poisson's ratio ($\nu = 0.34$).

Compliant mechanisms exhibit relatively large, geometrically nonlinear deformations. This nonlinearity, combined with the snap-through behaviour between two stable configurations, makes this a non-trivial modelling problem. To avoid the tangential stiffness matrix becoming singular at the global maximum in the force displacement curve, a displacement control rather than load control method must be used [25]. The x-displacement of the point A in Figure 5 is incrementally increased, causing stresses in the structure to develop, resulting in a reaction force measurable at point A.

For beams to buckle properly in simulation, a slight curvature ($r=130$ mm) is added to each beam to mimic imperfections [23].

Parameters for the design presented in this paper are shown in Table 3. Parameters in the first row describe the prosthesis at the proper scale. The design was prototyped at a scale of 3:1. The parameters determined for the prototype are shown in the second row of Table 3.

	l	θ_0	t	l_{base}	h	w_1	w_2	n_i
Design dimensions	1.6	10	0.25	4	0.6	0.25	0.2	2
Prototype dimensions	4.86	8	0.06	12	1.76	0.76	0.59	2

Table 3: Final dimensions of design and 3:1 prototype. Length dimensions are in mm, angle in degrees.

Figure 6 shows a Von Mises stress plot of the bistable mechanism simulation. The load step shown is the point with the highest internal stresses. The maximum stress is 940 MPa. According to the simulation, the force required to open the prosthesis is 850mN. Closing requires 65mN.

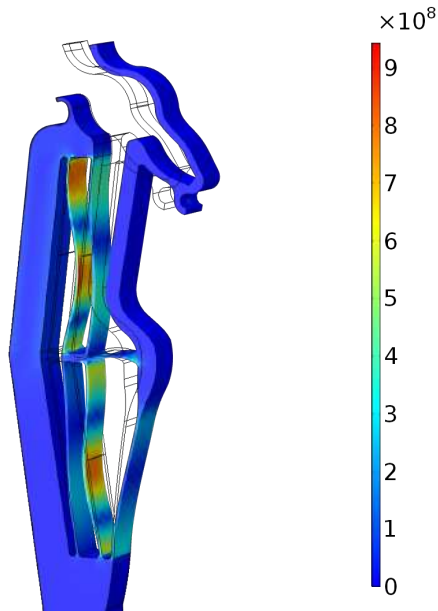


Figure 6: Results of COMSOL stress simulation for actuating the bistability. Units: N/m^2

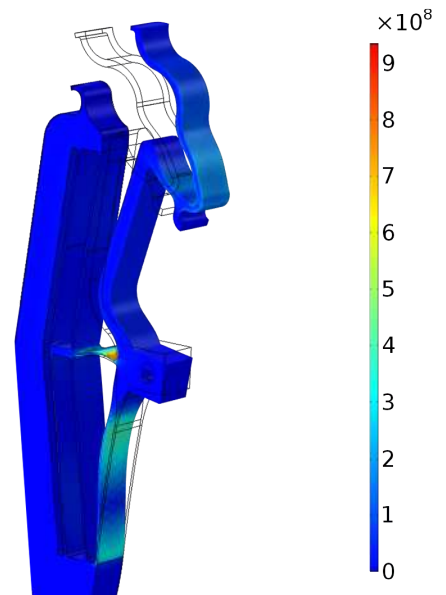


Figure 7: Results of COMSOL stress simulation of clamp opening. Units: N/m^2

3.3.3 Clasping mechanism

It has been established that the force the prosthesis exerts on the incus is crucial to the success of the operation, hence the dimensions of the clasp are tuned accordingly.

The proposed design consists of an arm that rotates via a fixed beam with distributed compliance, actuated by the deflection of the bistable mechanism. This rotating arm pushes the incus into the large-deformation holding mechanism: a clip-type mechanism resembling current prosthesis attachments. The arm and the flexure connecting it to the bistable mechanism form a pair of intersecting flexures. A feature of this configuration is that it has very low rotational stiffness around the point of intersection. Due to the large range of incus diameters to be accommodated, this low stiffness is desirable.

COMSOL was again used to model the force deflection behaviour and stress distribution of the mechanism. The clamp was dimensioned such that for a deflection range of 0.65mm, the reaction force is in the range 50mN-200mN. Figure 8 shows the final dimensions determined for prototyping.

The Von Mises stresses for when the clamp is at the maximum diameter are shown in Figure 7. The maximum stress is 915 MPa. The clamping force for the minimum incus diameter is 50mN, and 200mN for the maximum diameter.

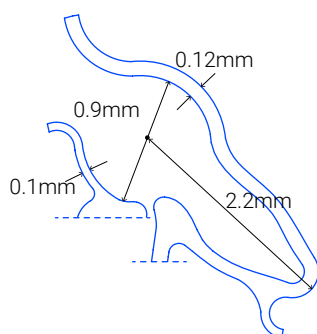
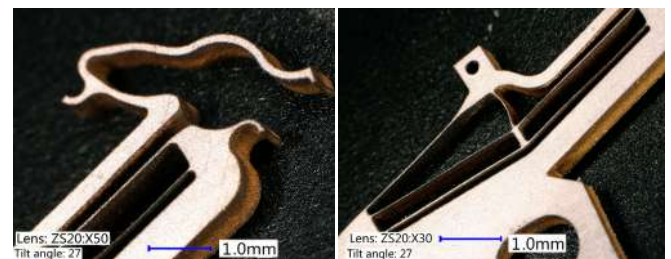


Figure 8: Final clamp dimensions

3.4 Prototyping

A titanium prosthesis is made using wire EDM at a scale of 3:1. This prototype is used to test the performance of the mechanism. A bracket is added for mounting to a baseplate, and a 0.4mm hole is drilled to attached a probe. Figure 9 shows images of the clasping mechanism and bistable mechanism of the manufactured prototype. A major advantage of wire EDM is the large aspect ratios that can be easily achieved. The diameter of the wire can be as small as 20 μm , with a precision of $\pm 1 \mu\text{m}$. The 3:1 prototype was made with a wire thickness of 150 μm .

Limitations of the available wire EDM machine imposed some design restrictions on the prototype. The beam thickness must be greater than 60 μm , and



(a) Clasp mechanism (a) Bistable mechanism

Figure 9: Digital microscope images of titanium prototype

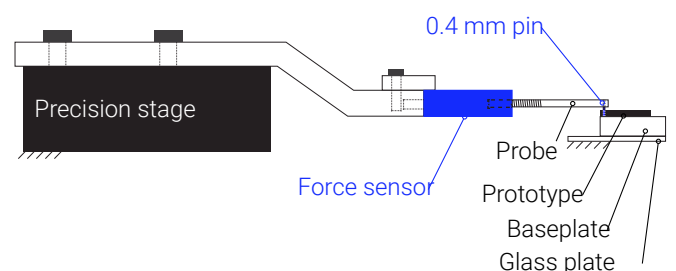


Figure 10: Schematic of the test setup

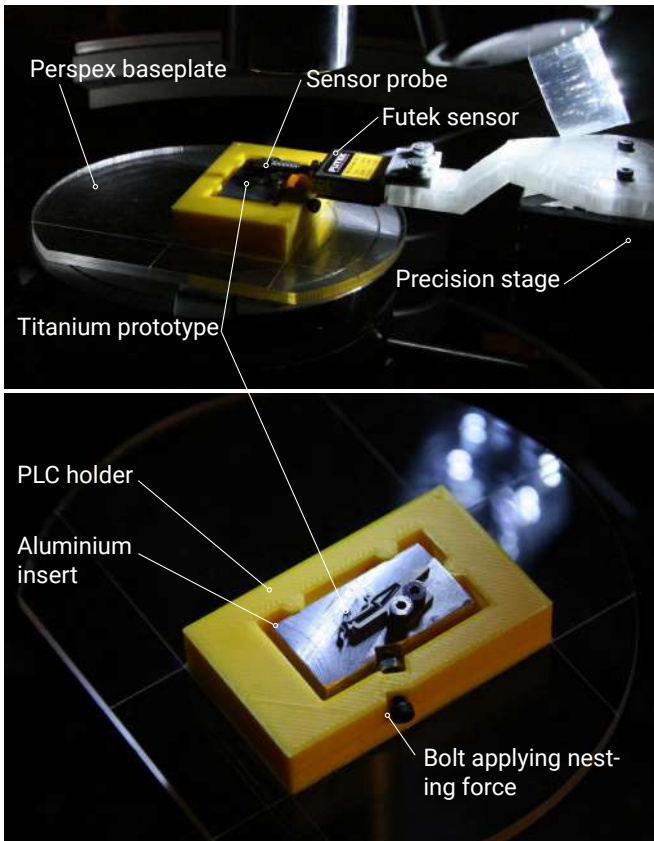


Figure 11: Force-displacement test setup.

the minimum corner radius is $75\ \mu\text{m}$ due to the wire thickness. An investigation is done on the sensitivity of the force displacement behaviour to the beam thickness. The tolerance is $\pm 30\ \mu\text{m}$.

3.5 Measurement

Beam widths are measured from high resolution images taken with a Keyence VHX-6000 digital microscope. Simulations are verified by measuring the force-displacement relationship.

The prototype is bolted to an aluminium machined block, and this block is nested inside a 3D printed component. There are three points of contact between the block and the printed holder, plus a nesting force (provided by another bolt) which ensures the block lies against these contact points. The 3D printed component is glued to a perspex plate. Fixation of the glass plate to the setup is achieved with a vacuum pump. A 100 gram Futek sensor is mounted onto a precision stage (PI Q-545) which has a resolution of 1 nm. Images of the force displacement measurement setup used to measure the device are shown in Figure 11.

Since bistable behaviour is being measured, the force

is expected to change sign during the measurement. Therefore, a custom probe was manufactured that could both push and pull the mechanism. Holes with a diameter of 0.4 mm are drilled into both the prototype and a threaded probe which can be attached to the force sensor. A pin of the same diameter is inserted through these holes to form a connection. The same probe is used to test the force-deflection behaviour of the clasp. A schematic is shown in Figure 10.

In order to verify repeatability of the measurements, the prototypes are completely demounted after the first set of measurements, and then remounted for a second set.

4 Results

Three prototypes were manufactured for testing purposes. Images of prototype #3 in its first and second stable positions are shown in Figure 12. Measured dimensions of the manufactured prototype differed from the simulated design due to manufacturing tolerances. Average, minimum and maximum beam widths are outlined in Table 4.

For prototypes 1 and 2 the average beam widths are $54\ \mu\text{m}$ and $50\ \mu\text{m}$ respectively. The third prototype comes closest to the design width of $60\ \mu\text{m}$, with an average width of $58\ \mu\text{m}$ over all its flexures. Figure 13 compares the measured force deflection curves of prototype 1 with the COMSOL simulated behaviour and the PRBM analytical model. Figure 14 does the same for prototype 3.

The third prototype is indeed bistable, and follows the trend of the COMSOL simulation. The repeatability of the measurements was good. An input force of 580 mN is required to open the third prosthesis. 60 mN is required

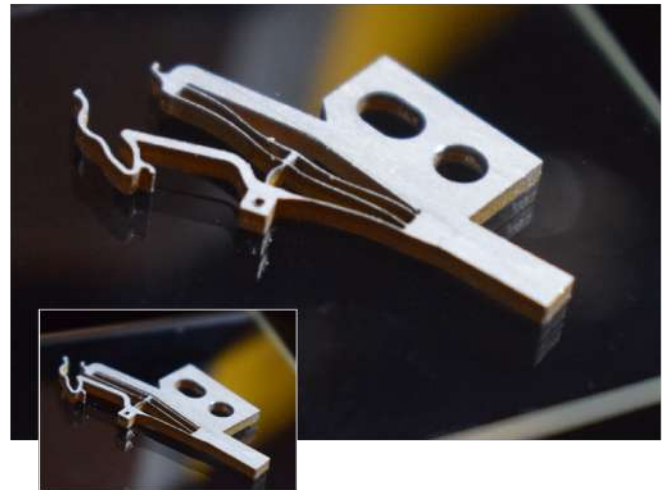


Figure 12: Main image: photograph of titanium prototype in second stable position. Bottom left: manufactured position.

Prototype #	Beam	1 (top left)			2 (top right)			3 (bottom left)			4 (bottom right)			All beams		
		avg.	max.	min.	avg.	max.	min.	avg.	max.	min.	avg.	max.	min.	avg.	max.	min.
1		55.1	68.7	44.9	45.7	71.5	33.0	57.2	70.2	58.0	58.1	78.3	53.2	54.0	58.3	33.0
2		47.0	60.3	35.0	51.7	65.0	39.0	62.8	72	56.7	38.3	44.9	34.0	49.9	72.0	34.0
3		57.1	63.7	45.0	58.0	67.6	45.1	59.6	65.7	54.5	58.9	41.5	72.8	58.4	72.8	38.4

Table 4: Average, minimum and maximum measured beam widths of manufactured beams.

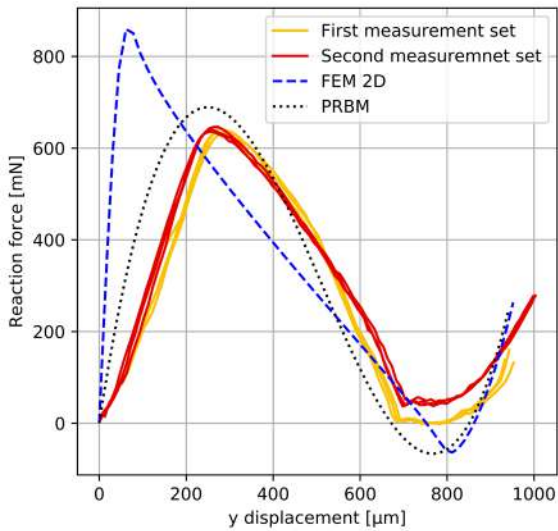


Figure 13: **Prototype 1** force-displacement measurement results for titanium prototype compared with FEM simulation and PRBM.

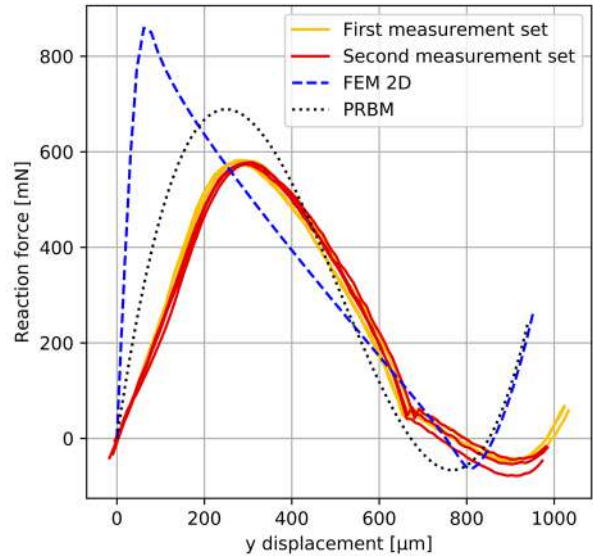


Figure 14: **Prototype 3** force-displacement measurement results for titanium prototype compared with FEM simulation and PRBM.

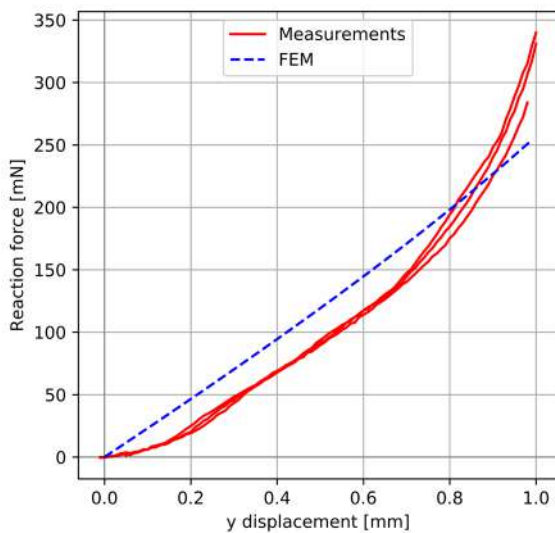


Figure 15: Force-deflection behaviour of the clamp (prototype 3)

to snap the device back to its original position.

The simulated and measured force-deflection curves of the clasp mechanism are shown in Figure 15. A deflection of 0.2 mm corresponds to the clasp of an incus with 0.5 mm diameter. At this deflection the measured force is 25 mN. A deflection of 0.8 mm corresponds to the clasp of an incus with 1.1 mm diameter. At this deflection the force is 180 mN.

5 Discussion

Measurements of the prototype confirm the bistability modelled in FEM. Though they follow the same trend, some discrepancies exist between simulation and experiments. In the bistability curves, the model overestimates the stiffness in the initial displacements until the point the reaction force starts to decrease. The measured curve is also rounder than the modelled one. These discrepancies are possibly due to the differences between the intended design dimensions and what

was manufactured in reality, since the manufacturing imperfections are significant. Beam widths of the prototypes, which should be 60 μm , vary as much as 50% ($\pm 30 \mu\text{m}$). To be able to have reliable medical devices, variance in manufacturing should be minimised.

The device was manufactured at 3:1 rather than 1:1 due to the limitations of the manufacturing equipment on hand. The measured data follows the trends predicted in the FEM and PRB models. Due to the miniaturisation of monolithic compliant mechanisms, the same FEM and PRB models for the 3:1 prototype can be used for simulating the 1:1 device, given different parameters. We can expect the 1:1 measurements to also follow the trend of simulation.

Two sets of measurements were made of the prototypes. Between measurement sets, the prototype was removed from the test setup and then remounted. The two sets of curves are virtually the same. With the first prototype, there are some discontinuities in the curve at around 700 μm . A potential cause for this is the method of measuring the force-displacement behaviour. We can assume there are small gaps between the probe pin and the holes, and so some discontinuity in the measurements is to be expected.

Although substantial steps were undertaken towards a clinically viable stapes prosthesis, it is not there yet. Below are some steps that should be taken to make the prosthesis ready for clinical trial.

1. Firstly, the next prototype should be manufactured, with several improvements. A prototype must be made at actual scale. A properly scaled prototype could conceivably be manufactured using a more precise EDM machine, via laser cutting, or by deep reactive ion etching (DRIE). A method of bulk micromachining high-aspect-ratio titanium structures with DRIE was developed by Aimi *et al.* [24]. Titanium sheets with thicknesses up to 500 μm have been successfully etched using this method. A masking

approach is advantageous since many devices can be made simultaneously. More research is required to verify the surgeon's improved user experience when inserting into the middle ear, and to test the dynamic performance of the mechanism. Also, the piston in the first prototype is a rectangular prism, whereas in reality it needs to be cylindrical. For the first prototype this was not a concern, since we were focussing on verifying the force-deflection behaviour of the attachment unit.

2. The frequency response of the mechanism must be tested, to verify 1:1 transmission from the incus to the inner ear.

3. To make the prosthesis suitable to be implanted into the body, an investigation should be done on how to reduce the surface roughness.

4. An investigation must be done on the usability of the design, to verify that it does in fact make the stapedotomy procedure less difficult. This could be done by first 3D printing a model of the middle ear and ear canal, and asking a number of surgeons to insert the prosthesis into the model. They could also be required to insert existing prostheses into the same model. Qualitative data can be gathered and compared, such as a ranking of the difficulty, or how safe the model operation felt. Quantitative data such as the time taken to operate can also be compared.

5. After testing on plastic 3D printed models, the prosthesis should be tested on real cadaver specimens.

The completion of these steps, and hence the introduction of this stapes prosthesis to the market, would have a significant impact on future stapedotomy surgeries. The insertion of the prosthesis is easier for the surgeon, and therefore safer for the patient. Also, since the clamping force is more controlled, it is expected that there will be less need for revision surgeries, which would be cheaper and less invasive for the patient.

6 Conclusion

In this paper, a new bistable stapes prosthesis is presented. Featured in the design is a bistable mechanism that actuates a rotating arm, the end of which clasps the incus. Bistability is achieved through tuning of the design parameters using FEM. The force required to close the mechanism is designed to be 65 μm , and is measured as 60 μm . The force deflection behaviour of the clamp has been designed to apply an appropriate pressure regardless of incus size. It applies a clamping force between 50 and 200 μm . This prosthesis should be easier and safer to insert, since the surgeon does not need to rely on intuition to secure the prosthesis to an appropriate clamping force. The design is fully compliant and two dimensional, and has been prototyped in titanium using wire EDM. The prototype successfully demonstrates the bistable behaviour and the adaptability of the prosthesis to different incus sizes. However, more research is required to advance the design to the stage of clinical trials.

7 References

- [1] Alexander M. Huber *et al.* "Stapes Prosthesis Attachment: The Effect of Crimping on Sound Transfer in Otosclerosis Surgery". In: *Laryngoscope* 113. May (May 2003), pp. 853–858. issn: 0023-852X. doi:10.1097/00005537-200305000-00015.
- [2] Albrecht Eiber. "On the Simulation of Human Hearing". In: *International Journal for Computational Vision and Biomechanics* 2.2. issn: 0973-6778.
- [3] Joachim A. Hornung *et al.* "First experience with a new titanium clip stapes prosthesis and a comparison with the earlier model used in stapes surgery". In: *Laryngoscope* 119.12 (Dec. 2009), pp. 2421–2427. issn:0023852X. doi:10.1002/lary.20641.
- [4] Christof Roosli and Alexander M. Huber. "Mid-term results after a newly designed nitinol stapes prosthesis use in 46 patients". In: *Otology and Neurotology* 34.7 (Sept. 2013), e61–e64. issn: 15317129. doi:10.1097/MAO.0b013e318299a973.
- [5] Juuso Kujala. "Modern surgical treatment of otosclerosis". July. 2009. isbn: 9789529254804.
- [6] B. Camescasse, A. Fernandes, and J. Pouget. "Bistable buckled beam and force actuation: Experimental validations". In: *International Journal of Solids and Structures* 51.9 (May 2014), pp. 1750–1757. issn: 0020-7683. doi:10.1016/J.IJSOLSTR.2014.01.017.
- [7] B J Hansen *et al.* "Plastic latching accelerometer based on bistable compliant mechanisms". In: *Smart Materials and Structures* 16.5 (Oct. 2007), pp. 1967–1972. issn: 09641726. doi:10.1088/0964-1726/16/5/055.
- [8] Larry L. Howell, Spencer P. Magleby, and Brian M. (Brian Mark) Olsen. "Handbook of compliant mechanisms". isbn: 9781118516485.
- [9] Miklós Tóth *et al.* "Anatomic Parameters of the Long Process of Incus for Stapes Surgery". In: *Otology & Neurotology* 34.9 (Dec. 2013), pp. 1564–1570. issn: 1531-7129. doi:10.1097/MAO.0b013e3182a43619.
- [10] Redaktion P K Plinkert *et al.* "Stapeschirurgie bei Otosklerose mit einer neuen Titanprothese mit superelastischem Nitinol-Clip". In: *HNO* 64 (2016), pp. 111–116. doi:10.1007/s00106-015-0100-z.
- [11] Suresh Mahendran, Richard Hogg, and James M. Robinson. "To divide or manipulate the chorda tympani in stapedotomy". In: *European Archives of Oto-Rhino-Laryngology* 262.6 (June 2005), pp. 482–487. issn:09374477. doi:10.1007/s00405-004-0854-5.
- [12] KURZ Middle Ear Intelligence. Passive middle ear implants. <https://www.kurzmed.com/products/otologie/stapedioplasty>
- [13] Ugo Fisch. "Tympanoplasty, Mastoidectomy, and Stapes Surgery". 2008, p. 396. isbn: 158890167X. doi:10.1308/003588410X12518836440441D.
- [14] K R Williams, A W Blayney, and H J Rice. "Middle Ear Mechanics as Examined by the Finite Element Method". In: *Middle Ear Mechanics in Research and Otosurgery* (1996), pp. 67–75.
- [15] Meredith E. Adams and Hussam K. El-Kashlan.

"Tympanoplasty and Ossiculoplasty". In: *Cummings Oto-laryngology - Head and Neck Surgery*. 2010, pp. 1999–2008. doi:10.1016/B978-0-323-05283-2.00142-7.

[16] P. W. Alberti. "The blood supply of the incudostapedial joint and the lenticular process." In: *The Laryngoscope* 73.5 (May 1963), pp. 605–628. issn: 0023852X. doi:10.1288/00005537-196305000-00012.

[17] P. W. R. M. Alberti. "The Blood Supply of the Long Process of the Incus and the Head and Neck of Stapes". In: *The Journal of Laryngology & Otology* 79.11 (Nov. 1965), pp. 964–970. issn: 0022-2151. doi:10.1017/S0022215100064653.

[18] Gregorio G Babighian and Silviu Albu. "Failures in stapedotomy for otosclerosis". In: *Otolaryngology - Head and Neck Surgery* 141.3 (2009), pp. 395–400. issn: 01945998. doi:10.1016/j.otohns.2009.03.028.

[19] Robert H. Todd, Dell K. Allen, and Leo Alting. "Manufacturing processes reference guide". *Industrial Press*, 1994, p. 486. isbn: 0831130490.

[20] F Schön and J Müller. "Measurements of ossicular vibrations in the middle ear." In: *Audiology & neuro- otology* 4.3-4 (1999), pp. 142–9. issn: 1420-3030. doi:10.1159/000013833.

[21] Wasil H.M. Salih et al. "Open access high-resolution 3D morphology models of cat, gerbil, rabbit, rat and human ossicular chains". In: *Hearing Research* 284.1-2 (Feb. 2012), pp. 1–5. issn: 03785955. doi:10.1016/j.heares.2011.12.004.

[22] Michael Lauxmann et al. "Experimental study on admissible forces at the incudomalleolar joint." In: *Otology & neurotology* 33.6 (Aug. 2012), pp. 1077–84. issn: 1537-4505. doi:10.1097/MAO.0b013e318259b34b.

[23] J. Lassoij et al. "A statically balanced and bi-stable compliant end effector combined with a laparoscopic 2DoF robotic arm". In: *Mechanical Sciences* 3.2 (Dec. 2012), pp. 85–93. issn: 2191-916X. doi:10.5194/ms-3-85-2012.

[24] Marco F. Aimi et al. "High-aspect-ratio bulk micromachining of titanium". In: *Nature Materials* 3.2 (Feb. 2004), pp. 103–105. doi:10.1038/nmat1058.

4

Reflection

This chapter contains a reflective overview of the work carried out in the past year. It is divided into four sections. Section 1 provides a chronological account of the line of thought followed throughout the project. In Section 2 the original plan is compared with the actual events of this thesis, and in Section 3 an overview is given of its contributions. Future steps for the project are discussed in Section 4.

4.1. Line of thought

During the first few weeks, I spent the majority of my time becoming familiar with the medical and biological facets of the project. Although the human body has always interested me, I have never formally studied it. In these initial weeks I focused on educating myself on topics such as the anatomy of the ear, in particular mechanics of the middle ear, mechanical properties of conductive hearing loss, the stapedotomy procedure and causes of failure. During this time I also followed the TU Delft course: Tissue Biomechanics of Bone, Cartilage and Tendon, which gave me an understanding of the more fundamental mechanics involved. This was most relevant when researching the effects of crimping on the incus ossicle. The first few months were spent conducting the literature review, the result of which is the classification and evaluation system which was used to evaluate all the prostheses I could find.

The initial meetings with the surgeon Dr. Henk Blom were crucial in gaining an understanding of what is problematic in current prosthesis designs. The literature review was useful in expanding and quantifying the points from these discussions. In November I went to observe a live stapedotomy performed by Dr. Blom. This experience helped me gain an appreciation of just how little space is available for the operation. I was given the stapes bone of the patient - not just a fun souvenir, but also a proper indication of scale.

Following on from the literature review was the conceptual design phase of the project - possibly the most enjoyable part of the project. I noticed that the work I did during this phase followed a curve similar to a bell curve: from the more basic, obvious ideas, to the more left-of-centre concepts, and finally bringing the ideas back to earth. There was a phase where I was considering introducing softer solutions, such as relaxing glues, to dampen the impact of the prosthesis on the incus. These ideas were ultimately rejected for a purely mechanical solution. The intention was to instead absorb some of the impact in the deflection of the mechanism. Originally the chosen design featured a tristable mechanism. Snapping to the second stable position would correspond to the mechanism closing loosely around the incus. Snapping to the third would result in a tightening of the mechanism. During dimensioning, the tristable design proved to be too bulky for the space-limited middle ear. Therefore it was necessary to step back to the concept phase, and a simpler, bistable mechanism was selected.

The minimum beam thickness (60 μm) imposed by the available manufacturing method and equipment meant that we could not, in the scope of this thesis, manufacture the design at the actual size. Once we were aware of this restriction, we identified four options on how to proceed:

1. Make a much larger, 3D printed prototype, and a small, non-functioning model as a demo.
2. Still try and make a prototype at actual size, even if the behaviour is compromised.
3. Make a prototype that is still small, but around 2-3x bigger than actual size.

4. Go back to the drawing board and come up with an entirely new concept that can be manufactured 1:1.

The first option would certainly have been the easiest, especially since large-scaled prototypes are far easier to test. However, at this stage I felt that I still had the time to do something more challenging. If I had gone with the second option, it is likely that the force in the force-deflection behaviour of the bistable mechanism would have been always positive. The bistable behaviour would have therefore been compromised, which would be very dissatisfying. Option 4, going again back to the drawing board to find a new solution, is, I think, problematic. The limitations we encountered in the manufacturing are not absolute limits. With this option we would be restricting the design possibilities to solutions that we can manufacture with equipment on-hand, even though it could be conceivably manufactured elsewhere. Such a restriction could unnecessarily be eliminating the more optimal solutions. Therefore we went with the third option: preserving the design but increasing the size three-fold.

4.2. Timeline review

The initial timeline for the project is shown in Appendix F.3. This plan was in fact followed quite closely. Limitations in time did, however, require me to leave out a milestone: the modelling and testing of the dynamic behaviour of the device. The function of the prosthesis is to transfer sound vibrations from the incus ossicle into the fluid-filled inner ear. The transmission from the incus motion perpendicular to the stapes footplate, to the motion of the end of the prosthesis piston should be approximately 1:1. Testing this experimentally would involve constructing a setup that uses a loudspeaker to input vibrations, and a laser doppler vibrometer to measure the phase and amplitude of the vibrations transmitted to the piston end.

4.3. Contributions

An extensive overview of the various kinds of stapes prostheses and a method to fairly compare them does not exist in current literature. A classification and evaluation system was therefore created to fill this gap. The other major contribution of this research is the development of a novel stapes prosthesis, which is designed to be simpler and safer to insert compared with existing prostheses.

4.4. Future steps

Although substantial steps were undertaken towards a clinically viable stapes prosthesis, it is not there yet. This section discusses the next steps that should be taken to make the prosthesis ready for clinical trial.

1. Firstly, the next prototype should be manufactured, with several improvements. Most importantly, the scale should be reduced to 1:1. Also, the piston in the first prototype is a rectangular prism, whereas in reality it needs to be cylindrical. For the first prototype this was not a concern, since we were focussing on verifying the force-deflection behaviour of the attachment unit. The piston is inconsequential.
2. The frequency response of the mechanism must be tested, to verify 1:1 transmission from the incus to the inner ear.
3. To make the prosthesis suitable to be implanted into the body, an investigation should be done on how to reduce the surface roughness.
4. An investigation must be done on the usability of the design, to verify that it does in fact make the stapedotomy procedure less difficult. This could be done by first 3D printing a model of the middle ear and ear canal, and asking a number of surgeons to insert the prosthesis into the model. They could also be required to insert existing prostheses into the same model. Qualitative data can be gathered and compared, such as a ranking of the difficulty, or how safe the model operation felt. Quantitative data such as the time took to operate can also be compared.
5. After testing on plastic 3D printed models, the prosthesis should be tested on real cadaver specimens.

5

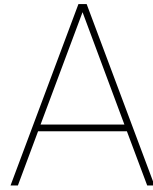
Conclusion

Current prostheses reportedly give excellent hearing results, however they are difficult to implement and the success of the surgery relies heavily on the skill of the surgeon. By systematically reviewing current prosthesis designs, a classification and evaluation system was set up and applied to a set of existing and patented prostheses. From the results of this examination, observations could be made on the most promising directions for designing the next generation prosthesis. Prostheses which work in the elastic regime of the material to clasp onto the incus bone came out as the most likely to be able to fill all requirements.

Informed by the results of the literature review, a novel prosthesis for stapedotomies was designed to improve the surgeon's experience in performing the procedure, and to further minimise the need for revision surgery. In this thesis, the new bistable stapes prosthesis is presented. Featured in the design is a bistable mechanism that actuates a rotating arm, the end of which clasps the incus. Bistability is achieved through the tuning of the design parameters using FEM. The force deflection behaviour of the clamp has been designed to apply an appropriate force (between 50mN and 200mN) regardless of incus size. This prosthesis should be easier and safer to insert, since the surgeon does not need to rely on intuition to secure the prosthesis to an appropriate clamping force. The design is fully compliant and two dimensional, and a 3:1 titanium prototype has been manufactured using wire EDM. The prototype verifies the intended bistability of the design. It has two stable positions, and requires a force of 60mN to switch from the second positions back to the first, zero-energy state position. This force was designed in the modelling stages to be 65mN.

Moving forward in making this prosthesis design clinically viable, a prototype must be made at actual scale. A properly scaled prototype could conceivably be manufactured using a more precise EDM machine, via laser cutting, or by deep reactive ion etching (DRIE). A method of bulk micromachining high-aspect-ratio titanium structures with DRIE was developed by Aimi *et al.* Titanium sheets with thicknesses up to 500 μm have been successfully etched using this method. A masking approach is advantageous since many devices can be made simultaneously. More research is required to verify the surgeon's improved user experience when inserting into the middle ear, and to test the dynamic performance of the mechanism.

Appendix



Conceptual process

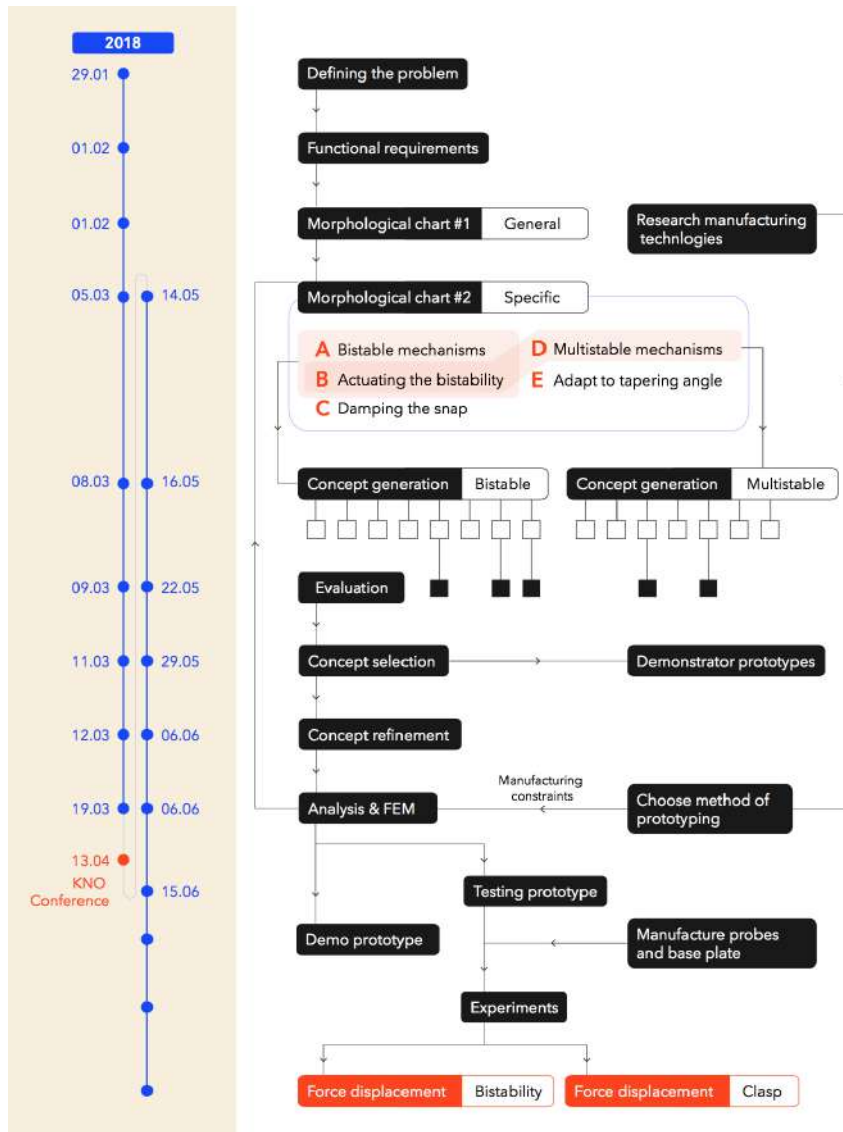


Figure A.1: Flowchart and timeline of the design process

A schematic of the design process and a corresponding timeline is shown in Figure A.1. Starting by setting up a framework for the problem (problem definition, design specifications and functional requirements), a set of concepts was generated using the morphological chart system. Two morphological charts were constructed: the first highly general, and the second to investigate specific mechanisms. Both charts are included in the Appendices A.5-A.7. The concepts generated were evaluated according to a set of weighted criteria, resulting in a shortlist of possible concepts. Tables of this evaluation process are found in Appendix A.8 and Appendix A.9. A selection was finally made, and the chosen concept was refined, analysed and modelled using COMSOL.

Due to constraints in manufacturing, it was necessary to step back to the concept phase. The minimum beam thickness ($60\ \mu\text{m}$) imposed by the available manufacturing method and equipment prompted a revisit to the bistable mechanism concepts in the second morphological chart. The process of concept generation, evaluation, selection, refinement, analysis and modelling was repeated. In the design dimensioning process, a final design was arrived at, with the desired force-displacement characteristics and permissible stresses.

A.1. Morphological chart process

Within the first morphological chart all types of solutions are considered - even somewhat obscure ideas such as utilising pneumatics, magnetics, relaxing glues, etc. From this chart an initial set of concepts was generated, shown in Figure A.14. During this part of the design process a very wide net was cast, and every idea was considered. However, the solution space was eventually narrowed to only include purely mechanical designs. This decision was based off the feasibility of manufacturing at the required scale, and the desire not to unnecessarily complicate the design.

The second morphological chart explores these purely mechanical solutions. From literature and pre-existing mechanisms, 32 examples of bistable mechanisms and 14 multistable mechanisms were collected. These were further organised into categories: distributed compliant/lumped compliant, origami and shell mechanisms. Mechanical solutions for actuating the bi/tristability were also compiled, as were compliant mechanisms with only a rotational degree of freedom, since this could be used to adapt to the tapered geometry of the incus. A map of the sections of morphological chart 2, and how they stem from the energy profiles from morphological chart 1, is shown below in Figure A.2. Sections A-F can be found in Appendix A.7.

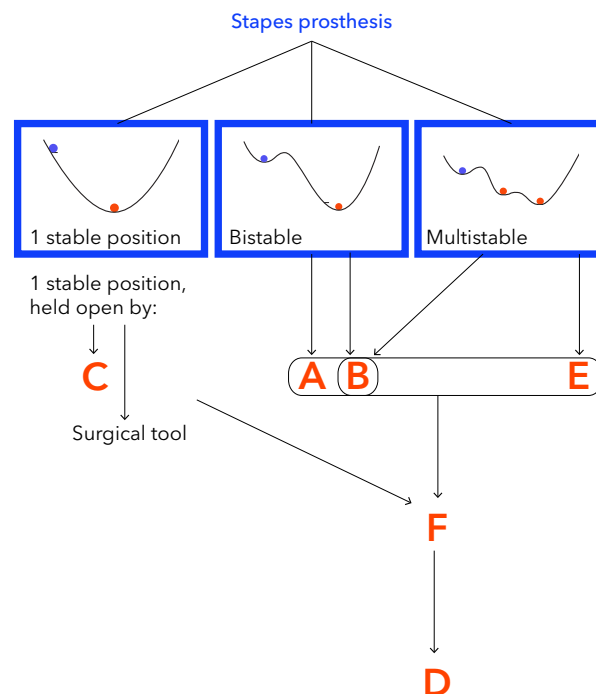


Figure A.2: Map of second morphological chart

A.2. Concept generation and evaluation

From this morphological chart an extremely large number of solutions can be generated - far too large to go through individually. A systematic method is required to prune the solution space. The choice of bi/tri stable mechanism and the method of actuating the bi/tri stability are the two aspects that have the largest influence on the final design. Therefore, a subset of concepts are compiled by considering combinations of [bistable mechanism + actuation mechanism] and [multistable mechanism + actuation]. Before doing so, the bistable, multistable and actuation sets are reduced to the mechanisms that are the smallest and least complex.

Generated solutions are evaluated according to how they would perform according to a set of weighted criteria. For every concept, each criteria is evaluated as either -1 (bad), 0 (okay) or 1 (good). Since most of these concepts aren't developed past the preliminary sketch stage, their evaluations are based mainly on common sense. A list of the criteria and their weightings are shown in Table A.3. The evaluation table and results for the bistable concepts are shown in Table A.15. Table A.16 give the results for the evaluation of tristable concepts. These tables are found in Appendix A.8 and A.9 respectively.

CRITERIA	WEIGHTING
Pressure controllability	7
Ease of implantation	8
Shape adaptability to LPI	1
Size	6
Complexity	5
Miniaturisation	4
Ease of manufacture	3
Strength of stability	2

Figure A.3: Prosthesis design criteria and weightings

A.3. Shortlisted concepts

From the many concepts generated from the procedure described above, 6 high-scoring designs were expanded upon. These are described below.

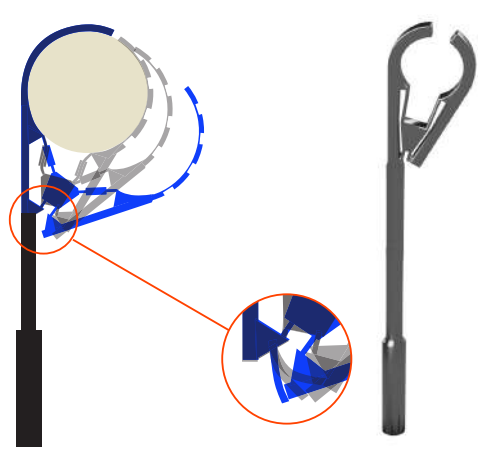
#	DIAGRAM	DESCRIPTION
1		<p>This design consists of two bistable units in series, which allow for the rotation of an arm in three distinct orientations. The idea behind introducing tristability when only bistability is strictly necessary is to reduce the velocity of the arm as it comes in contact with the incus ossicle. In the third stable position the arm is fully open. When closed to the second it comes in partial contact with the incus. Finally in the first (the manufactured position) the arm closes around the incus, making full contact.</p>

Figure A.4: Description of shortlisted concepts

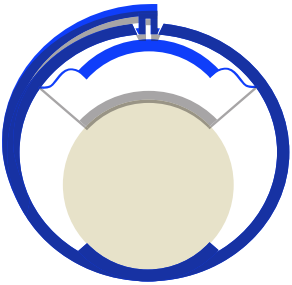
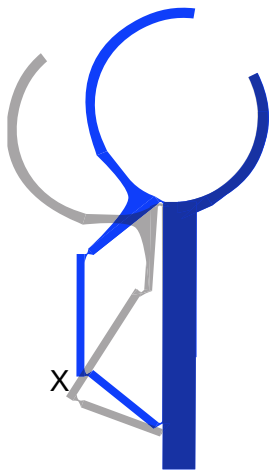
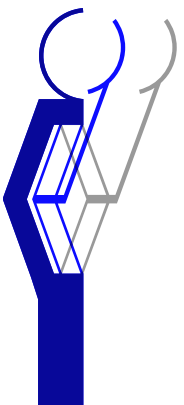
#	DIAGRAM	DESCRIPTION
2		<p>The attachment end of this design fully encompasses the incus. It is slid over the distal portion of the incus in the open position. When in place, the surgeon actuates the bistability by pressing the flexure at the top, thereby closing the prosthesis around the incus. This flexure has a locking mechanism, so that once it is pressed closed it can not open again, unless forced out of plane by the surgeon in the case of revision surgery.</p> <p>The idea of adding this flexure is to minimise the possibility of the prosthesis closing prematurely, or opening unintentionally.</p>
3		<p>This mechanism was adapted from one of the tristable mechanisms in the synthesis of 4-bar mechanisms (Section A9). It consists of rigid bars and living hinges and has two stable positions: open and closed.</p> <p>In the event of revision surgery it is easy to reopen. The surgeon must press on the point marked X. This location is accessible from the surgeon's view through the ear canal.</p>
4		<p>This prosthesis design consists of two sets of bistable flexure pairs moving in parallel. The extra set of bistable flexures restricts the rotation of the centre shuttle, thus restricting allowable motion and making the bistability stronger.</p> <p>The bistable mechanism causes an arm to translate. This translating arm causes the opening and closing of the prosthesis.</p>

Figure A.5: Description of shortlisted concepts

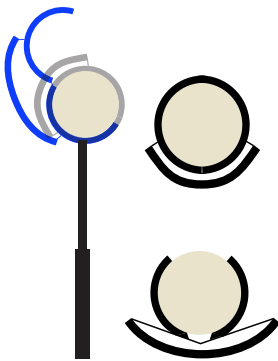
#	DIAGRAM	DESCRIPTION
5		<p>The gripper design shown here is a symmetrical design with two arms that can either be open or closed around the incus. Two versions are drawn here: a version with living hinges and a version with distributed compliant members.</p>

Figure A.6: Description of shortlisted concepts

A.4. Final concept

The initial concept choice (concept 1) was revised due to constraints in manufacturing, which caused the design to be far bulkier than intended. Going back to the concept phase, a different design was selected (concept 4). In this second iteration of concept evaluation, more importance was placed on reducing the amount of deflection in the elements. Designs with less local strain were favoured over those with apparent higher strains.

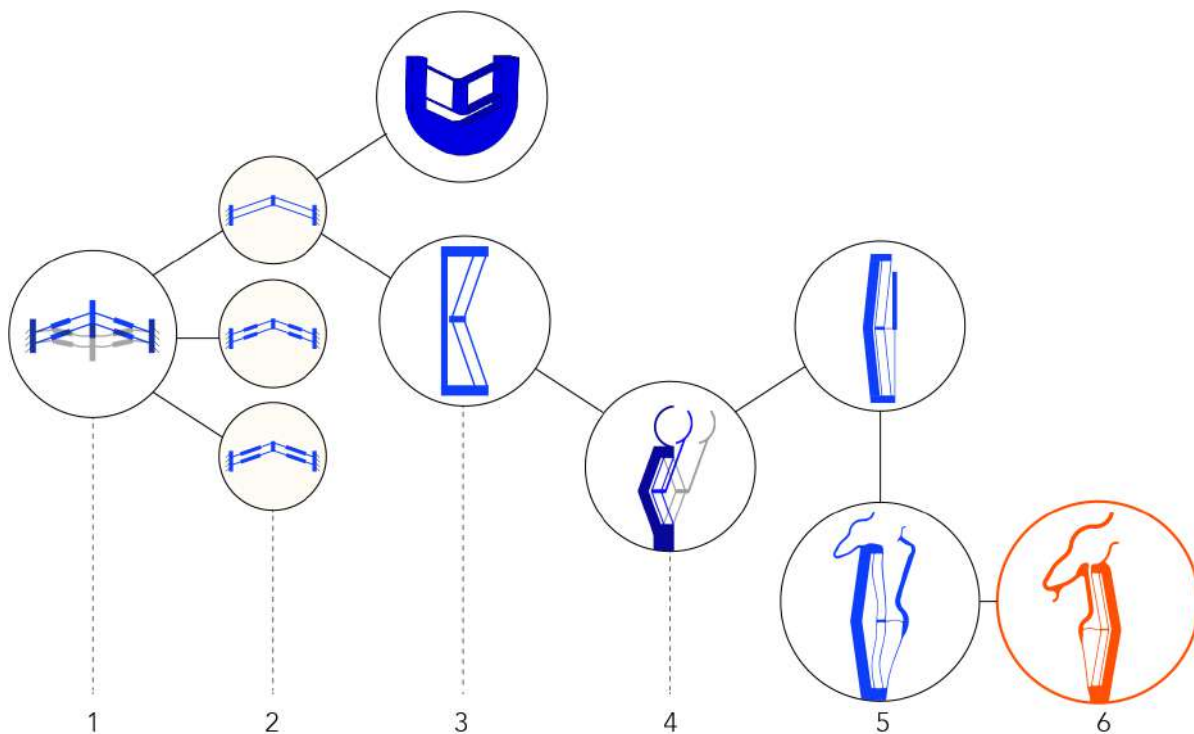


Figure A.7: Design evolution

The flowchart in Figure A.7 gives an overview of the design iterations involved in refining the concept from the generic bistable mechanism to a fully functioning stapes prosthesis. Each revision step is summarised below:

1. The parallel guided mechanism was chosen from the library of bistable mechanisms compiled in the

second morphological chart. The basis of this choice was the relatively small deflection in the beams.

2. The mechanism could either be a distributed compliant mechanism, or lumped compliant to various degrees. There exists a tradeoff between the strength of the bistability and the stresses and strains in the material. The distributed compliant case exhibits the smallest stresses, but also the weakest bistability. Due in part to manufacturing limitations (minimum thickness of the flexures), and in part to the maximum size constraints, the distributed compliant case was chosen. This is because the design is operating at a safety factor of just 1, and the higher stresses induced by the lumped compliance would cause it to be deformed beyond the yield stress.
3. Since the beams need to be quite long to properly exhibit bistability, the decision was made to orient them along the length of the piston. When the bistable mechanism is pushed outwards, to the second stable position, the prosthesis must be open enough to easily allow the incus into the clasp.
4. The clasp opens since part of it is connected to an arm which is fixed to the horizontally translating, bistable shuttle. The dimensions of this arm and the clasp will determine the force of the prosthesis on the incus - crucial to the success of the operation.
5. To arrive at the final design, a few more design modifications were made. The flowchart shown here is not exhaustive. Firstly, the translational movement of the shuttle was not large enough to provide adequate space to place the incus. Therefore, the arm is connected by a flexure to the bottom of the device, thereby allowing it to rotate rather than translate. Some geometric modifications are made on the design to minimise its size. Also, the clasp geometry is modified, influenced by current prosthesis designs, to allow for the whole range of incus diameters.
6. In the final concept iteration, the relative orientation of the clasp with respect to the bistable mechanism is flipped. Only one side of the prosthesis is easily accessible from the viewpoint of the surgeon when looking through the ear canal. This side should be the point of actuation. In flipping the clasp mechanism, the surgeon is able to actuate the bistability more easily.

Sketches of the required function steps are illustrated in Figure 4 below. Before entering the ear of the patient, the surgeon pulls open the device to the second stable position. During its decent into the middle ear, the prosthesis holds itself in this position. The surgeon places the piston into the hole drilled into the inner ear, and hooks the prosthesis loosely onto the incus. It is important that the prosthesis is not able to fall into the inner ear. This is one reason why configuration (a) was favoured over configuration (b) (Figure A.7, 2). By tapping the notch at the back of the mechanism, the bistable mechanism is pushed past its unstable equilibrium position, back to the manufactured, closed position. During this motion, the rotating arm pushes the incus into the wedge shaped clip.

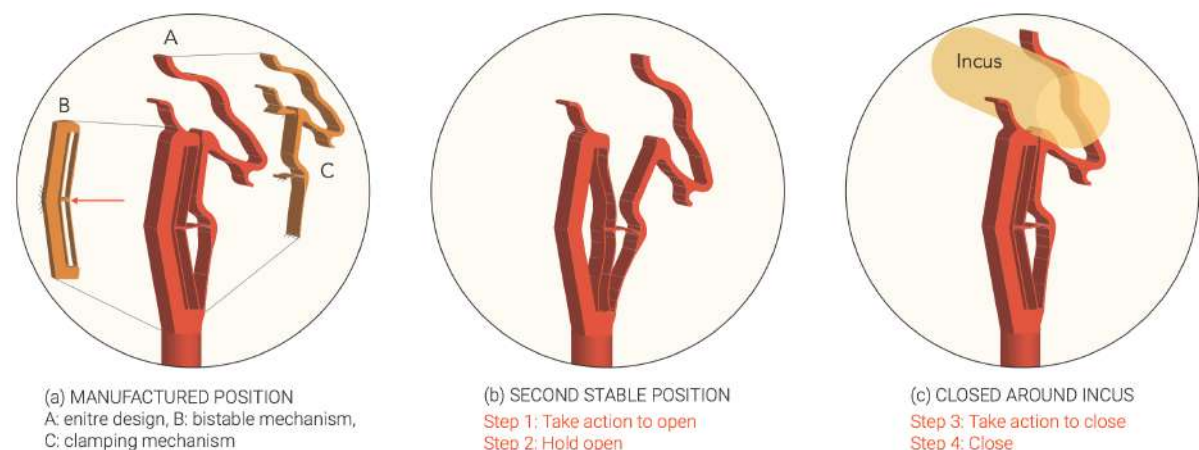


Figure A.8: Illustration of final concept

It is not desirable to have too much snapping action, due to the delicacy of the ossicles and joints. The idea is that some of this kinetic energy is transformed into elastic strain energy of the deformed clasp as the incus is pushed into place. This idea is illustrated in Figure A.9.

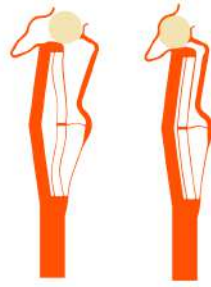


Figure A.9: Illustration of prosthesis closing over incus

A CAD rendering of the final device is shown in Figure A.10. This is not exactly the design that was ultimately prototyped. Manufacturing constraints meant that the smallest prototype that we could make was 3 times the actual size. Internal dimensions were scaled accordingly.



Figure A.10: CAD render of final concept

A.5. Morphological chart 1: general solutions

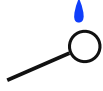
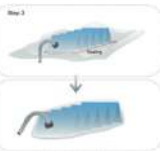
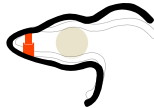
Function	Systems				
User input: switch from closed to open	Surgical tools	Custom case	Magnetic	Thermal	Solution
					
	Pneumatics				
Hold in open position					
	Surgical tools	Mechanical stop	Removable piece	Stop	Stable position
					
Pneumatics	Glue				
					
User input: placing around incus	Hook	Clip	Push over distal end		
					

Figure A.11: Morphological chart A: general functions | Part 1

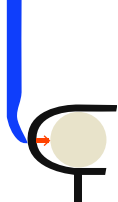
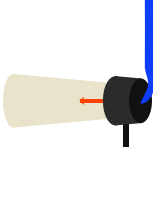
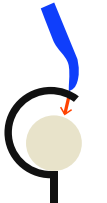
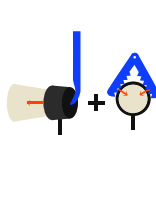
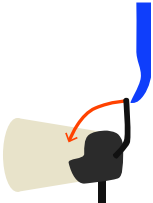
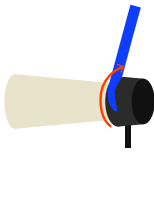
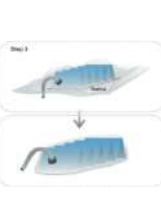
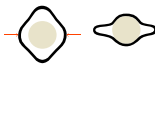
Function	Systems				
User input: secure to incus	Compress LPI	Compress piston	Push perp LPI	Push parallel LPI	Parallel piston
					
	Tap perp LPI	SMA	Push parallel LPI + push perp LPI	Follow path	Solution
					
	Twist	Pneumatics	Hydraulics	Remove sheath	Apply voltage
					
Clasp mechanism	Bistable gripper	Deformable clip	Shell mechanism	Origami	
					
Hold in closed position	Stable position: lowest energy	Shape memory state	Clip		

Figure A.12: Morphological chart B: general functions | Part 2

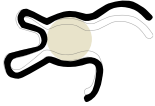
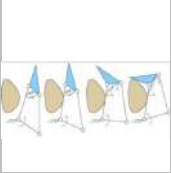
Function	Systems				
Adapt to incus diameters	Elastic clip	Hard clip	Self-adaptive fingers	SMA	
					
Adapt to tapered geometry	Spiral path	Leaf spring		SMA	
					
Dampen impact	Coating on incus	Coating on prosthesis	Damping in tool	Artificial muscle	Damping in hand of surgeon
					
	Soft spring				
					
Energy profiles					

Figure A.13: Morphological chart C: general functions | Part 3

A.6. Concept brainstorm

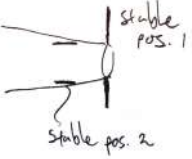
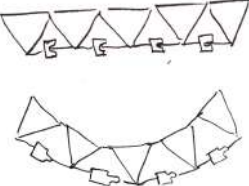
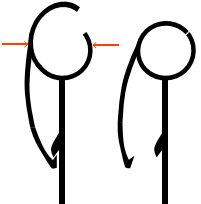
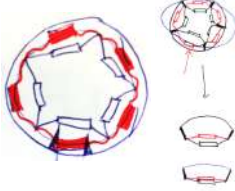
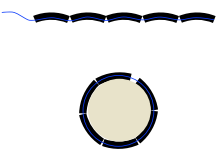
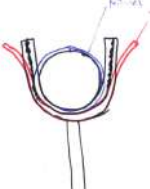
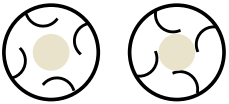
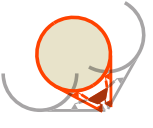
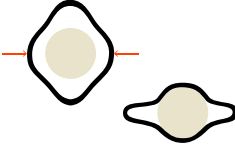
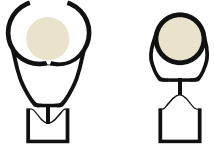
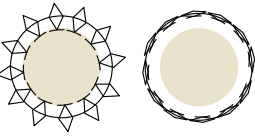
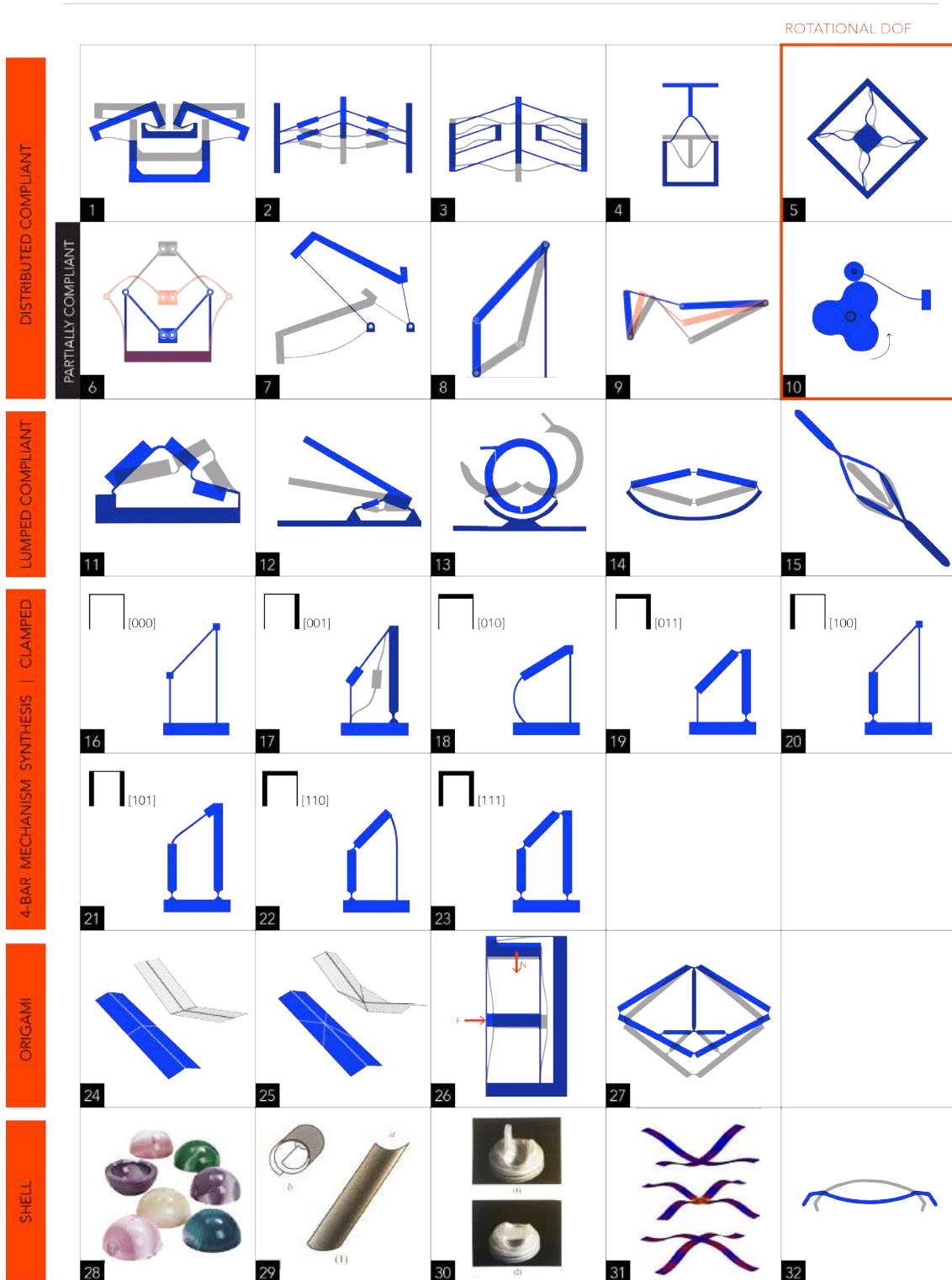
Hook	Push over end	Fold	Fold
			
			
			
			
			

Figure A.14: Brainstorm of concepts generated from first morphological chart

A.7. Morphological chart 2: mechanical solutions

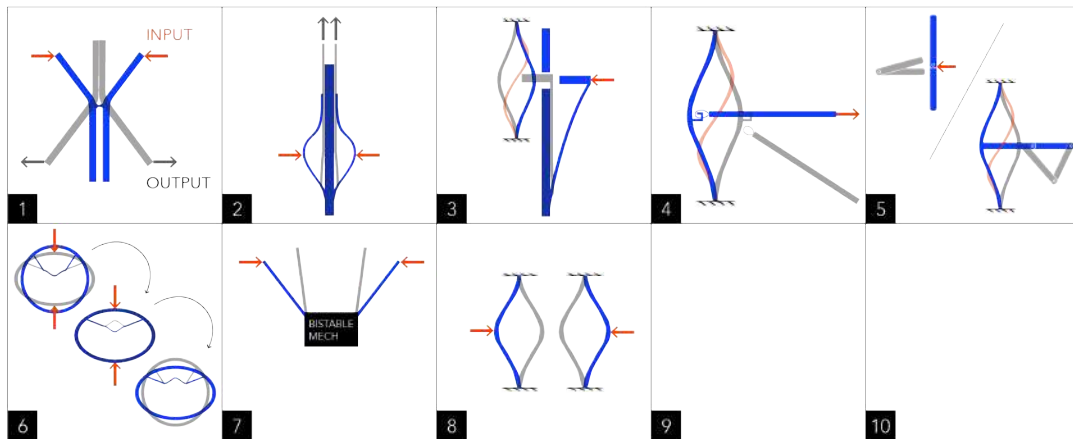
A

Bistable compliant mechanisms



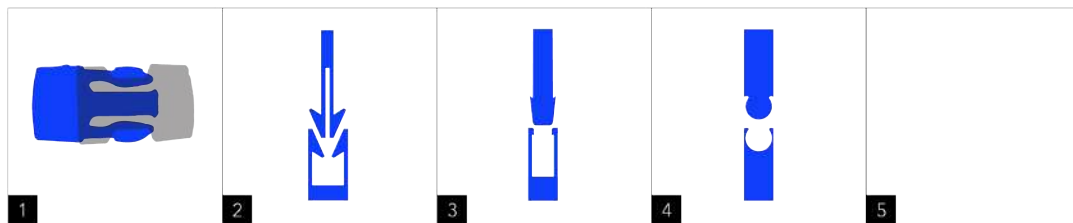
B

Actuating the bistability



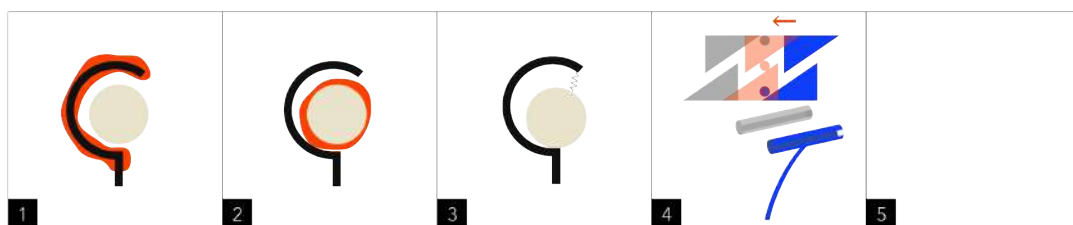
C

Connecting mechanisms



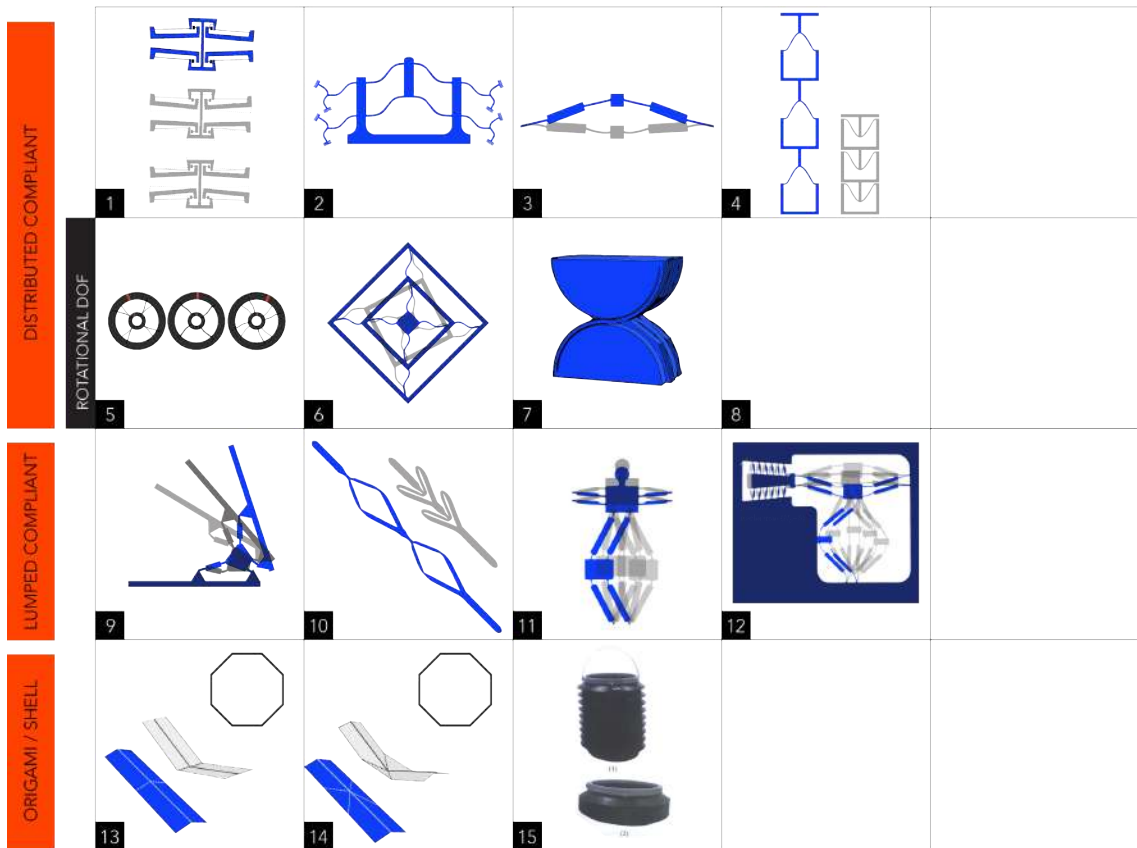
D

Damping the snap



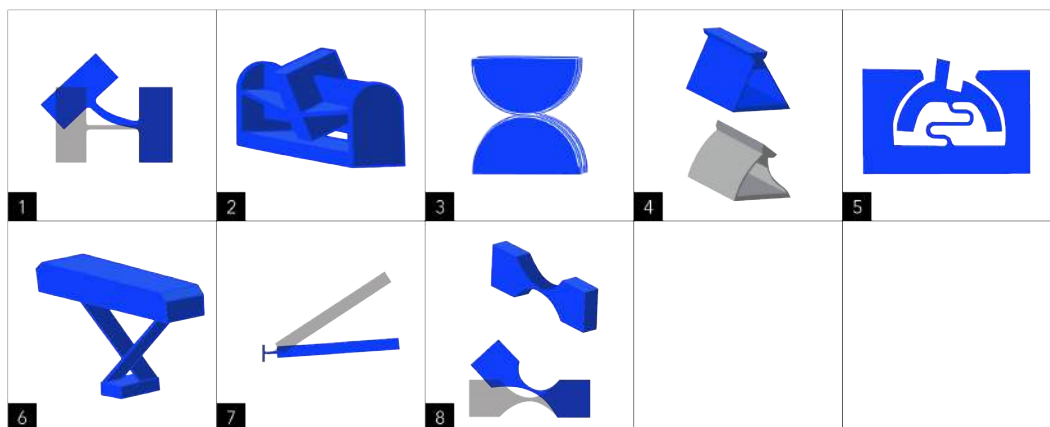
E

Multistable



F

Compliant rotation | Adapt to tapered geometry



A.8. Evaluation: bistable concepts

BISTABLE CONCEPTS		A	B	C	D	E	F
0		0	0	0	0	0	0
		0	1	0	1	1	0
		1	1	1	1	1	1
		0	0	0	1	0	0
		1	0	1	1	1	0
		1	1	1	1	1	0
		1	1	1	1	0	-1
		0	0	0	1	1	0
1		0	0	0	0	0	0
		1	X	0	X	1	1
		1	X	-1	X	1	1
		0	X	0	X	-1	-1
		1	X	1	X	0	0
		1	X	1	X	-1	-1
		1	X	1	X	0	0
		-1	X	-1	X	-1	-1
2		0	0	0	0	0	0
		1	1	0	1	1	1
		1	1	1	1	1	1
		1	0	-1	0	1	-1
		1	0	0	0	-1	0
		1	1	1	1	0	1
		1	1	1	1	-1	-1
		1	0	1	1	0	0
3		0	0	0	0	0	0
		1	1	0	X	1	0
		1	0	-1	X	1	1
		1	0	0	X	-1	0
		0	1	1	X	1	1
		0	1	1	X	0	-1
		-1	0	1	X	0	0
		-1	-1	-1	X	-1	-1

TOTAL SCORES

	A	B	C	D	E	F
0	8	11	15	24	3	-7
1	18	X	4	X	-10	-5
2	24	11	4	13	2	-1
3	13	11	-1	X	9	-8

Figure A.15: Evaluation of bistable concepts

A.9. Evaluation: multistable concepts

	A	B	C	D	E
TRISTABLE CONCEPTS					
0	0 1 1 -1 0 1 1 -1 1	0 1 1 1 0 1 -1 -1 1	0 1 1 1 0 1 1 1 1	0 1 1 -1 -1 0 -1 0 0	0 0 0 0 0 0 -1 -1 1
1	0 0 1 -1 -1 0 0 0 1	0 1 1 1 0 1 -1 1 1	X		
2		0 1 1 1 0 1 -1 1 1	0 1 1 -1 -1 1 1 1 1	X	
3			0 1 1 1 -1 -1 1 1 1	0 1 1 1 -1 -1 0 0 1	X

TOTAL SCORES

	A	B	C	D	E
0	13	28	29	-5	-5
1	-5	25	X	X	X
2	0	25	12	0	X
3	0	0	12	15	X

Figure A.16: Evaluation of multistable concepts

A.10. 4-bar tristable mechanism synthesis

One method of generating mechanism concepts was to create a synthesis of tristable mechanisms constructed from a simple four-bar bistable mechanism. This graphical synthesis is shown in Figure A.17. Mechanisms under *A* are joined by the longest member of the 4-bar unit mechanism. Mechanisms under *B* are joined by the opposite member. Mechanisms under *C* are joined by one of the side members. Under each heading (*A*, *B*, *C*) the three stable states of the mechanism are sketched for the cases of each member being held fixed. Symmetrical cases are not considered.

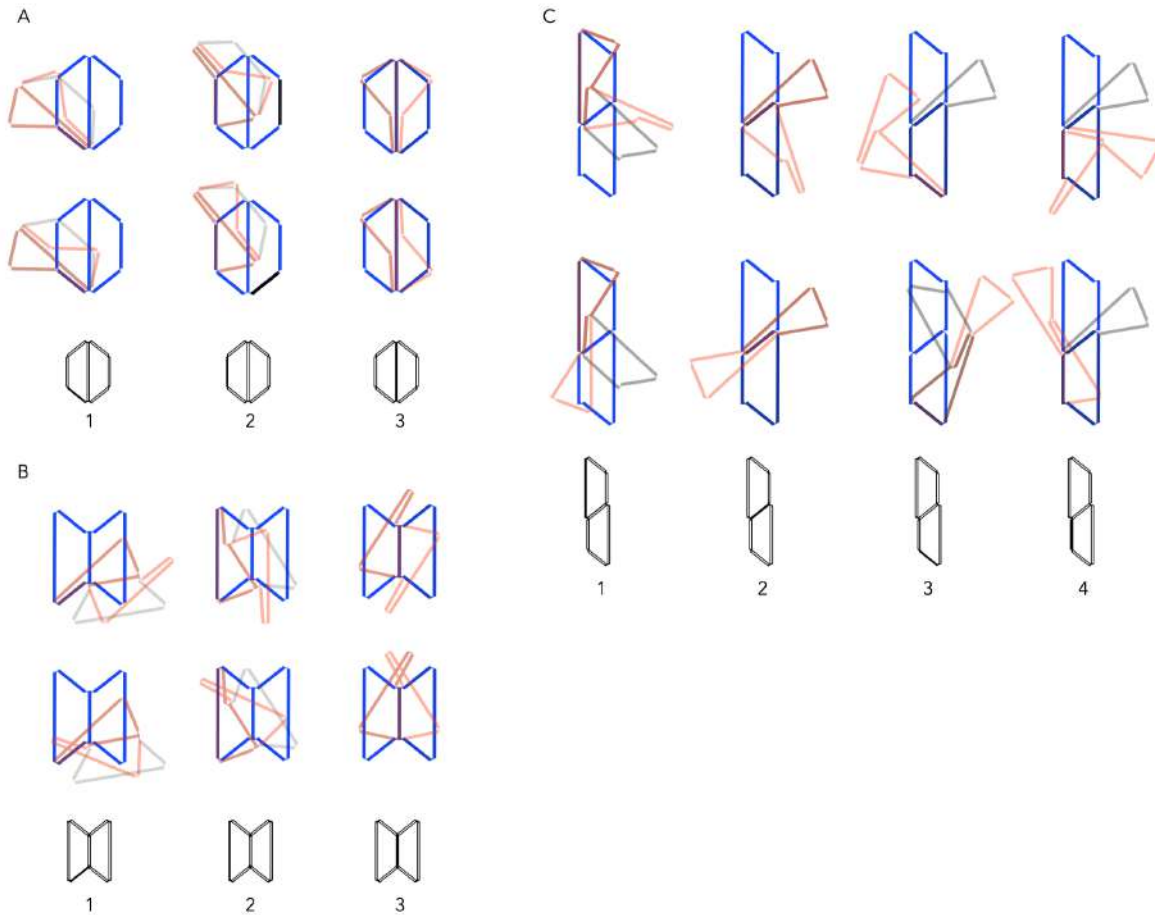


Figure A.17: Graphical synthesis of four-bar tristable mechanisms

B

Dimensional design

B.1. PRBM: initial concept

A labelled schematic of the underlying mechanism in the initial concept is shown below in Figure B.1. The mechanism is symmetric, hence just one symmetrical half is analysed using the PRBM method. We expect this half to be bistable.

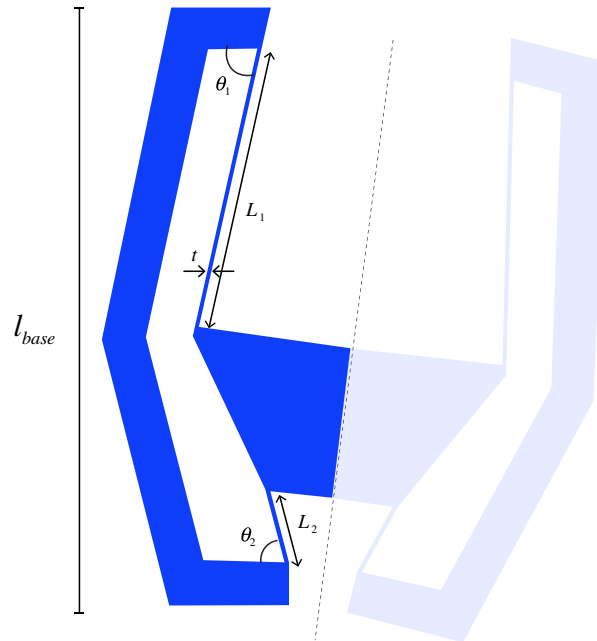


Figure B.1: PRBM schematic of the initial concept

Two PRBM options were considered to analyse this system. If L_2 is very short, then it could be approximated by a single torsional joint. A drawing of this option is shown in Figure B.2(a). Otherwise, the flexure of length L_2 would be approximated by two torsional springs, at a distance of $\frac{(1-\gamma)L_2}{2}$. This option is sketched in Figure B.2(b)

Schematics of the PRBM approximations of each case are shown in Figure B.2. Relevant dimensions have been labelled. $\gamma = 0.85$, from standard pseudo rigid body mechanism equations [4]. Case 1 is described below.

For the torsional springs that approximate a fixed-fixed compliant member, the torsional spring stiffness can be approximated by:

$$K_t = 2 \frac{\gamma}{L_0} K_{\Theta} (EI)_{bending}$$

Therefore, the torsional springs replacing the compliant members in case 1 can be approximated by:

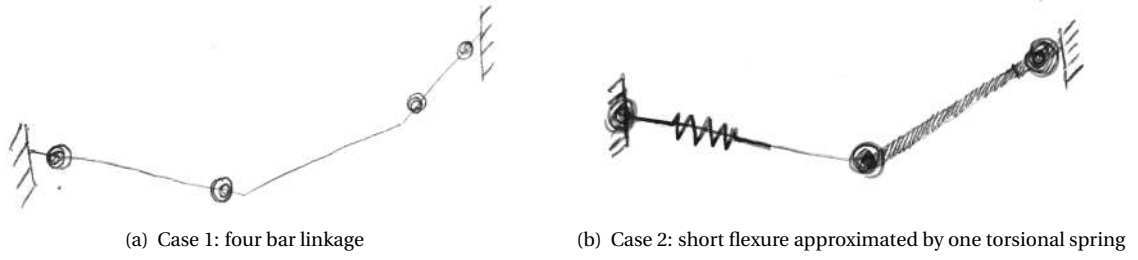


Figure B.2: Two cases for PRBM

$$K_{t1} = 2 \frac{\gamma}{L_1} K_{\Theta}(EI_1)_{bending} \quad K_{t2} = 2 \frac{\gamma}{L_2} K_{\Theta}(EI_2)_{bending}$$

where

$$I_1 = \frac{d_1 w_1^3}{12} \quad I_2 = \frac{d_2 w_2^3}{12}$$

where w_1 , w_2 are the widths of flexures 1 and 2, and d_1 , d_2 are their depths into the page.

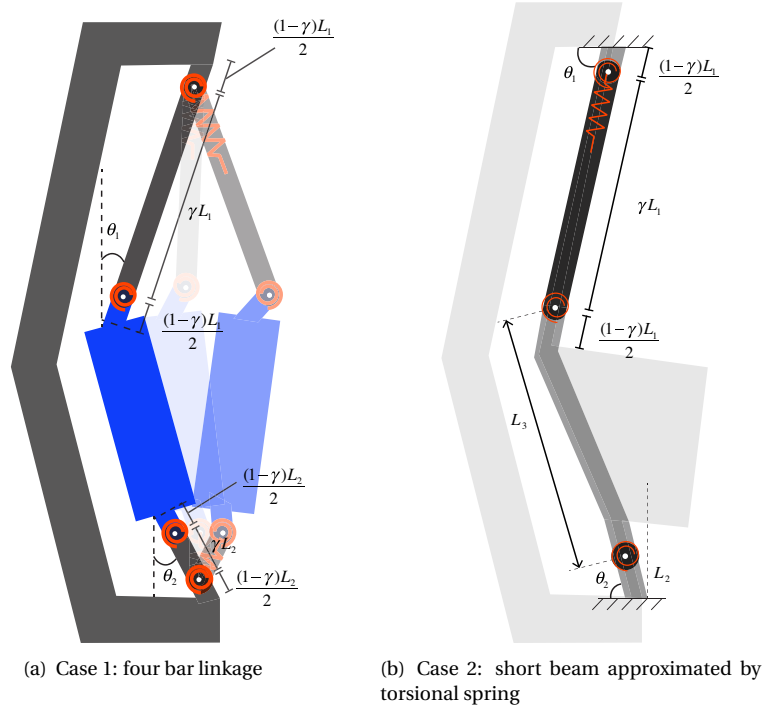


Figure B.3: PRBM schematic of the initial concept

The total strain energy is approximated by adding all the energies stored by the deflected torsional springs.

$$U = \frac{1}{2} K_{t1} (d\phi_1^2 + d\phi_2^2) + \frac{1}{2} K_{t2} (d\phi_3^2 + d\phi_4^2)$$

where $d\phi_n = \phi_{ni} - \phi_{n0}$, $n = 1, 2, 3, 4$ is the angular deflection of each torsional spring.

B.2. PRBM: final concept

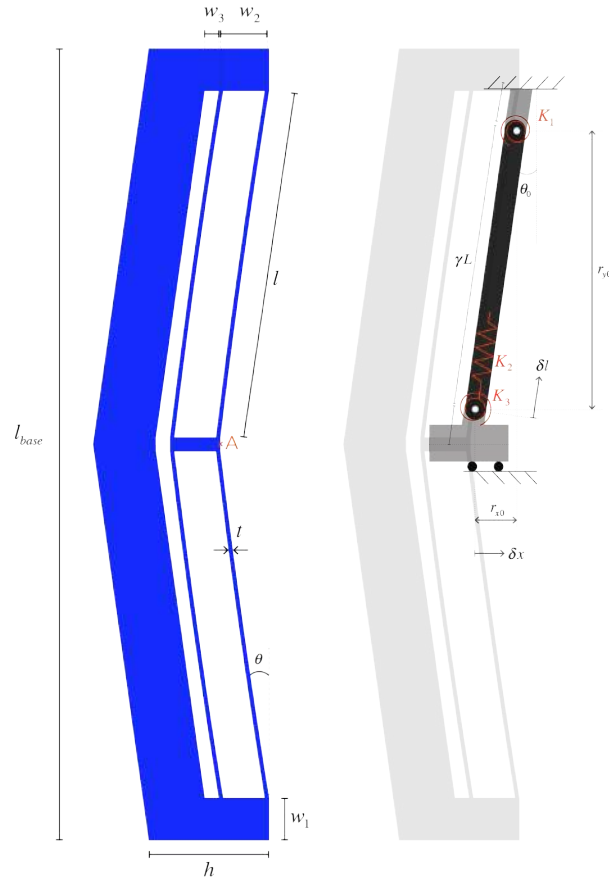


Figure B.4: PRBM schematic of the final concept

A schematic of the pseudo rigid body equivalent used to approximate the fully compliant bistable mechanism is shown in Figure B.4. Torsional springs represent the bending stiffness of the flexure beams. Their stiffness is given by:

$$K_t = 2\gamma K_\Theta \frac{EI_B}{l}$$

where $K_\Theta = 2.65$ and $\gamma = 0.85$, from standard pseudo rigid body mechanism equations [8]. The distance between the torsional springs, r , is also determined by PRBM standards: $r = \gamma L$.

The axial spring stiffness is calculated from the bending stiffness of the backbone:

$$\frac{1}{K_a} = \frac{(w_2 + w_3)^3}{3EI_1} + \frac{(l_{base})^2}{3EI_2} \quad I_1 = \frac{dw_1^3}{12} \quad I_2 = \frac{dw_4^3}{12}$$

Linear and torsional springs deflections are found for varying deflections of the centre shuttle in the x direction - δx_i , where $i = 1, 2, \dots, n$ is the number of load steps. Upon deflection:

$$r_{xi} = r_{x0} - \delta x_i = r \sin(\theta_0) - \delta x_i$$

$$\theta_i = \tan^{-1} \left(\frac{r_{xi}}{r_{y0}} \right)$$

Hence the deflection of the first linear spring becomes:

$$\delta r_i = \sqrt{r_{xi}^2 + r_{y0}^2}$$

Torsional spring deflections:

$$\phi_{xi} = \theta_0 - \theta_i$$

$$\phi_{yi} = \theta_i - \theta_0$$

The total force on the shuttle at load step i is then:

$$F_i = 4 \cdot g_{1i} \cdot K_t \cdot (\phi_{xi} - \phi_{yi}) + g_{2i} \cdot K_a \cdot \delta_{xi} - F_{arm}$$

where $g_{1i} = \frac{1}{r_{xi}}$ and $g_{2i} = \frac{r_{yi}}{r_{xi}}$ are the kinematic coefficients.

F_{arm} is due to the deflection in the rotating arm. It is determined through the standard beam deflection formula for a concentrated load at the free end of a cantilever:

$$F_{arm,i} = \frac{3EI_{arm}}{l_{arm}^3} \delta_{xi} \quad I_{arm} = \frac{dt^3}{12}$$

where δ_{xi} is the deflection of point A at step i , and I_{arm} is the moment of inertia of the rotating arm.

B.3. FEM modelling process

This section addresses the process of finite element modelling using COMSOL. In the first part, the steps to set up the 2D COMSOL model are stated. Notes on convergence are given in Section 2, and some results for parameter sensitivity are given in Section 3.

B.3.1. Setting up COMSOL model

The steps involved in setting up the COMSOL model for the final design are detailed below, so that the model could be replicated if desired. These steps refer to the 2D model - which was the primary model used in dimensioning the design due to the relatively low computational time. In the final modelling stages a 3D model was used. For the 3D model, the CAD model was imported directly into COMSOL.

Model setup

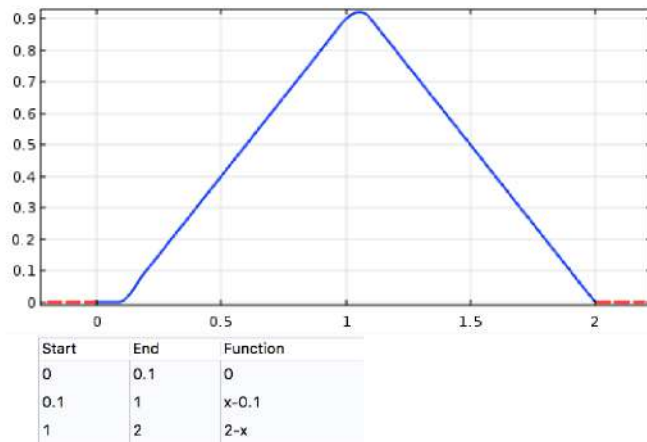
From the *Model Wizard*, select 2D. From the *Select physics* menu, select structural mechanics > Solid mechanics (solid). From *Select study* menu, select stationary study.

Parameters

Parameters shown in Appendix B.3.1(a) and the piecewise function in Appendix B.3.1(b) are defined in *Global Definitions*.

Name	Expression	Value
t1	0.06[mm]	6E-5 m
t2	t1	6E-5 m
t3	0.26[mm]	2.6E-4 m
theta1	8[deg]	0.13963 rad
theta2	theta1	0.13963 rad
l1	4.947[mm]	0.004947 m
l2	l1	0.004947 m
step	1	1
nbeam	2	2
ubeam	0.636[mm]	6.36E-4 m
w1	0.76[mm]	7.6E-4 m
h1	1.6[mm]	0.0016 m
base	9.85[mm]	0.00985 m
scale	3	3

(a) Parameters



(a) Piecewise function

Figure B.5: Global definitions: parameters and piecewise function

Geometry

The geometry shown in Appendix B.3.1 is constructed using the parameters defined above. Input values for each of the polygons are shown in Appendix B.3.1. Polygons 1 and 3 are given a fillet of 40 mm. This has the effect of giving the beams a very slight curvature, so that the structure behaves as it would in real life.

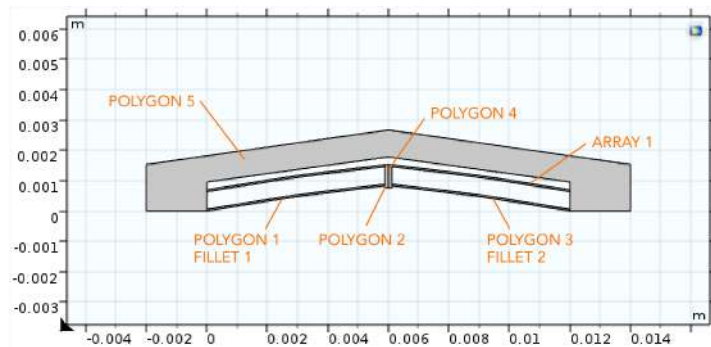


Figure B.6: Geometry of COMSOL model

x (m)	y (m)
0	0
-w1	0
-w1	h1
base/2	(base/2)*sin(theta1[deg]) + h1+0.3e-3
base + w1	h1
base + w1	0
base	0
base	(nbeam-1)*ubeam+t3 + t1
base/2	l1*sin(theta1[deg])+(nbeam-1)*ubeam+t3+t1
0	(nbeam-1)*ubeam+t3 + t1

(a) Polygon 1

x (m)	y (m)
0	0
0	t1
l1*cos(theta1)/2	l1*sin(theta1)/2 + t1 + t1
l1*cos(theta1)	l1*sin(theta1) + t1
l1*cos(theta1)	l1*sin(theta1)
l1*cos(theta1)/2	l1*sin(theta1)/2 + t1

(b) Polygon 2

x (m)	y (m)
l1*cos(theta1)	l1*sin(theta1)-0.06[mm]
l1*cos(theta1)	l1*sin(theta1)+t1+(nbeam-1)*ubeam
base/2	l2*sin(theta2)+t1+(nbeam-1)*ubeam
base/2	l2*sin(theta2)-0.06[mm]

(c) Polygon 3

x (m)	y (m)
base-l2*cos(theta2)	l2*sin(theta2)
base-l2*cos(theta2)	l2*sin(theta2) + t2
base-l2*cos(theta2)/2	l2*sin(theta2)/2 + t2 + t2
base	t2
base	0
base-l2*cos(theta2)/2	l2*sin(theta2)/2 + t2

(d) Polygon 4

x (m)	y (m)
base/2	l1*sin(theta1)-0.06[mm]
base/2	l1*sin(theta1)+t1+(nbeam-1)*ubeam
base-l2*cos(theta2)	l2*sin(theta2)+t1+(nbeam-1)*ubeam
base-l2*cos(theta2)	l2*sin(theta2) -0.06[mm]

(e) Polygon 5

Material

Titanium is used as the material for the entire model, with material properties:

- $E = 113 \cdot 10^9$ Pa
- $\nu = 0.34$

Solid mechanics

- **Fixed constraint** on boundary 3
- **Prescribed displacement** on point 21: $-1.7e-3 \cdot pw1$ (step). Select '*Use weak constraints*'.

Study

- Include geometric nonlinearity
- Parameter sweep: $step = range(0,0.01,2)$
- Linear solver: direct
- Non-linear method: Automatic (Newton)

Results

In order to plot the force-displacement behaviour, create a point graph for point 25. Plot the Lagrange multiplier ($-v_lm0$) against the displacement ($-v$).

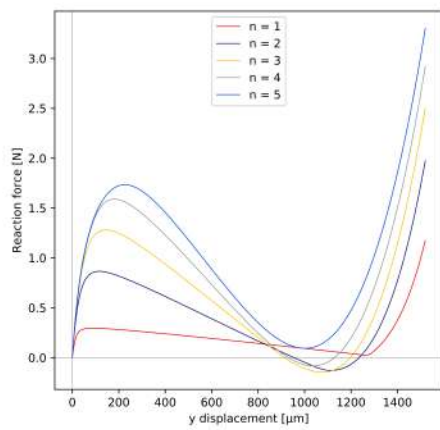
B.3.2. Convergence

Compliant mechanisms exhibit relatively large, geometrically nonlinear deformations. This nonlinearity, combined with the snap-through behaviour between two stable configurations, makes this a non-trivial modelling problem. To avoid the tangential stiffness matrix becoming singular at the global maximum in the force displacement curve, a displacement control rather than load control method must be used. The x-displacement of a point is incrementally increased, causing stresses in the structure to develop, resulting in a reaction force measurable at that point.

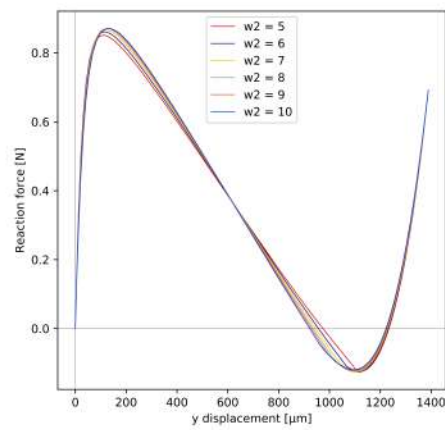
Some imperfections must be added to the beams for them to buckle in a natural way. If completely straight, COMSOL will perfectly compress the beams for as long as possible, resulting in a convergence to higher order buckling modes. Consequently, the stresses found in the deformed beams will be excessively high. In real life no beam is perfectly straight, therefore a very slight curvature ($r = 130\text{mm}$) is added to each of the beams, thereby removing the symmetry of compression. This step is essential to improve the accuracy of the finite element solution.

B.3.3. Varying parameters

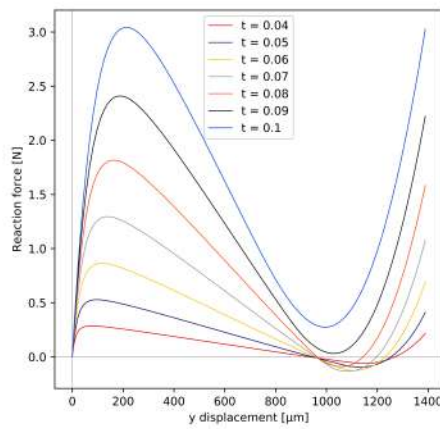
In dimensioning the design and to gain a proper understanding of the mechanism a parameter sweep was done on each of the design parameters in the FEM model and the resulting force-displacement curves compared. Results of this analysis are shown in the Appendix B.3.3 on the following page.



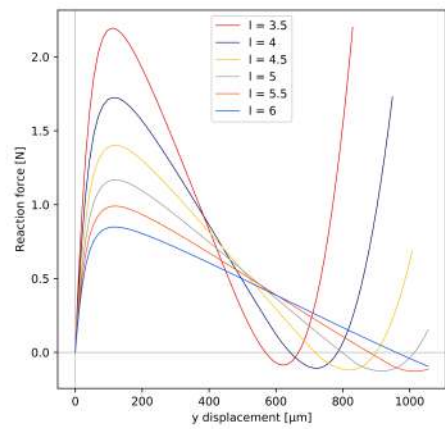
(a) Varying number of parallel flexures



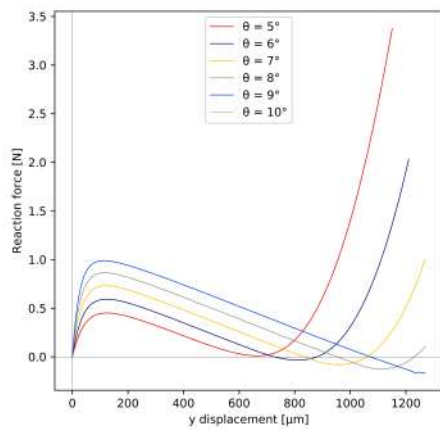
(b) Varying distance between parallel flexures



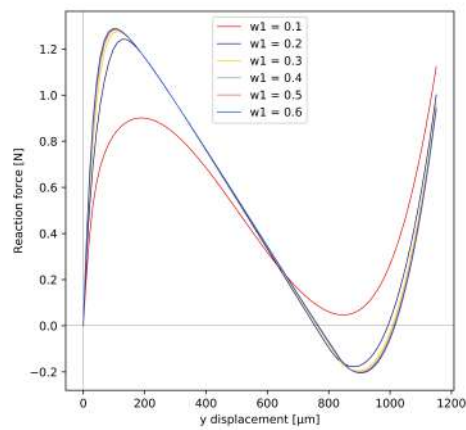
(c) Varying thickness of flexures



(d) Varying length of flexures



(e) Varying angle of flexures

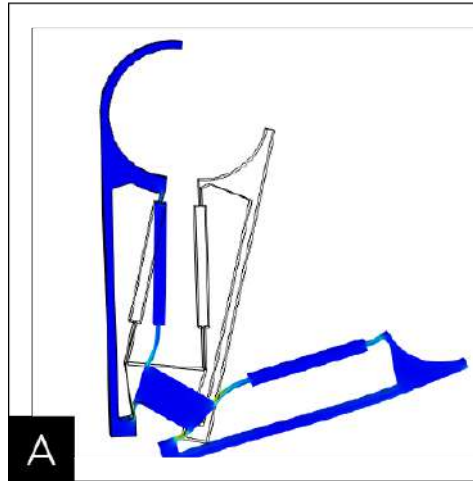


(f) Varying w_1 (see Figure B.4)

Figure B.7: Force displacement behaviour for varying parameters n , u , t , l , θ and w_1 independently

B.4. Concept revision

From simulations of the initial design, the behaviour was not quite as intended. Long beams and very large displacement were required to achieve a second stable state. The required displacement was too big for the size restrictions in the middle ear. Appendix B.4 shows a COMSOL displacement and stress plot of the initial design.



First we took two steps back, to the first morphological chart. The possibility of having a bistable rather than tristable mechanism was reconsidered, since a tristable mechanism perhaps is too complex for the limited space and miniature scale of the device.

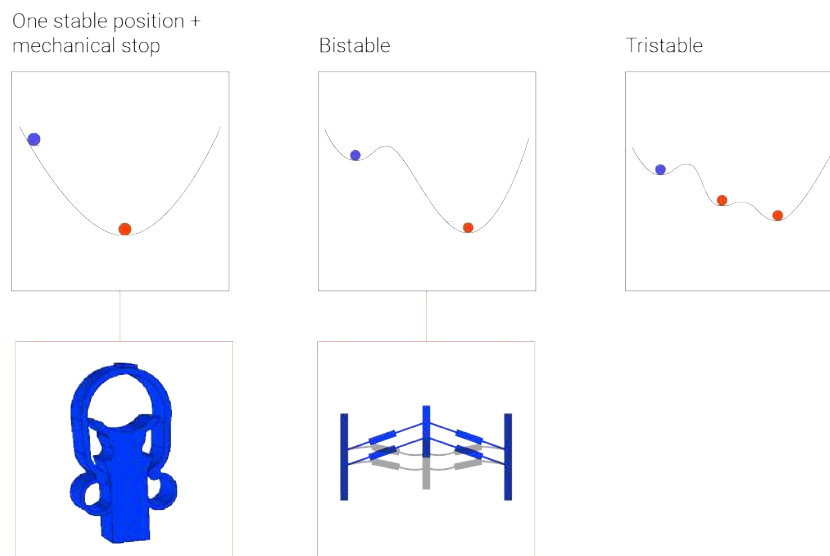


Figure B.8: Two steps back: revisiting the general morphological chart

Looking back to the second morphological chart, the bistable mechanisms were re-evaluated. Figure B.9 shows three mechanisms which were selected in this second iteration of concept evaluation. The first two are fully compliant and properly bistable. At this stage some 3D printed models were made to assist with decision making - some of these can be seen in Figure C.4 in the following section. Comparisons were also made using COMSOL. The parallel fixed-guided beam mechanism (mechanism 2 in the second morphological chart) was chosen since a stronger bistability could be achieved with the same dimensions.

Concept 4 (Figure A.5) was selected as a promising alternative to the original design. Two variations of the design are shown below. The first has the direction of actuation parallel to the vibrational motion of the incus. The second is perpendicular to this motion. Simulations of early versions of the final design are shown

in Figure B.10. The version shown in Figure B.10(b) fulfilled the force design parameters, however it did not open wide enough to easily slip over the incus. Due to the symmetry of the design (compared with the initial design where one of the flexures is shorter than the other) the clasp only translates (no rotation).

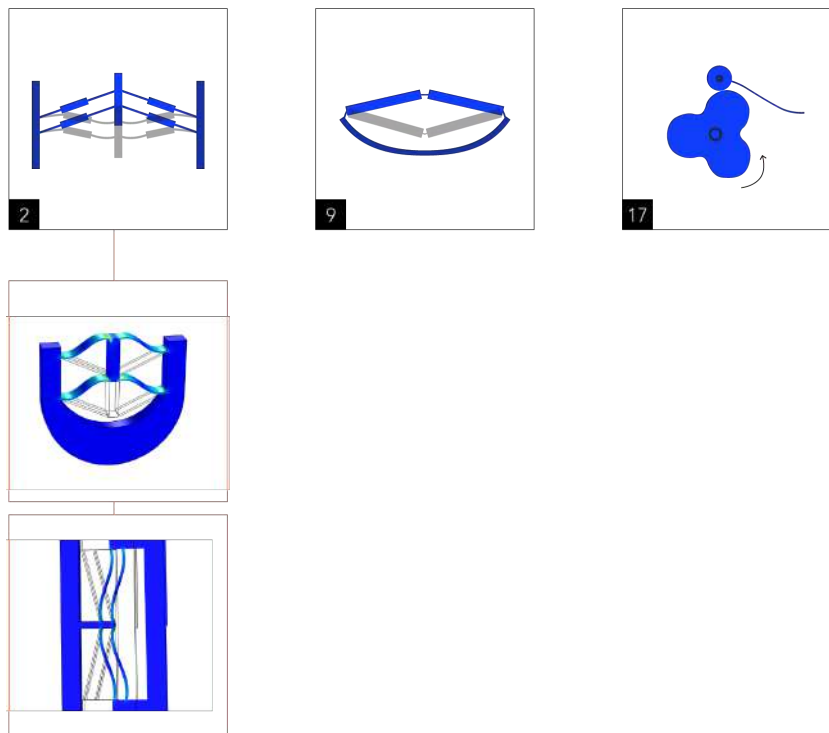


Figure B.9: One step back: revisiting the chart of mechanical solutions. Two embodiments of the first mechanical solution are shown: one with the direction of actuation parallel to the vibrational motion of the incus. The second is with the actuation direction perpendicular to this motion

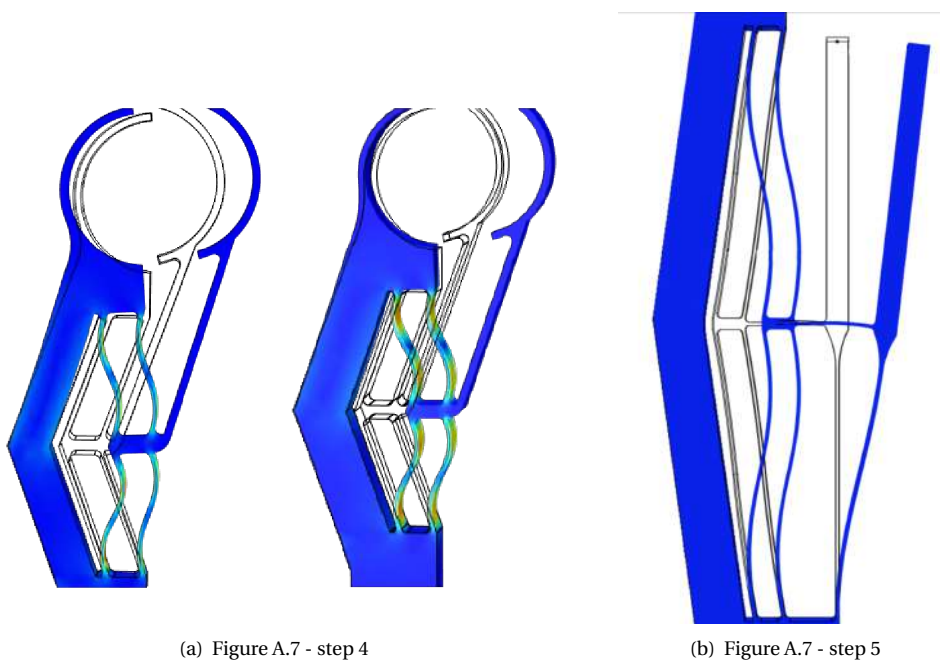
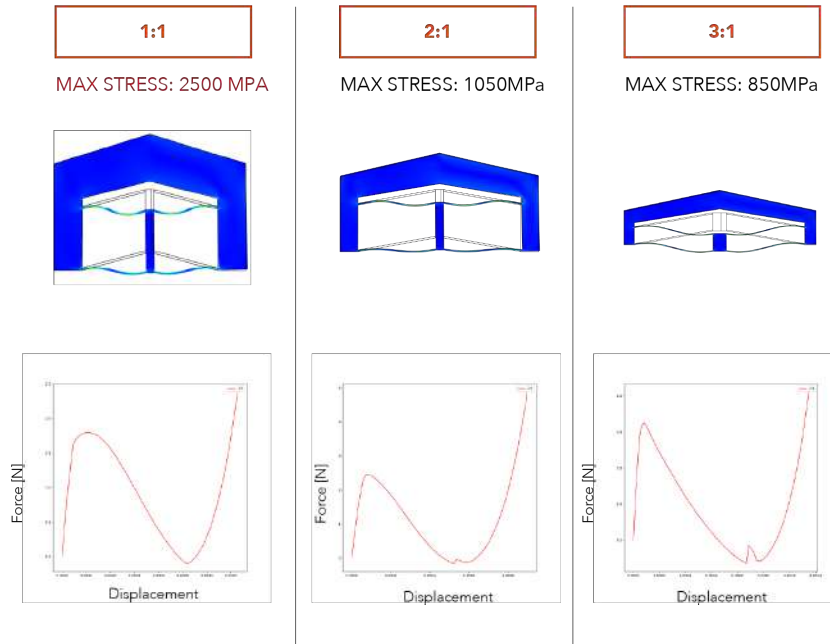


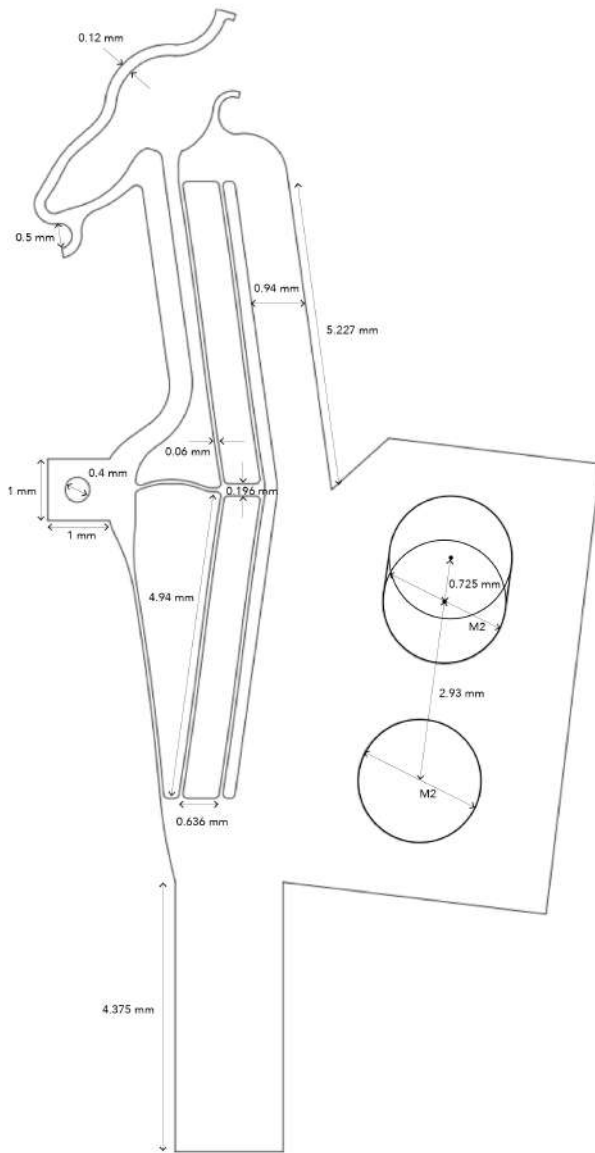
Figure B.10: COMSOL simulations of early versions of the final concept

B.5. Determining minimum prototype scale

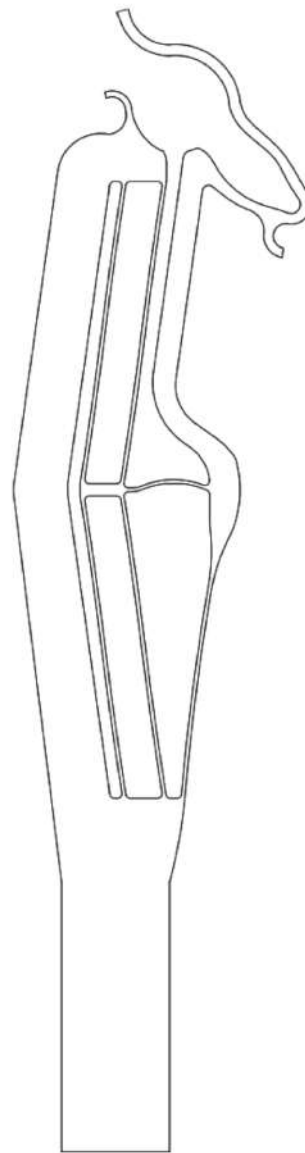
An analysis was done to determine how close we could get to the actual scale of the device. The mechanism was dimensioned at increasing scales, and the maximum stress in the beams was determined. Appendix B.5 shows the results of analysing prototypes at 1:1, 2:1 and 3:1 scales. The length was set as the longest it could be to fit in the middle ear, and the beam thickness at the thinnest according to the manufacturing restrictions. The 3:1 prototype has a maximum stress of 850 MPa, which is just below yield stress (880MPa). Since a low number of load cycles are required in the functioning of the device, the 3:1 version was chosen for prototyping. The factor of safety is therefore about 1.



B.6. CAD drawings



CAD drawing: testing prototype



CAD drawing: demo prototype

C

Manufacturing and measurements

C.1. Manufacturing techniques

While still in the conceptual phase, manufacturing techniques were already being examined. By considering manufacturing options early on, a more realistic prosthesis design could be obtained in the concept selection. Current prostheses were studied with respect to manufacturing, and five distinct categories were identified. These categories purely address the geometry of the prostheses, ignoring additional manufacturing steps such as the setting of shape memory alloys. The five different types of prosthesis attachment geometries are shown in Figure C.1.



Figure C.1: Overview of manufacturing approaches to incus attachment

- 1D: prostheses which consist simply of a wire bent into shape
- 2D: two dimensional manufacturing techniques are used to form a shape from a flat plate
- 2D + bending: a shape is manufactured from a flat plate, and later bent into shape
- 2D + assembly: multiple 2D shapes are manufactured, and later assembled (i.e. stacked)
- 3D: a structure is formed via three-dimensional manufacturing techniques. In the case of the bucket prosthesis, assembly is also required.

The overview of manufacturing techniques below are split up into the categories 2D and 3D.

C.1.1. 2D | Laser cutting

Laser cutters typically use optics to concentrate a laser beam onto the substrate, removing the material where desired. Laser cutting is one of the key technologies used to manufacture coronary stents, another implantable micro mechanism. Laser cutters can have positioning accuracy as low as 10 μm [5].

C.1.2. 2D | Wire Electron Discharge Machining (EDM)

Wire EDM cuts through a conductive material via an electric discharge between a continuously moving wire and the workpiece. The wire moves through a spool, passing through the material and into a collection bin. The workpiece is completely submerged in a dielectric fluid - typically deionised water. As the distance between the wire and the workpiece becomes small enough, the dielectric breaks down, allowing a spark to jump between the wire and the workpiece. This electric discharge process repeats constantly, eroding at the workpiece. The wire also erodes, but is continuously being replaced.

Being able to form internal shapes is essential for the application of a bistable stapedotomy prosthesis. All of the bistable/multistable units that were compiled in the concept generation phase of this project include at least one hole. This can be addressed with wire EDM by first drilling a pilot hole, and then threading the wire. Threading and cutting of the wire can be done by the machine automatically.

The diameter of the wire can be as low as $20\ \mu\text{m}$, with a precision of $\pm 1\ \mu\text{m}$. In this case, the smallest internal corner radius would be about $10\ \mu\text{m}$. The cutting width is always slightly larger than the diameter of the wire since the distance between wire and workpiece where electric discharge begins to occur is non-zero. A simple schematic demonstrating this principle is shown in Figure C.2.



Figure C.2: Wire EDM offset

A major advantage of wire EDM for the manufacturing of bistable compliant mechanisms is the high aspect ratio that can be achieved.

C.1.3. 2D | Deep Reactive Ion Etching (DRIE)

DRIE is a method of etching deep, straight walled structures, by alternating passivation and etching steps. In the passivation step a protective layer is deposited. The etch step involves bombardment of ions through a mask. The sidewalls of the structure are protected, however the bottom layer is directly hit by ions, resulting in an etched layer.

This process is traditionally used to etch silicon, however silicon is not biocompatible and therefore cannot be used in the design of the implantable stapes prosthesis. Deep reactive ion etching of titanium is also possible. Aimi et al. [1] developed a method (MARIO) to bulk micromachine high-aspect-ratio titanium structures. At the time of their paper publication, MARIO had been used to etch titanium sheets with thicknesses ranging from $10\ \mu\text{m}$ to $500\ \mu\text{m}$.

C.1.4. 3D | Selective laser melting

SLM is a form of additive manufacturing whereby a laser is used to selectively melt powdered metal, forming a solid 3D structure. The process, as with standard polymer 3D printers, works layer-by-layer. Highly complex 3D structures not possible with traditional manufacturing techniques can be easily created. SLM varies from SLS (Selective Laser Sintering) by its higher density. It is possible to produce near 100% dense structures, with properties close to that of structures made with traditional manufacturing processes. SLS structures, on the other hand, are porous.

For the bistable stapedotomy prosthesis designs explored in this research, the minimum allowable feature size possible with SLM is not small enough. S. Campanelli *et al.* [7] studied the performance of SMA, and found the minimum feasible thin wall thickness to be 0.2mm, with a maximum error of 15%.

C.1.5. 3D | Micro milling

Micro milling is essentially a minimisation of traditional machining techniques, such as milling, drilling and turning. It is a popular machining method due to its potential to create complex 3D geometry with feature sizes ranging from tens of micrometers to a few millimetres [2].

When working with titanium micro milling is a particularly expensive process, mainly due to the high rate of tool turnover [6]. Due to titanium's low conductivity, the heat is not able to quickly dissipate through the workpiece, but rather concentrates at the tool tip. Plastic deformation and wear of the tool tip due to high speeds also contribute to this high turnover.

C.2. Materials

Biocompatible materials that are already being used in existing stapes prostheses are listed in Table 3, along with their material properties. The two materials that were seriously considered for the new prosthesis design were titanium and Nitinol. These two materials are typical for modern stapes prostheses.

Material	Young's Modulus (GPa)	Yield strength (MPa)	Poisson's ratio	Density (g/cm ³)
Titanium	116	880	0.32	4.506
Nitinol	Austenite	195-690	0.33	6.45
	Martensite	70-140		
Gold	79		0.4	19.30
Teflon	0.55	0.862 - 41.4	0.46	2.16
Platinum	168	35-180	0.38	21.45

Table 3: Material properties for materials used in current prostheses

C.3. Prototypes

C.3.1. Design process demonstrators

Periodically during the design process various mechanisms were 3D printed from PLA. The purpose was always to test ideas and get a feeling for what is and isn't working. Photos of some of these large demonstrators are shown in Figure C.4 (a)-(g).



Figure C.3: First 3D printed prototype of initial design

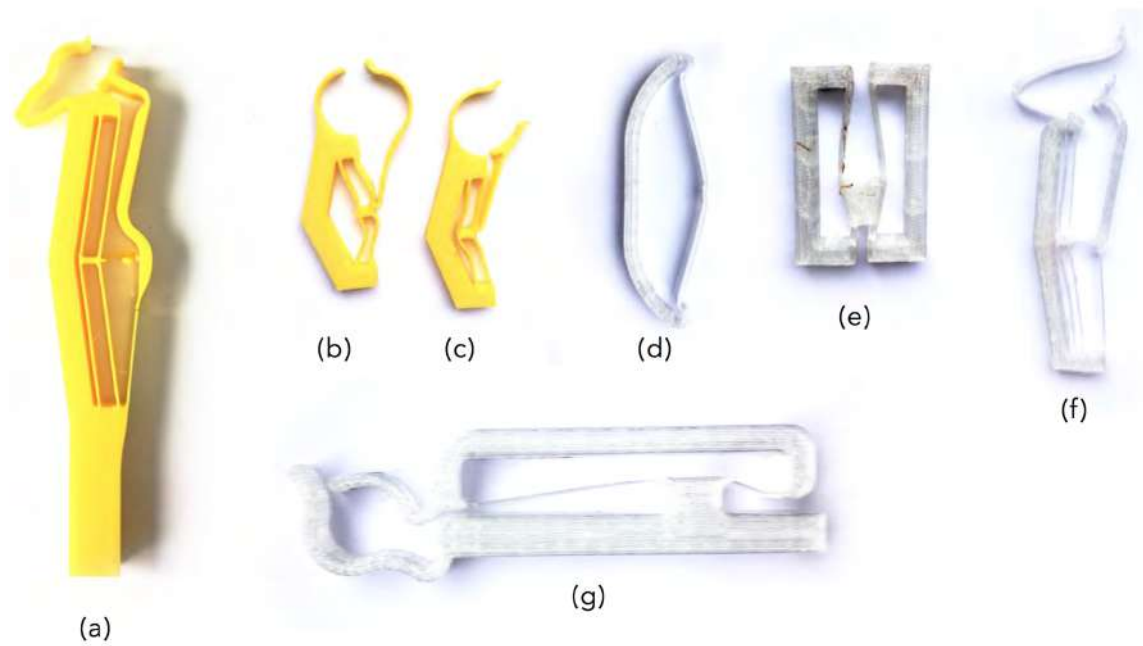


Figure C.4: Various 3D printed demonstrators. (a) Penultimate iteration of the design. (b),(c) Early version of the final design (Figure A.7-4). (d) Exploring alternative bistable mechanisms. (e) First 3D printed prototype of initial design. (f) Early version of the final design. (g) Simplified version of initial design

C.3.2. Wire EDM: copy of existing prosthesis

A copy was made of an existing prosthesis to test the performance of the wire EDM machine, and to determine whether or not we can manufacture in titanium at this scale. If this test had not been successful then micro laser cutting would have been looked into further. As a last resort the ‘proof-of-concept’ in the scope of this project would have simply been a large 3D printed demonstrator. It was worth pursuing a prototype closer to the actual size to further illustrate the feasibility of the design. For this prototype, the design was cut from a 5mm titanium rod using wire EDM. It was then sliced, so that many identical prototypes were made at once. As a result the entire surface is quite rough. This can be seen in Figure C.5.

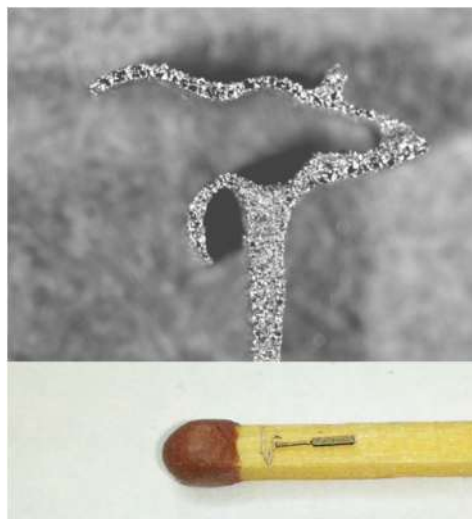


Figure C.5: Wire EDM copy of existing prosthesis

C.3.3. Wire EDM: bistable prosthesis

Wire EDM test prototype: first attempt

In the first attempt at manufacturing the prototype, some of the flexures broke during the wire EDM process. This initial attempt, though not successful in itself, allowed us to properly calibrate the offset of the wire. Images of this attempt are shown below in Figure C.6. The bottom right image is a photograph of the wire EDM machine with the workpiece clamped in place, and the wire threaded through one of the pilot holes.



Figure C.6: Left: Keyence microscope image of first attempt at wire EDM prototype. Top right: image of first wire EDM attempt. Bottom right: Wire EDM setup during manufacture of first prototype.

Issues and solutions

During the manufacturing of the first wire EDM prototype, many issues were encountered. Table ?? below details the issues that were encountered, and the solutions that were found.

Issue	Reason	Fix
Corner between clamp and base too sharp → Machine error.		Add a radius between each segment
Still same error	Segment before corner is extremely short	Back to CAD model: add fillet in Inventor Manually add fillet into EDM code
Receiving wheel clogged	Wire stuck in machine	Open up machine and remove wire
Threading into holes: machine not able to do it itself	Near end of wire spool... so wire had curvature with small radius Wire nozzle was quite far away from the sample plate, since the piece was being machined close to the clamp (chosen because there is less deflection of the sample)	Had to thread each hole manually
Wire getting tangled and not able to pass through feeding tube	Reason unknown.. was not working properly Near end of wire spool	Manual threading and untangling... Patience
First prototype: two beams broke during EDM process	Offset was set too high	Measure resulting beam thickness and use measurements to determine proper offset

Issues encountered in manufacturing EDM prototype, and the solutions found

Mass production

Some considerations have been made into how the device could be produced at a higher rate. One of the major issues that slowed down the production of the prototypes was the wire had to be fed into the pilot holes by hand. The wire EDM machine should be able to feed the wire through automatically. The nozzle should be located very close to the material, so that the machine can cut and thread the wire on its own. In the production of the prototypes, the workpiece was clamped at just one end. The prototype was then cut from a section of the workpiece quite close to the clamp, since this is where the displacements due to bending are smallest. However, this meant that the wire feeder was quite far away from the workpiece in order to clear the clamp. A solution could be to clamp the workpiece at two ends, and cut somewhere closer to the middle. In this way the wire feeder could be located very close to the workpiece.

Another way to increase the chance of the wire feeding automatically into the pilot holes would be to place another sheet of material directly above the workpiece, with conical shaped holes above the workpiece pilot holes. The purpose of the conical holes is to direct the wire into the pilot holes.

Wire EDM test prototype: second attempt

In the second iteration of manufacturing the titanium prototype the wire offset was adjusted. This time the flexures did not break. Three prototypes were manufactured for measuring. Appendix C.3.3 shows a Keyence microscope image of one of the three prototypes.



Details of the prototypes are shown in Figure C.7. The top left image shows one of the prototypes in its second stable state - proving its bistability. The surface finish of the edges is very rough and this is most clearly seen in the bottom left and top right images of Figure C.7. The purpose of this prototype is as a 'proof-of-concept' - to prove the bistability. Surface finish is not a concern at this point of the design process. The top right image shows a detail of a pilot hole that was drilled in the titanium sheet. The wire from the EDM machine was threaded through this hole to create an internal shape. The wire from the EDM machine was threaded through this hole to create an internal shape.



Figure C.7: Keyence microscope images of second attempt at wire EDM prototype

Wire EDM demo prototype

One prototype was manufactured without the baseplate and hole for the probe. This is the 'demo' prototype, and is the closest we got to the actual device within the scope of this thesis. Images of the demo prototype in its first and second stable positions are shown in Figure C.8. In order for it to be suitable for implanting into a patient a few things would need to be addressed. Firstly, the size needs to be reduced by a factor of 3. Secondly, the piston end of the prosthesis must be cylindrical. This was not attempted in these initial prototypes since the aim was to primarily to verify the bistability of the attachment end. A cylindrical titanium piston attached to a 2D attachment is the structure of many existing prostheses, so it is not necessary to prove its feasibility. In future prototypes a cylindrical end could be manufactured by micro milling, and then the attachment end could be cut with wire EDM in the same way as done here.

C.4. Test setup and measurements

Experiments were conducted with the purpose of verifying the FEM simulations and PRBM analysis of the mechanism. In particular, the force-displacement relationship of the bistable mechanism and of the clasp mechanism were measured and compared with simulation results. An existing setup was modified and used for the experiments. After the first set of measurements, further modifications were made to the setup to improve repeatability of the experiments.



Figure C.8: Wire EDM demo prototype in two stable positions

C.4.1. First test series

Since bistable behaviour was being measured, small modifications to the existing setup had to be made to allow for the change in direction of the force mid-stroke. A schematic of the resulting setup is shown in Figure C.9. In the original setup the probe was an acupuncture needle, directed into the substrate at an angle. In the modified setup, the holder for the sensor was modified so that the probe is parallel to the workpiece. A new probe was machined with a 0.4 mm pin, perpendicular to the workpiece. This pin is inserted into a 0.4 mm hole in the test prototype. In this way, the probe can both push and pull the mechanism. There may be a small backlash due to the gap between the pin and the 0.4 mm holes in the probe and prototype.

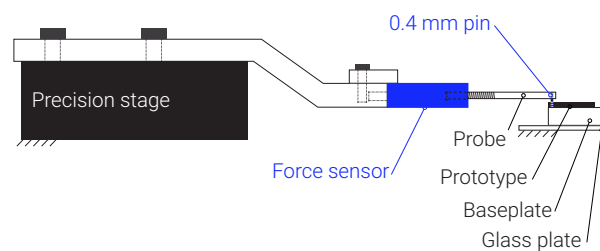


Figure C.9: Schematic of modified test setup

A Futek 100 gram sensor was used to take the force-displacement measurements. Figure C.10 shows the test setup for the first test series, before improvements were made on the mounting technique. The prototype is screwed into a 3D printed base plate. The screws quickly degrade the 3D printed material, hence impacting the precision of the measurements.

A CAD model of the modified sensor holder is shown in Figure C.11(a). Figure C.11(b) is the CAD design of the new probe for measuring bistability.

Measurements of prototype 1 and prototype 2 are shown in Figure C.12(a) and Figure C.12(b) respectively. Two sets of measurements were taken of prototype 3. These are plotted in Figure C.13.

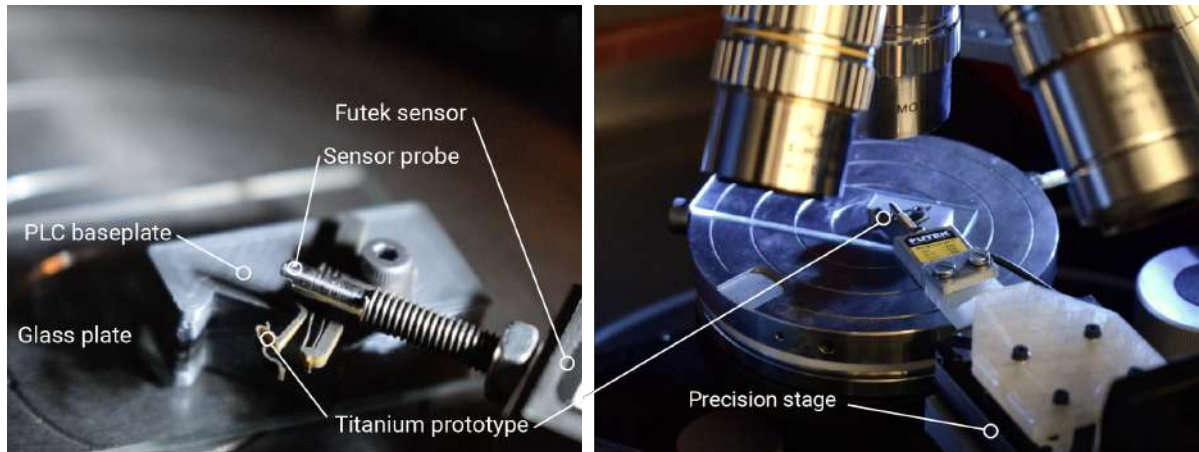
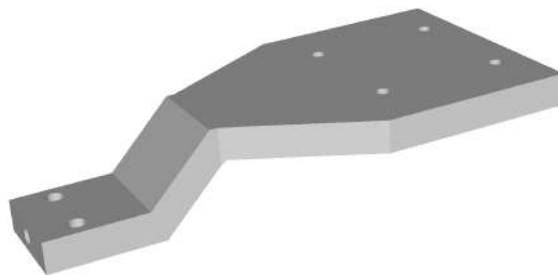


Figure C.10: Images of test setup during the first test series

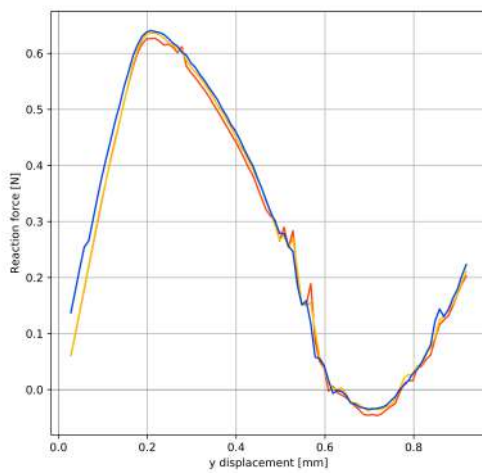


(a) CAD design of new sensor mounting

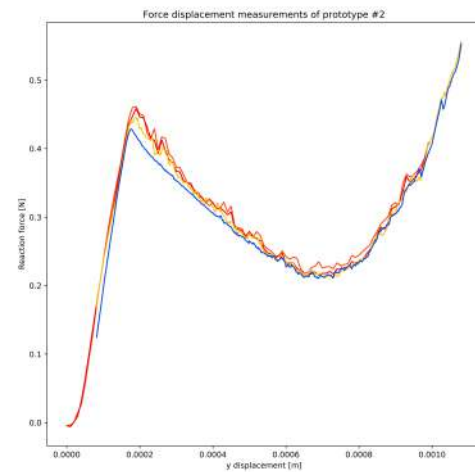


(b) Design of bistable probe

Figure C.11: CAD designs for parts of new setup



(a) Prototype 1



(b) Prototype 2

Figure C.12: Force-displacement measurements of prototype 1 and 2

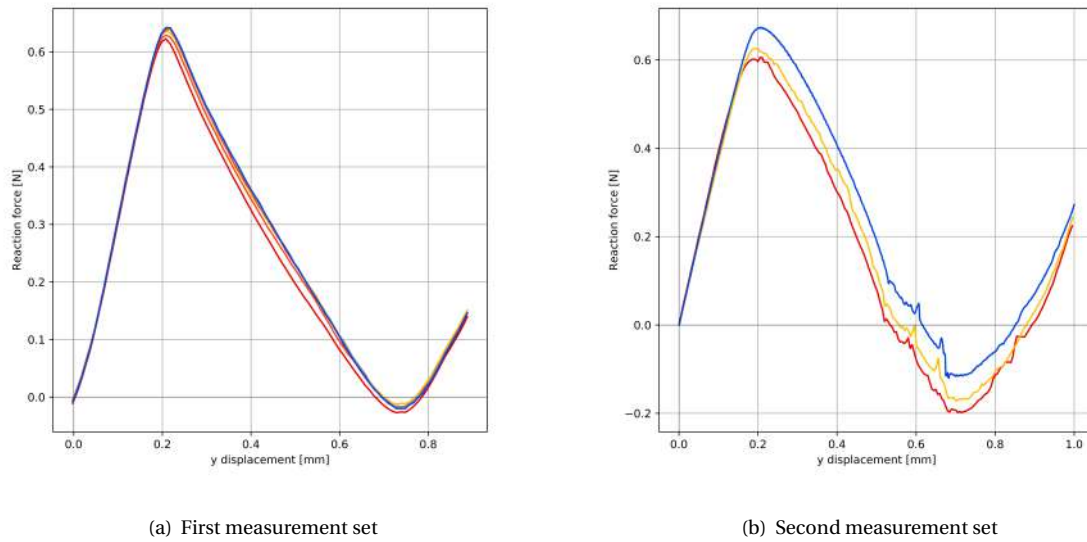


Figure C.13: Force-displacement measurements of 3rd prototype

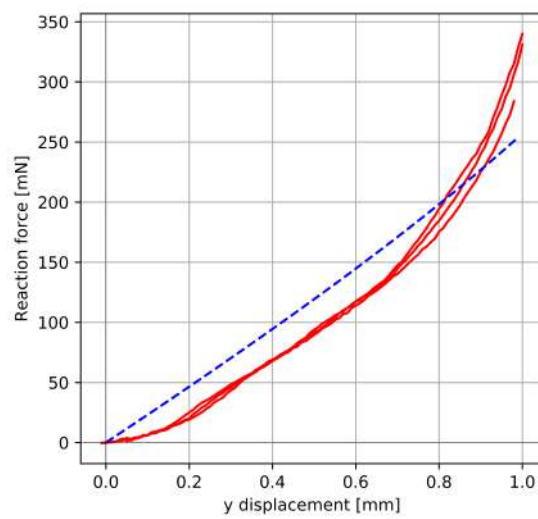
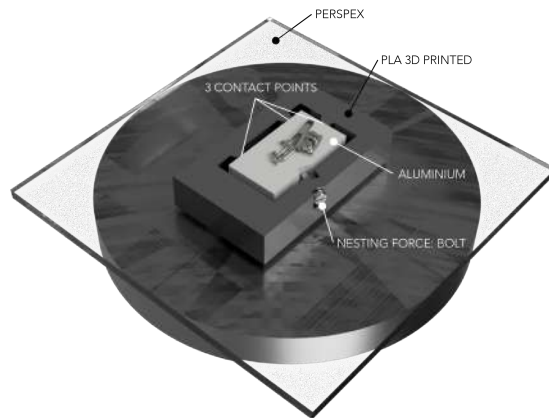


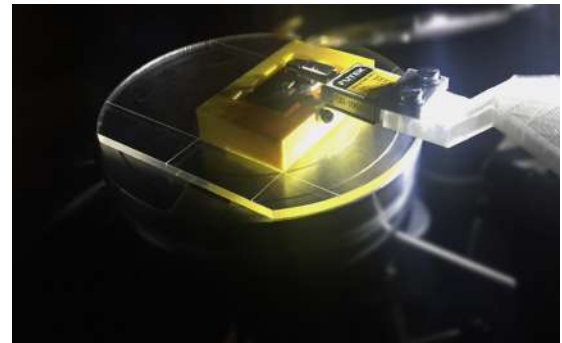
Figure C.14: Measurement of clasp force-displacement behaviour compared with COMSOL simulation

C.4.2. Second test series

In order to improve the repeatability of experiments, the test setup was revised and an alternative mounting method was designed. A CAD render of this schematic is shown in Figure C.15(a). The perspex base is much larger than in the original test setup, and as a result, the vacuum pump was able to provide a much stronger hold, minimising one possible cause for error (moving of baseplate). A 3D printed base is glued onto the perspex base. There is a kinematic coupling between this base and the aluminium piece that sits in it. There are three contact points between the 3D printed base and the aluminium insert, plus a nesting force provided by a bolt that is screwed into the base. Two threaded holes are placed in the aluminium insert in the precise location such that when the sensor probe moves rectilinear to the base, the prototype is actuated along the desired path. Using Aluminium threaded holes rather than screwing into 3D printed PLA further improves the accuracy of the mounting.



(a) CAD render



(b) Photograph in action

Figure C.15: Render and photo of new measurement setup

Two sets of measurements were made to verify repeatability. The prototype is mounted and a first set of force-displacement curves are measured. The Aluminium insert is demounted, and the prototype is then completely unscrewed. The setup is then reassembled and a final set of measurements is made. These two measurement sets are compared for prototypes 3 and 1 in Figure C.16(a) and Figure C.16(b) respectively. Prototype 2 was broken during demounting in the first measurement series, so was not tested again. This measurement setup has far more repeatable results compared with the first version.

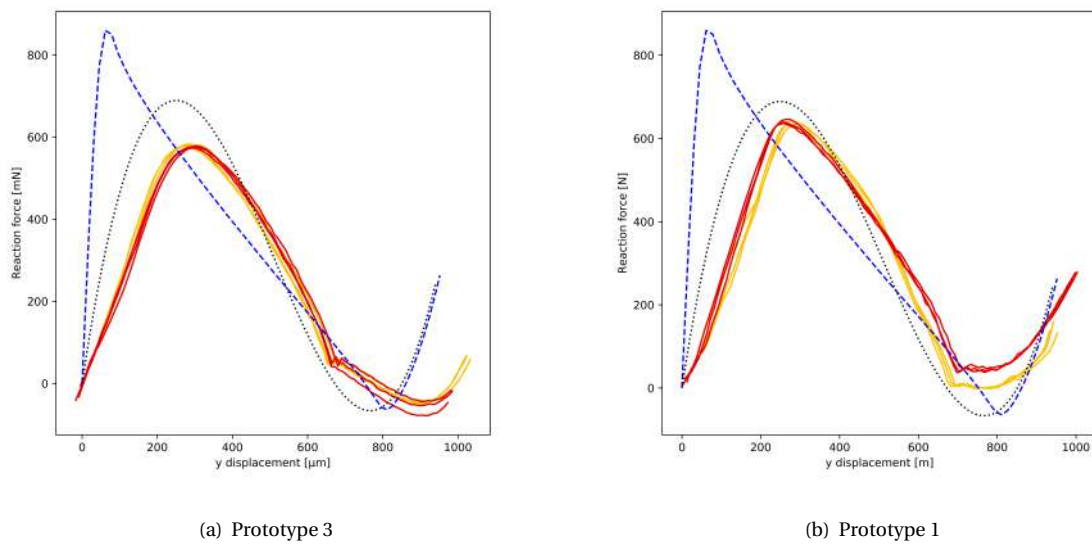


Figure C.16: Measurement results for second test setup, prototype 3 and 1. Red: first measurement set. Yellow: Measurement set after demounting and remounting

D

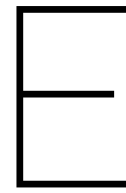
Final design



Figure D.1: Photograph of test prototype



Figure D.2: Renders of test prototype



Code

E.1. PRBM python code

```
1 import numpy as np
2 import pandas as pd
3 import pylab
4 import matplotlib.pyplot as plt
5 from operator import add
6 import math
7
8 # ----- Parameters ----- #
9 gamma=0.85
10 K_Theta = 2.65
11
12 lbase = 12.2e-3
13 t = 0.06e-3
14 d = 1e-3
15 l = 4.9e-3
16 w1 = 0.4e-3
17 h1 = 1.76e-3
18 theta0 = np.deg2rad(8)
19
20 w2=0.9e-3
21
22 E = 1.138E+11
23
24 # Determine r
25 r = l*gamma
26 r10 = r*np.cos(theta0)
27 r20 = r*np.sin(theta0)
28
29 # Moments of inertia
30 lbeam = (d*t**3)/12
31 I2 = (d*w1**3)/12
32 I3 = (d*w2**3)/12
33
34 # PREM equivalent torsional stiffness
35 kt = 2*gamma*K_Theta*E*lbeam/l
36
37 # PREM equivalent axial stiffness
38 ka1 = 3*E*I2/(1e-3**3)
39 ka12 = 3*E*I2/(0.3e-3**3)
40 ka2 = 3*E*I3/((3e-3)**3)
41 ka = 1/((1/ka1)+(1/ka1)+(1/ka2))
42
43 ksensor = 0.01
44
45 # For deflection d2i, find linear spring deflections
46 step = 0.01e-3
47 d2 = np.arange(0,2.5*r20, step)
48 d1 = np.zeros(len(d2))
```

```

49 r2 = np.zeros(len(d2))
50 r1 = np.zeros(len(d2))
51
52
53 theta = np.zeros(len(d2))
54
55 phi2 = np.zeros(len(d2))
56 phi1 = np.zeros(len(d2))
57
58 g1 = np.zeros(len(d2))
59 g2 = np.zeros(len(d2))
60
61 F = np.zeros(len(d2))
62 E = np.zeros(len(d2))
63
64 # Construct E[i] and F[i] arrays
65 for i in range(len(d2)):
66     r2[i] = r20-d2[i]
67
68     theta[i] = np.arctan(r2[i]/r10)
69
70     r1[i] = math.sqrt(r2[i]**2+r10**2)
71
72     d1[i] = r0-r1[i]
73
74 # Angle deflections
75     phi1[i] = theta0 - theta[i]
76     phi2[i] = -phi1[i]
77
78 # Kinematic coefficients
79     g1[i] = 1/(r1[i])
80     g2[i] = r2[i]/(r1[i])
81
82 # Force
83     F[i] = 8*g1[i]*kt*(abs(phi1[i])+abs(phi2[i])) + g2[i]*ka*d1[i] - ksensor*d2[i] - 700*d2[i]
84
85 # Energy
86     E[i] = 0.5*kt*(8*abs(phi1[i])**2) + 0.5*ka*d1[i]**2
87
88
89 # ----- Import Measurements ----- #
90 Prob3_1 = pd.read_table('0307/Prob3_1.txt', delim_whitespace=True, names=('t', 'u', 'F'))
91 Prob3_2 = pd.read_table('0307/Prob3_2.txt', delim_whitespace=True, names=('t', 'u', 'F'))
92 Prob3_3 = pd.read_table('0307/Prob3_3.txt', delim_whitespace=True, names=('t', 'u', 'F'))
93 Prob3_4 = pd.read_table('0307/Prob3_4.txt', delim_whitespace=True, names=('t', 'u', 'F'))
94 Prob3_5 = pd.read_table('0307/Prob3_5.txt', delim_whitespace=True, names=('t', 'u', 'F'))
95
96 # ----- Import COMSOL simulation ----- #
97 Comsol_0507 = pd.read_table('0507_force.txt', delim_whitespace=True, names=('u', 'F'))
98
99 # Plot PRBM results
100 plt.plot(d2,F,'k:')
101
102 # Plot COMSOL simulation results
103 plt.plot(Comsol_f_19_06['u'], Comsol_f_19_06['F'], 'b--')
104
105 # Plot measurement data
106 plt.plot(Prob3_1['u'], Prob3_1['F'],'r')
107 plt.plot(Prob3_2['u'], Prob3_2['F'],'r')
108 plt.plot(Prob3_3['u'], Prob3_3['F'],'r')
109 plt.plot(Prob3_4['u'], Prob3_4['F'],'r')
110 plt.plot(Prob3_5['u'], Prob3_5['F'],'r')
111 plt.plot(Prob3_6['u'], Prob3_6['F'],'r')
112
113
114 plt.legend(['Comsol simulation', 'PRBM', 'Measurements'])
115 plt.axhline(0, color='black', linewidth = 0.2)
116 plt.axvline(0, color='black', linewidth = 0.2)
117 plt.xlabel('y displacement [mm]')
118 plt.ylabel('Reaction force [N]')
119 plt.title('Prototype 3, Test 1')

```

```

120 plt.grid()
121 plt.savefig('pro3_test1.png', format='png', dpi=1000)
122 plt.rcParams['figure.figsize'] = [5, 5]
123
124 plt.show()

```

Listing E.1: Python code for PRBM analysis of final design and plotting against COMSOL simulation and measurement data

E.2. ANSYS code

```

1 FINISH
2
3 /CLEAR,START
4
5 !Set parameters
6
7 result_file_path = '/Users/lolagiuffre/University/02 MSc TU Delft/Thesis/Analytical/ADPL'
8
9 L1 = 1.3e-3
10 L2 = 0.3e-3
11 t1 = 50e-6
12 t2 = 50e-6
13 theta1 = 15
14 theta2 = 20
15 base = 2e-3
16 gap = 50e-6
17 w = 200e-6
18
19
20 /PREP7
21 !element selection
22 ET,1,BEAM188
23
24 !define cross section
25 SECTYPE, 1,BEAM,RECT,0
26 SECOFFSET,CENT
27 SECDATA,t1,w
28
29 SECTYPE, 2,BEAM,RECT,0
30 SECOFFSET,CENT
31 SECDATA,w,w
32
33 !material properties
34 MPIEMP,1,0
35 MPDATA,EX,1,,80e9
36 MPDATA,PRXY,1,,0.3
37
38 !define keypoints
39 *AFUN,DEG
40 K,1,0,0
41 K,2,L1*cos(theta1),L1*sin(theta1)
42 K,3,base-L2*cos(theta2),L2*sin(theta2)
43 K,4,base,0
44 K,5,0,-gap
45 K,6,L1*cos(theta1),-L1*sin(theta1)-gap
46 K,7,base-L2*cos(theta2),-L2*sin(theta2)-gap
47 K,8,base,-gap
48 K,9,0,-600e-6
49 K,10,base,-600e-6
50
51 !define lines
52 *GET,Line_ID1,LINE,0,NUM,MAXD
53 L,1,2
54 L,3,4
55 L,5,6
56 L,7,8
57
58 *GET,Line_ID2,LINE,0,NUM,MAXD
59
60 L,5,9
61 L,9,10

```

```

62 L,8,10
63 L,2,3
64 L,3,7
65 L,6,7
66 L,2,6
67
68 *GET, Line_ID3 ,LINE,0 ,NUM,MAXD
69
70 !meshing of lines
71 TYPE,1 !element type1
72 SECNUM,1 !section num1
73 LSEL, S, LINE, , Line_ID1+1,Line_ID2 !select lines
74 LESIZE ,ALL, , ,20 !mesh 20 elements per line
75 LMESH,ALL !mesh all selected elements
76 ALLSEL,ALL !reselect everything
77
78 TYPE,1
79 SECNUM,2
80 LSEL, S, LINE, , Line_ID2+1,Line_ID3
81 LESIZE ,ALL, , ,5
82 LMESH,ALL
83 ALLSEL,ALL
84
85 /ESHAPE,1
86
87
88 ! Get nodes under keypoints
89
90 ID_ground1 = 1
91 ID_ground2 = 4
92 ID_shuttle = 9
93
94 KSEL, S, KP, , ID_ground1
95 NSLK, S
96
97 *GET, ID_ground1 ,NODE, ,NUM,MIN
98 KSEL, S, KP, , ID_ground2
99 NSLK, S
100
101 *GET, ID_ground2 ,NODE, ,NUM,MIN
102 KSEL, S, KP, , ID_shuttle
103 NSLK, S
104
105 *GET, ID_shuttle ,NODE, ,NUM,MIN
106
107 ALLSEL,ALL
108
109 NSEL, ALL
110
111 D, ID_ground1 , ALL, 0
112 D, ID_ground2 , ALL, 0
113 D, ID_shuttle , UY, -1.4e-3
114
115 /SOLU
116 ANTYPE,0 !static analysis
117 NLGEOM,ON
118 OUTRES,ALL,ALL !save all substep information
119
120 nSubsteps = 100
121 NSUBST, nSubsteps , , nSubsteps
122
123 TIME, 1
124
125 SOLVE
126
127 /POST1
128 PLDISP, 0
129
130 /POST26
131 TIMERANGE, 0 , 2
132 RFORCE, 2 , ID_Shuttle , F, Y, FY

```

```
133 NSOL,3, ID_Shuttle,U,Y,UY
134 XVAR,3
135 PLVAR,2
136
137 *CREATE, scratch , gui
138 *DEL, VAR_export
139 *DIM, VAR_export, TABLE, nSubsteps+1,4
140 VGET, VAR_export(1,0),1
141 VGET, VAR_export(1,1),2
142 VGET, VAR_export(1,2),3
143 /OUTPUT, 'Lola_ANSYS_results', 'txt', result_file_path
144 *VWRITE, VAR_export(1,0),VAR_export(1,1),VAR_export(1,2)
145 %G, %G, %G
146 /OUTPUT,TERM
147
148 *END
149
150 /INPUT, scratch , gui
```

Listing E.2: ANSYS code to run simulation on the initial design and plot force-displacement relationship

F

Extra material

F.1. Photographs from stapedotomy surgery

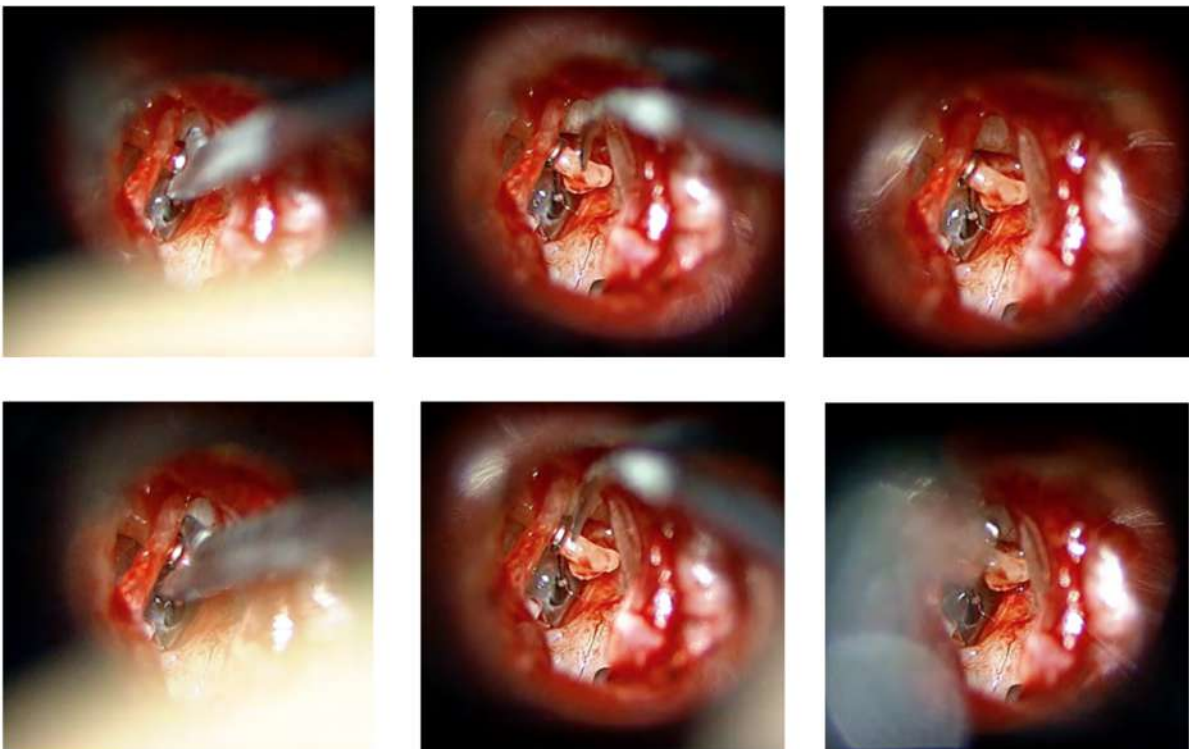


Figure F.1: Video stills from stapedotomy surgery

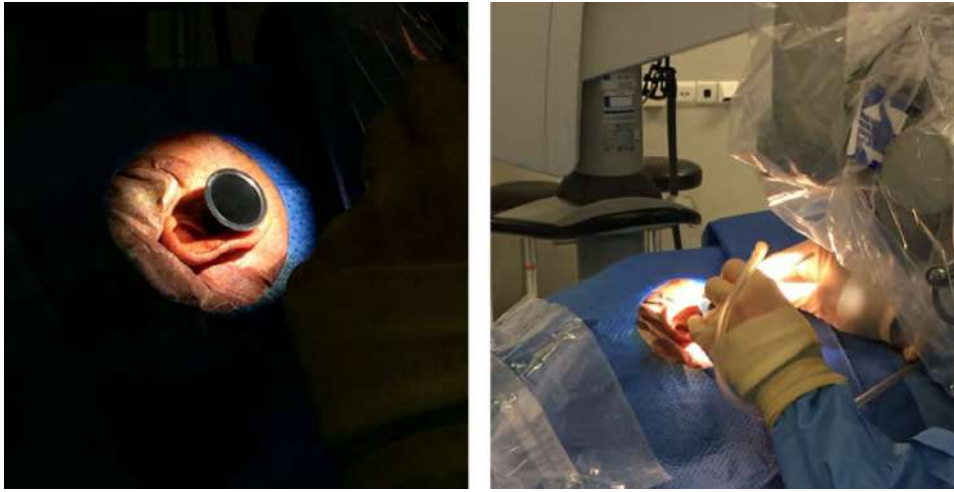
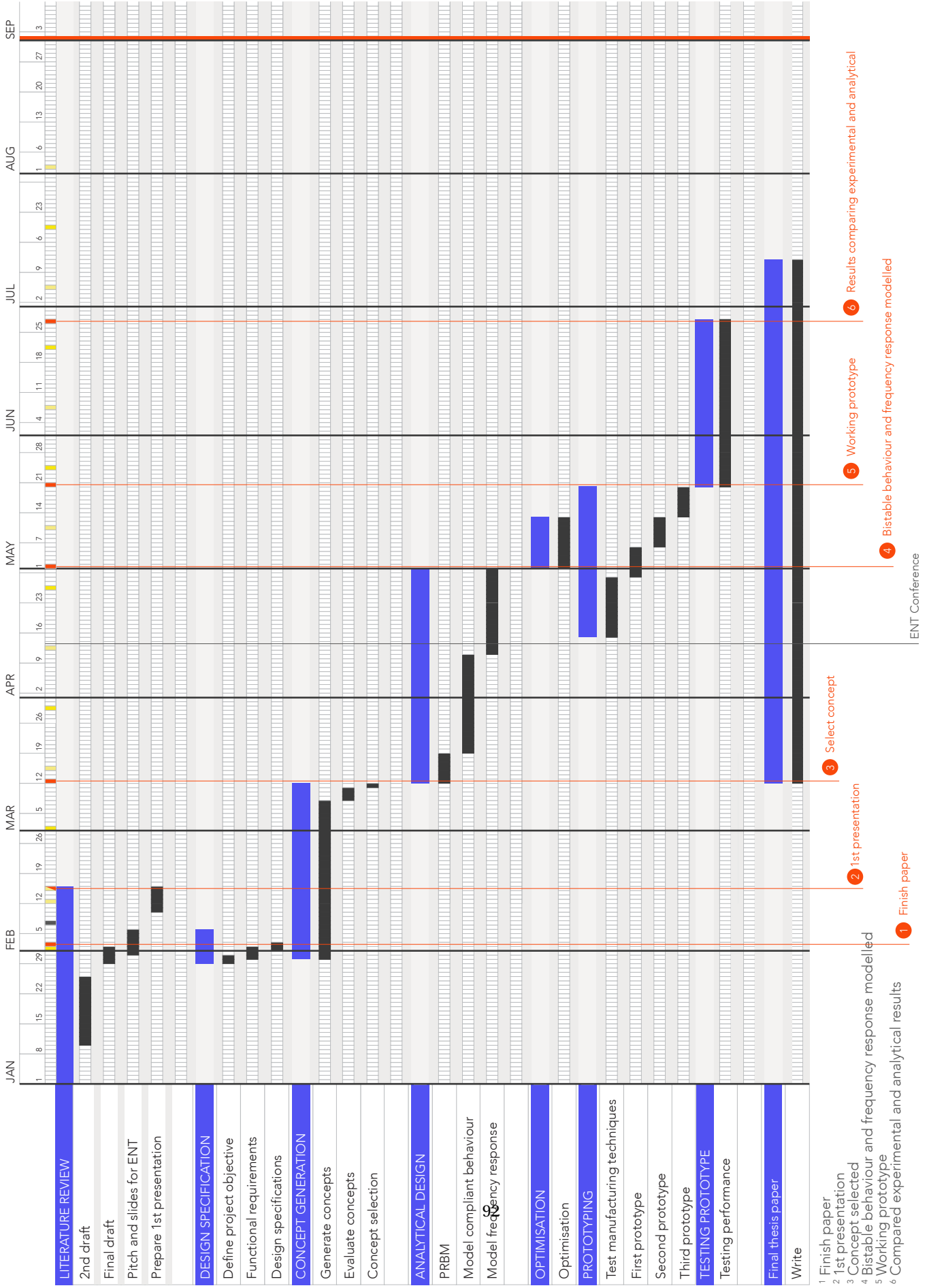


Figure E2: Photographs from viewing live stapedotomy surgery



Figure E3: KNO Vergadering 2018

F.3 Timeline



References

- [1] M. F. Aimi et al. "High-aspect-ratio bulk micromachining of titanium". In: *Nature Materials* 3.2 (Feb. 2004), pp. 103–105.
- [2] J. Chae, S. Park, and T. Freiheit. "Investigation of micro-cutting operations". In: *International Journal of Machine Tools and Manufacture* 46.3-4 (Mar. 2006), pp. 313–332.
- [3] U. Fisch. *Tympanoplasty, Mastoidectomy, and Stapes Surgery*. 2008, p. 396.
- [4] L. L. Howell, S. P. Magleby, and B. M. (M. Olsen. *Handbook of compliant mechanisms*.
- [5] R. H. Todd, D. K. Allen, and L. Alting. *Manufacturing processes reference guide*. Industrial Press, 1994, p. 486.
- [6] X. Zhao, Z. Zhou, and J. Ni. "Micro-Structural Analysis of WC-Co Carbide Tool in Titanium Machining - Knovel". In: ()).